Novel Hydrogen-bonded Supramolecular Assemblies from Resorcinarene-derived Macrocycles & Elucidation of the Prerequisites for Terpene Cyclizations inside the Resorcinarene Capsule

Inauguraldissertation

zur Erlangung der Würde eines Doktors der Philosophie

vorgelegt der

Philosophisch-Naturwissenschaftlichen Fakultät

der Universität Basel

von

Severin Merget

2021

Genehmigt von der Philosophisch-Naturwissenschaftlichen Fakultät

auf Antrag von

Prof. Dr. Konrad Tiefenbacher, Prof. Dr. Marcel Mayor und Prof. Dr. Alessandro Scarso.

Basel, den 30. 03. 2021

Prof. Dr. Marcel Mayor

(Dekan)

Die vorliegende Arbeit wurde von Mai 2017 bis April 2021 an der Universität Basel unter Leitung von Prof. Dr. Konrad Tiefenbacher angefertigt. Teile dieser Arbeit wurden veröffentlicht:

(1) **Merget, S.**, Catti, L., Piccini, G.M., Tiefenbacher, K. Requirements for Terpene Cyclizations inside the Supramolecular Resorcinarene Capsule: Bound Water and its Protonation Determine the Catalytic Activity, *J. Am. Chem. Soc.* **2020**, *142*, 4400−4410

(2) **Merget, S.**, Catti, L., Zev, S., Major, D. T., Trapp, N., Tiefenbacher, K., Concentration-dependent Self-assembly of an Unusually Large Hexameric Hydrogen-bonded Molecular Cage, *Chem. Eur. J.* **2021**, *27*, 4447−4453.

Acknowledgements

First and foremost, I would like to thank my supervisor Prof. Dr. Konrad Tiefenbacher for giving me the opportunity to work in his group on a very interesting subject. I am truly thankful for his unwavering support, his assistance and motivation also during the more difficult times of the project.

For extremely valuable discussions and always worthwhile scientific input I am also deeply grateful to my second supervisor Prof. Dr. Marcel Mayor.

I am happy to acknowledge my colleagues from the Tiefenbacher research group for a pleasant working atmosphere and never a dull moment in the lab. Thanks goes to Dr. Lorenzo Catti who introduced me to the group and taught me most of the practical and theoretical background for my studies and contributed significantly to the publications. Special mention deserves Suren Nemat mainly for proofreading this manuscript but also for his constant and relentless bad taste concerning the music he played in the lab. Further, I would like to thank Jonathan Pfeuffer-Rooschüz for great suggestions and discussions, while writing this thesis.

I am extremely grateful to our collaborators who added valuable contributions to the publications presented in this thesis: Prof. Dr. Dan T. Major, Dr. Shani Zev and Dr. Giovanni-Maria Picini for computational studies as well as Dr. Nils Trapp for his help with challenging X-ray crystallographic experiments.

The entire staff of the chemistry department is greatly acknowledged for their support, with a special mention of PD Dr. Daniel Häussinger for his endless patience and support concerning our demands for unusual NMR spectroscopic experiments. I am also grateful to Isa Worni for always being of great help concerning any administrative issues.

Last but not least, I want to thank my family, friends and most of all my wonderful partner, Isabella, for the unconditional support over the last four years working on this thesis.

Deutsche Zusammenfassung

Die säurekatalysierte tail-to-head Zyklisierung von Terpenen mit dem Resorcinarene Hexamer als Co-Katalysator stellt eines der eindrücklichsten Beispiele für enzymmimetische Katalyse unter Verwendung von supramolekularen Kapseln dar. Die detaillierte Wirkungsweise und besonders die Gründe für die katalytische Inaktivität des verwandten Pyrogallolarene Hexamers waren jedoch bisher ungeklärt. Die vorliegende Arbeit zeigt die Möglichkeiten synthetischer Methoden auf um den Resorcinaren-Makrozyklus zu modifizieren, um neue Bausteine für unbekannte, selbstassemblierende Strukturen zu erhalten. Mit dem Ziel die Voraussetzungen für Säure-Katalyse im Inneren des Resorcinaren Hexamers genauer zu untersuchen, wurde zunächst eine Syntheseroute entwickelt, die es erlaubt neuartige Makrozyklen in reiner Form zu isolieren, welche unterschiedliche Verhältnisse von Resorcinol- und Pyrogallol-Einheiten aufweisen. Die basierend auf diesen Makrozyklen selbstassemblierenden Strukturen wurden im Folgenden bezüglich ihrer katalytischen Aktivität in der Zyklisierung von Monoterpenen untersucht. Des Weiteren erfolgte eine Charakterisierung der Strukturen in Bezug auf verschiedene Eigenschaften wie die Fähigkeit zur Gastaufnahme, die Stabilisierung von Ionenpaaren, die Fähigkeit zur Interaktion mit Säure (HCl), sowie die strukturelle Integration von Wassermolekülen in das Wasserstoffbrückennetzwerk. Die Resultate zeigten eine deutliche Korrelation zwischen der katalytischen Aktivität und der Inkorporation von Wassermolekülen was auf die besondere Rolle solch integrierter Wassermoleküle hindeutet. Diese fungieren als Protonenshuttle und ermöglichen somit die Aktivierung des enkapsulierten Substrates durch Protonierung. An einem Modellsystem durchgeführte Simulationen der molekularen Dynamik lieferten weitere Details bezüglich des genauen Verlaufs der Protonierung und stützen die experimentellen Ergebnisse. In einem zweiten Projekt wurde ein ähnlicher synthetischer Ansatz genutzt, um einen vom Resorcinaren abgeleiteten Makrozyklus mit zusätzlichen Amid-Funktionalitäten zu synthetisieren. In detaillierten ^{1}H- und DOSY-NMR Studien konnte gezeigt werden, dass dieser Makrozyklus konzentrationsabhängig und basierend auf der intermolekularen Dimerisierung der Amidgruppen, zu einem großen, hexameren Käfig assembliert. Mit einem Volumen von 2800 Å^3 und einem Durchmesser von 2.3 nm stellt dies die größte bisher bekannte Struktur dar, die ausschließlich auf Wasserstoffbrückenbindungen beruht. Die Resultate von DFT-Berechnungen deuten auf eine ungewöhnliche käfigartige Struktur hin, die an kovalent verbrückte Strukturen erinnert, im Gegensatz zu den häufig bei wasserstoffbrückenbasierten Kapseln beobachteten closed-shell Strukturen. Zusätzlich konnte gezeigt werden, dass in dem Käfig Fullerene (C_{60} and C_{70}) enkapsuliert werden können.

Abstract

The acid-catalyzed tail-to-head terpene cyclization promoted by the resorcinarene hexamer is a prime example of enzyme mimetic catalysis utilizing supramolecular capsules. The exact mode of activation and the reasons for the catalytic inactivity of the closely related pyrogallolarene hexamer however, remained elusive for some time. In this work we utilized synthetic chemistry to modify the resorcinarene macrocycle with the goal of obtaining new building blocks capable of self-assembly, forming new supramolecular structures with unprecedented properties. Firstly, a synthetic route was developed to access several new macrocycles with varying ratios of resorcinol and pyrogallol units, in order to elucidate the specific requirements for acid-catalyzed terpene cyclizations within the resorcinarene capsule. The resulting assemblies were characterized with respect to their catalytic activity in the cyclization of monoterpenes as well as several properties including guest uptake, stabilization of ion pairs, response to externally added acid (HCl) and water incorporated into the hydrogen bond network. The results revealed a correlation between the structural incorporation of water and the catalytic activity. This indicates the crucial role of the water molecules in the hydrogen bond network of the supramolecular capsule, which act as a proton shuttle activating the encapsulated substrate and enable efficient catalysis. Molecular dynamics simulation conducted using a model system provided additional details concerning the exact protonation pathway, supporting the experimental evidence. Secondly, a similar synthetic approach was used to synthesize a resorcinarene-derived macrocycle featuring four additional amide moieties capable of hydrogen bonding. Detailed ^{1}H- and DOSY-NMR studies revealed the concentration-dependent self-assembly of a large, hexameric cage based on intermolecular amide−amide dimerization. An internal cavity volume of 2800 Å^3 and a diameter of 2.3 nm make it the largest self-assembled cage/capsule structure self-assembled exclusively *via* hydrogen bonding. Supported by DFT calculations the results indicate that an unusual cage-like structure with large openings, reminiscent of covalently linked structures, is formed rather than a ‘closed-shell’ structure observed more commonly for hydrogen bonded assemblies. Additionally, the cage was found to form host-guest complexes with fullerenes (C_{60} and C_{70}).

Table of Contents

1. Introduction

The utilization of plants for medicinal purposes is a well-documented aspect of human history.[1] Our ancestors knew about the beneficial effect of certain plants and used them to alleviate pain, cure different illnesses or as psychoactive drugs. With the general advancement of natural sciences over the last two centuries, humanity's understanding of the underlying reasons for the potency of plants has improved significantly. Today we can isolate and synthesize the pharmacologically active molecules and have implemented numerous plant-derived drugs into modern pharmacotherapy. The approach to isolate significant amounts of the bioactive substances directly from plants is often limited by low contents of target compound or purification issues. With the advent of synthetic organic chemistry, it became possible to produce some of the most complicated natural product by highly sophisticated total synthetic routes. And while great feats have been achieved by organic chemists in this field the elegance and efficiency of the biochemical machinery producing complex molecules from simple precursors remains unmatched by any human efforts. The reason for this discrepancy are the highly sophisticated macromolecules enabling practically all life on earth, enzymes. Constituted of long amino acid chains, which fold and aggregate to form complex three-dimensional structures, enzymes have evolved over millions of years resulting in the unrivalled catalytic efficacy observed today. The three-dimensional structure of such proteins allows the formation of hydrophobic pockets, where molecules of complementary size and shape can be encapsulated through an interplay of different interactions with the amino acid side chains within the binding pocket (lock and key principle).[2] The binding within such active sites relies on non-covalent interactions and creates a unique microenvironment for catalysis isolated from the bulk solution. One aspect of supramolecular chemistry is to mimic this basic principle using man-made three-dimensional structures in order to overcome the limitations of conventional solution chemistry.[3] The focus lies on the imitation of the catalytically active part of enzymes leading to a reduction in overall structural complexity. This approach could simplify the total synthesis of scarce natural products and possibly access new derivatives not found in nature. The synthetic effort for artificial enzymes can be greatly reduced by using simple building blocks that self-assemble into defined supramolecular entities *via* non-covalent interactions. Especially hydrogen bonding, which is also crucial for the secondary structure of many natural enzymes, has been established as a powerful tool to construct supramolecular assemblies.

1.1 Enzyme Catalysis

The ability of enzymes to selectively bind and recognize substrate molecules is crucial for the functionality of biocatalysts within a complex *in vivo* setting (i.e., inside cells). The hydrophobic binding process relies on enthalpic as well as on entropic contributions. It also creates a defined, molecular environment activating the substrate(s) and stabilizing reactive intermediates.[4] Generally, three modes of enzyme mediated lowering of the activation free energy are distinguished:[5] 1) Transition state stabilization: Enzymes preferentially bind and stabilize the transition state (often involving a (partially) charged state) rather than the substrate or product molecules, which circumvents inhibition. 2) Ground state destabilization: The binding of a molecule within the active site of the enzyme causes a strain, which results in a more reactive orientation and/or conformation of the substrate. Similarly, non-covalent interactions with the amino acid side chains can lead to the activation of a particular functional group. 3) Covalent catalysis: The activation barrier is lowered by temporarily forming a covalent bond between enzyme and substrate. These modes of action result in the unmatched catalytic efficiency with high selectivity in combination with excellent regio- and stereocontrol, enabling the catalysis of biochemical reactions under mild *in vivo* conditions.

Among the numerous reactions catalyzed by enzymes, the cyclization of terpenes is considered one of the most intriguing transformations found in nature. Terpenes constitute one of the largest and diverse classes of natural products, with over 80 000 compounds known, many of them showing biological activity.[6-8] Some members exhibit promising antibacterial activity[9] while others such as Paclitaxel,[10-11] a potent anticancer drug, have already found practical application. Terpenes are distinguished based on the number of carbon atoms/isoprene units: hemi- (C_5), mono- (C_{10}), sesqui- (C_{15}), di- (C_{20}), sester- (C_{25}) and triterpenes (C_{30}) and even larger members. Albeit their structural diversity the majority of terpenes is derived from just a few acyclic precursors (Figure 1) such as geranyl diphosphate (**1**) (monoterpenes), farnesyl diphosphate (**2**) (sesquiterpenes), and geranylgeranyl diphosphate (**3**) (diterpenes).[7]

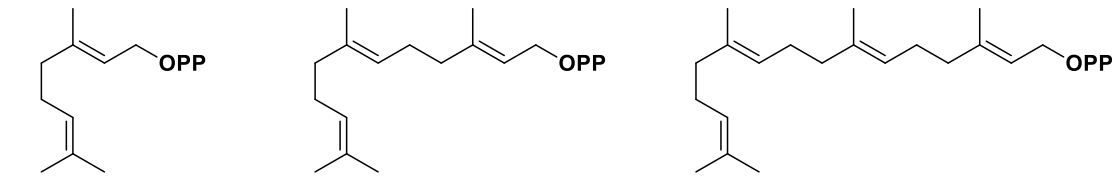

geranyl diphosphate (**1**) farnesyl diphosphate (**2**) geranylgeranyl diphosphate (**3**)

Figure 1: Acyclic precursors for the biosynthesis of complex terpenes.

1.1.1 Terpene Cyclases

The enzymes catalyzing these transformations are termed terpene cyclases and can be divided into two groups depending on the mode of activation.[8, 12-13] Class I cyclases trigger the cyclization by abstracting the allylic diphosphate leaving group utilizing a trinuclear metal complex (e.g., Mg^{2+}) which leads to the formation of a carbocation. In contrast, class II cyclases act by protonating a C–C double bond or an epoxide moiety. These different modes of activation result in different reaction pathways concerning the propagation of the positive charge during the cyclization cascade. Activating the terminal double bond (head) leads to a head-to-tail terpene (HTT) cyclization, while cleavage of the diphosphate leaving group (tail) induces a tail-to-head terpene (THT) cyclization cascade (Scheme 1a).[14] Independent of the mode of activation the resulting carbocation is attacked by a nucleophilic double bond to form a cyclic structure. The resulting positively charged species can then undergo further cyclization steps, rearrangements, or hydride migrations until the cascade is terminated either by elimination or by an intermolecular attack of a nucleophile. An important feature of class I cyclases is the complexation of the diphosphate leaving group which prevents premature quenching and enables a non-stop cyclization cascade. Considering the number of possible reaction pathways and resulting products, terpene cyclases show a remarkable selectivity often producing a single product. Equally noteworthy is the efficient transfer of chirality from the cyclase onto the prochiral substrate induced by the specific configuration of the active site.

To illustrate the complexity of this transformation scheme 1a shows the possible reaction pathways and common products (Scheme 1b) resulting from the cyclization of geranyl diphosphate (**1**).[12] The cyclization occurs in a tail-to-head fashion, starting with the cleavage of the diphosphate group to give the cationic species **4a**. Due to the (*E*)-configuration of the double bond intermediate **4a** cannot undergo cyclization directly. The preceding isomerization to the *cisoid*-isomer **4b** is believed to occur either directly[15] or *via* the linalyl diphosphate (**5**) and rotation of the double bond.[12] Cation **4b** can then cyclize to form the terpinyl cation (**6**), the common precursor of all cyclic products of this transformation. Elimination leads directly to limonene (**7**) and terpinolene (**8**), while α-terpinene (**9**), γ-terpinene (**10**) or α-phellandrene (**11**) are formed if the elimination is preceded by a 1,2- or 1,3-hydride migration. If water is present within the active site **6** can react to α-terpineol (**12**), which can be further cyclized to give the bicyclic ether eucalyptol (**13**). Other possible bicyclic products include β-pinene (**14**), camphene (**15**), 3-carene (**16**) and sabinene (**17**), as well as products formed by reaction of cationic bicyclic intermediates with water such as sabinene hydrate (**18**) and *endo*-fenchol (**19**).

If the initial isomerization is followed by an attack of water or deprotonation several acyclic products (geraniol (**20**), nerol (**21**), linalool (**22**), (*E*)-β-ocimene (**23**) and myrcene (**24**)) are formed. Additionally, products can be found that result from the reaction of cationic intermediates with the diphosphate group. The absolute configuration can be attributed to the helical conformation of geranyl diphosphate (**1**), which dictates the configuration of the optically active terpinyl cation (**6**).

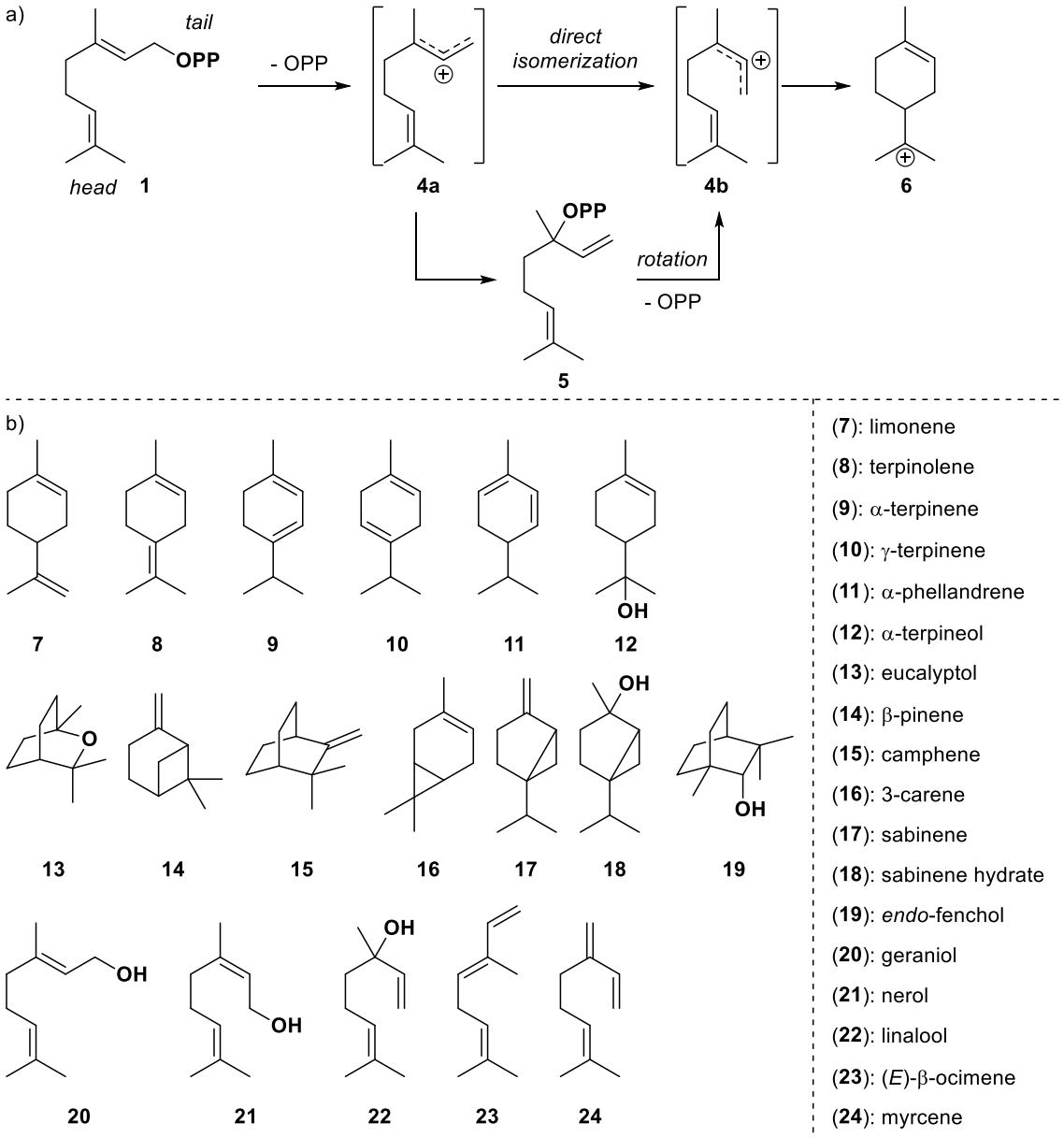

Scheme 1[*]: a) Formation of the α-terpinyl cation (**6**) catalyzed by class I cyclases. b) Common cyclic and acyclic monoterpene products of the THT cyclization.

[*] Reproduced from: *Application and Development of Resorcin[4]arene-Based Supramolecular Catalysts*, Lorenzo Catti, **2017**, Dissertation.

1.1.2 Towards Biomimetic Tail-to-Head Terpene Cyclization

Due to their remarkable structural diversity and their promising biological activity, terpenes have attracted considerable interest by synthetic chemists. Since the complex carbon skeletons are often tedious to access by other means, nature has served as an inspiration to numerous studies trying to imitate the processes occurring in terpene cyclases.[16] While there have been some reports concerning the tail-to-head cyclization of monoterpene alcohols in solution (Scheme 2a) using phosphoric acids[17] or ferric chloride,[18] these results proved difficult to reproduce and yielded in case of the phosphoric acids mostly the head-to-tail product cyclogeranyl acetate (**26**).[15] Comparable results were achieved employing zeolithes[19-20] or chlorosulfuric acid[21] with geraniol (**20**) and geranyl acetate (**27**) as substrates (Scheme 2b).

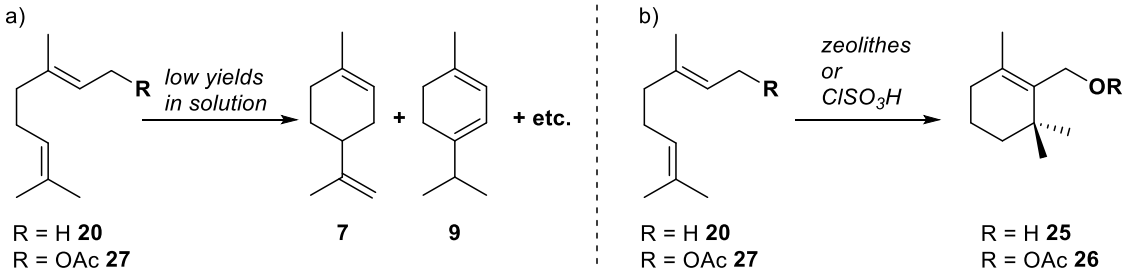

Scheme 2: a) THT cyclization in solution using conventional BRØNSTED and LEWIS acids. b) HTT cyclization forming cyclogeranyl acetate (**26**) derivatives in the presence of zeolithes and chlorosulfonic acid.

Other reports concerning the tail-to-head cyclization of sesquiterpenes in solution under similar conditions[19, 21-22] also suffered from low yields for cyclic terpenes due to competing side reactions, such as premature elimination and/or substitution of intermediates. These problems can be at least partially attributed to the presence of the counteranions, which can act as base and/or nucleophile. Additionally, they are probably held in close range to the cationic intermediates due to their negative charge. To circumvent this problem SHENVI and coworkers developed a method where the cleaved leaving group is immobilized efficiently by forming a covalent bond with the reagent.[14] For this purpose, they employed a modified sesquiterpene substrate **28** featuring a vinyl epoxide (Scheme 3a). When **28** is exposed to aluminium LEWIS acids the epoxide is activated, which allows the formation of the bisabolyl cation (**29**). The cationic leaving group remains covalently linked to the former LEWIS acid, enabling the cyclization cascade to proceed further towards the polycyclic frameworks of cedrene (**30, 31**) and funebrene (**32**), which have been isolated in 44% combined yield. Employing a similar strategy, the authors were also able to achieve the synthesis of the cumacrene/dunniene skeleton

34 where a trimethylsilyl (TMS) group was utilized to modulate the reactivity of the substrate **33** (Scheme 3b).

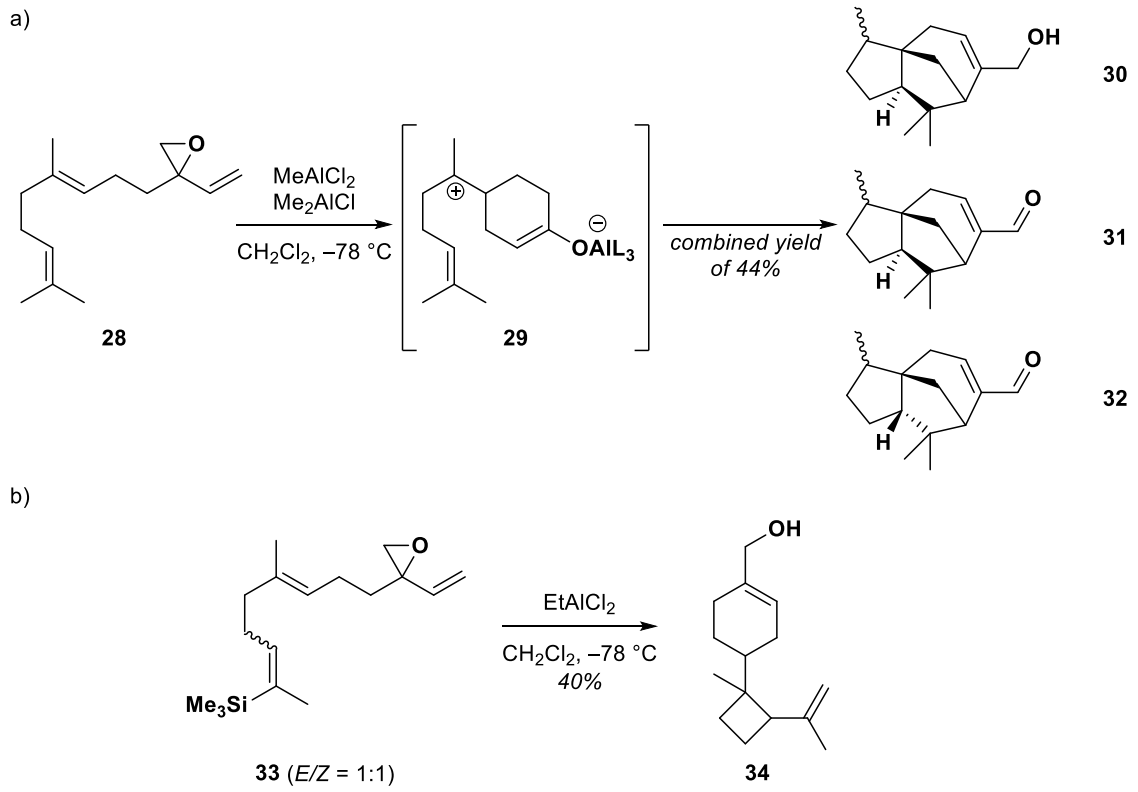

Scheme 3: a) Tail-to-head cyclization of sesquiterpene **28** developed by SHENVI and coworkers relying on aluminium LEWIS acids to immobilize the anionic leaving group. b) Tail-to-head cyclization of activated substrate **33** yielding the cumacrene/dunniene skeleton **34**.

Another important contribution to the field was recently reported by the JACOBSEN group. Based on earlier studies concerning the cyclization of polyenes catalyzed by thiourea derivatives[23] they were able to develop the first catalytic, enantioselective version of a tail-to-head terpene cyclization in solution (Scheme 4a).[24] In the presence of urea-derived catalysts neryl chloride (**35**) derivatives are converted to form mainly limonene (**7**) and terpinyl chloride derivatives (**36**) resulting in high enantiomeric excess (ee). The authors were able to show that substitution of the substrate with a bulky aryl substituent is crucial for steric and electronic reasons, as is the incorporation of an aromatic moiety into the carefully designed catalyst structure **37** (Scheme 4b), in order to stabilize the cationic intermediate by cation−π interactions. Additionally, evidence for a concerted mechanism involving two catalyst molecules is presented, which explains why geranyl chloride derivatives show only weak reactivity and enantioinduction, due to their unfavorable double bond configuration.

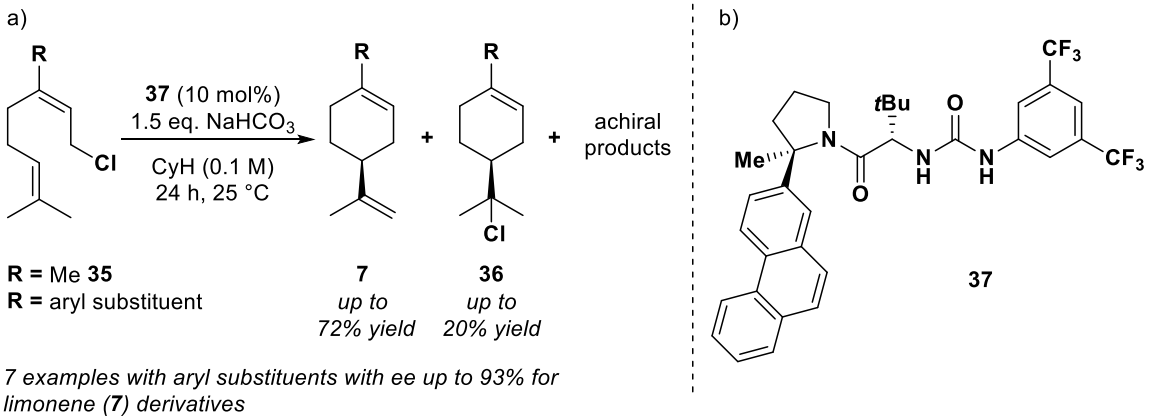

Scheme 4: a) First example of an enantioselective tail-to-head cyclization of neryl chloride (**35**) derivatives with aryl substituents employing b) Urea-derived catalyst **37**.

While there have been some significant advances in the field of biomimetic terpene cyclizations in solution some important limitations remain. The methods developed to date often require complex substrate synthesis, considerable catalyst optimization and their universality is generally rather limited. Furthermore, many of them lack sufficient control over the conformation of substrate and intermediates, resulting in poor product selectivity. Therefore, nature continues to serve as an inspiration, where these issues were elegantly solved by encapsulating substrates and intermediates within carefully designed cavities.

1.2 Supramolecular Host Structures

Supramolecular chemistry is often defined as relying on non-covalent bonding interactions between two or more chemical entities/molecules in contrast to molecular chemistry, which is predominantly concerned with covalent bonds connecting the atoms of a single molecule.[25] Based on non-covalent interactions such as hydrogen bonding, metal coordination, hydrophobic interactions or π-interactions complex two- and three-dimensional architectures become feasible. An important prerequisite for the formation of homogenous networks based on non-covalent interactions is a high degree of preorganization and rigidity of the individual molecular building blocks. This becomes even more vital for the assembly of discrete, molecular structures rather than the formation of extended networks.[26-27] Considering the diversity and functionality of naturally occurring biomolecules utilizing a complex interplay of non-covalent and covalent bonding, it can hardly surprise that chemists were intrigued by the thought of mimicking these processes to assemble sophisticated, molecular architectures.

1.2.1 Guest Binding and Catalysis in Supramolecular Host Systems

In nature, the first step in enzyme catalyzed reactions is usually marked by the process of molecular recognition.[25] Based on the specific chemical environment within the active site, the substrate is bound in a selective way. To mimic this basic concept, it is desirable to design/synthesize molecules with some type of cavity or binding pocket. Such molecules are then able to complex guest molecules forming a well-defined supramolecular host-guest complex. Molecular recognition in man-made system relies mainly on different non-covalent interactions often acting simultaneously, and strongly depends on the nature of the host as well as the solvent employed.[28-30] The binding process is entropy- and/or enthalpy-driven resulting in a total net negative free energy ΔG.

Many early examples utilizing covalently linked host structures such as the well-known crown ethers complexing alkali metal cations relied on ion-dipole interactions for guest binding.[31] Another type of bonding commonly observed is based on cation-π interactions e.g., between aromatic host structures and ionic guests such as quaternary ammonium ions.[32] In this context the electrostatic potential surface (ESP) was found to provide a good, qualitative measure for the strength of cation-π interactions.[33] Depending on their electronic properties aromatic surfaces have been observed to interact also *via* π−π-stacking and CH−π bonding.[34] Recently, anion-π interactions have come more into focus and have even been applied in a catalytic context.[35-37] In aqueous solvents the dominant force is usually the hydrophobic effect. In this

case the guest binding is mostly viewed to be entropy-driven, due to liberated solvent molecules upon encapsulation.[38] In contrast, the non-classical hydrophobic effect is enthalpy-driven due to favourable dispersive interactions, attraction of fluctuating dipoles and gains in solvent cohesive interactions. Yet another type of interaction frequently observed in molecular recognition events is hydrogen bonding. In the context of host-guest interactions hydrogen bonds are mostly observed in non-competitive media, such as apolar, organic solvents or within hydrophobic pockets. The strength of hydrogen bonds depends on the acidity of the hydrogen bond donor and likewise increases with the basicity of the hydrogen bond acceptor.[39] Generally, hydrogen bonds are considered highly directional and form along the direction of the unpaired electrons of the acceptor, however significant deviations are often tolerated. In some cases, bifurcated hydrogen bonds are observed, where a single hydrogen atom forms two weaker bonds with different acceptors.[40] In particular OH-groups can act as donor and acceptor simultaneously, leading to cooperative hydrogen bonding resulting in bond polarization and strengthening of the individual bonds.[41] Closely related to hydrogen bonds are halogen bonds, which rely on the interactions between LEWIS bases and the area of positive electrostatic potential (σ-hole) opposite of carbon-halogen bonds. The strongest halogen bonds are observed with increasing size of the halogen atom and are usually linear.[42]

Guest binding within supramolecular structures is a valuable tool on its own and has been, among other things, applied for sensing and separation purposes.[43] A significant part of the attractiveness of enzymes however, stems from their catalytic power. Isolation of a reaction from the bulk solution yields several advantages as demonstrated by the highly efficient biochemical machinery using this concept. Supramolecular catalysis attempts to mimic natural enzymes using artificial hydrophobic cavities as nano reaction chambers. The catalytic activity usually stems from the properties of the supramolecular host itself or alternatively from the encapsulation of a catalytically active guest (e.g., transition metal complex, organocatalyst) resulting in several favourable aspects:[44]

i) **Product Selectivity**: A reaction taking place within a confined environment can lead to different products compared to the bulk solution. Specific interactions between host and guest can lead to alternative reaction pathways e.g., by activating certain functional groups, by inflicting steric strain and thereby changing regio- and/or stereochemistry as well as favouring intramolecular over intermolecular reactions. Additionally, the encapsulation of reactive intermediates inside a

supramolecular cavity can result in the protection from counterions or solvent molecules often observed in solution chemistry.

ii) **Substrate Selectivity**: Due to the limited size of the hydrophobic cavity a size selectivity concerning the substrate is automatically inflicted. Only substrates that can enter and fit inside the cavity are converted while larger substrates with the same reactivity are unaffected.

iii) **Multicatalyst Tandem Reactions**: To avoid cost and time intensive work-up and purification steps, it is highly desirable to run multicatalyst tandem reactions. This would allow reaction sequences with multiple successive reactions in a one-pot fashion. The encapsulation of catalysts within supramolecular structures allows the spatial separation of different catalysts, which would be incompatible in bulk solution.[45] The size- and shape-selectivity of supramolecular hosts furthermore helps to achieve a defined order of substrate conversion in such a complex tandem reaction system.

The following sections summarize the different approaches to constructing and utilizing supramolecular host structures for different purposes with a focus on catalytic applications. Early on, mainly covalently linked host structures were developed and applied for host-guest studies. Gradually the strategy was broadened, and non-covalent interactions were employed to self-assemble larger, discrete entities, which are then able to act as host structures themselves. Both types of structures have their specific advantages and disadvantages and have been applied in enzyme mimetic catalysis with some selected examples presented hereafter.

1.2.2 Covalently Linked Host Systems

In 1987 the Nobel Prize in Chemistry was awarded to PEDERSEN, CRAM and LEHN for their pioneering work in developing functional molecules capable of guest binding.[46-48] PEDERSEN published the first examples of the so called "crown ethers" **38**, which are capable of selectively binding alkali metal ions depending on their size.[31] LEHN and CRAM expanded the concept further to three-dimensional crown ether derivatives, namely cryptands[49] **39** and spherands[50] **40**, with even higher binding constants and improved selectivity (Figure 2).

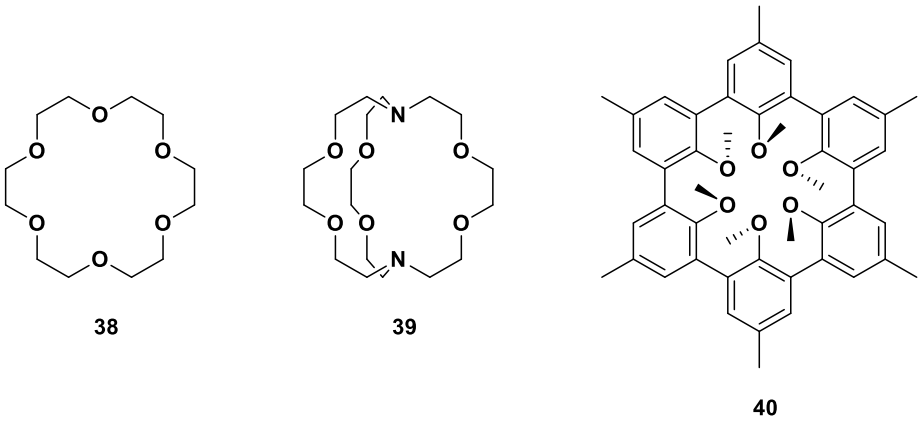

Figure 2: Crown ether **38** by PEDERSEN, cryptand **39** by LEHN and spherand **40** by CRAM.

Even though these results are considered milestones of supramolecular chemistry, their specific properties have also hindered the development of catalytic applications of such molecules to some degree. Due to their high binding affinities, they often suffer from product inhibition and their exceptional size selectively severely limits the substrate scope.[51-52]

Another important class of enzyme mimetic compounds employed for supramolecular chemistry in the early stages are cyclodextrins (Figure 3). These naturally occurring oligosaccharides are water soluble and feature a hydrophobic pocket in which small guest molecules can be bound, a property which has been used amongst other things in drug formulation.[53] α-Cyclodextrin (**41**) was shown to accelerate the chlorination of anisole in a regioselective way, by encapsulating the substrate, which leads to a blocking of the usually reactive *ortho*-position.[54] Circular macrocycles accessed *via* synthetic methods include amongst others the porphyrin based structure **42** and cyclophanes (e.g., **43**, Figure 3) which were utilized to catalyze an intermolecular acyl transfer reaction[55] and a catalytic oxidation of aromatic aldehydes,[56] respectively.

One of the covalently linked host structures with the highest binding affinities for charged guests (i.e., ammonium species) are cyclic cucurbiturils (e.g., **44**, Figure 3).[57] These macrocycles are composed of glycouril units linked by methylene units. They are synthesized by condensation of glyoxal, formaldehyde and urea with different oligomers favored depending on reaction conditions. They exhibit strong binding of cationic guest molecules by ion-dipole interactions with the oxygen atoms situated at both rims of the cavity. This property was exploited when employing cucurbit[6]uril in a 1,3-dipolar cycloaddition between azides and alkynes, each bearing an ammonium group to enhance binding within the cavity.[58] Several other reactions have been accelerated in the presence of these macrocycles in a biomimetic fashion.[57]

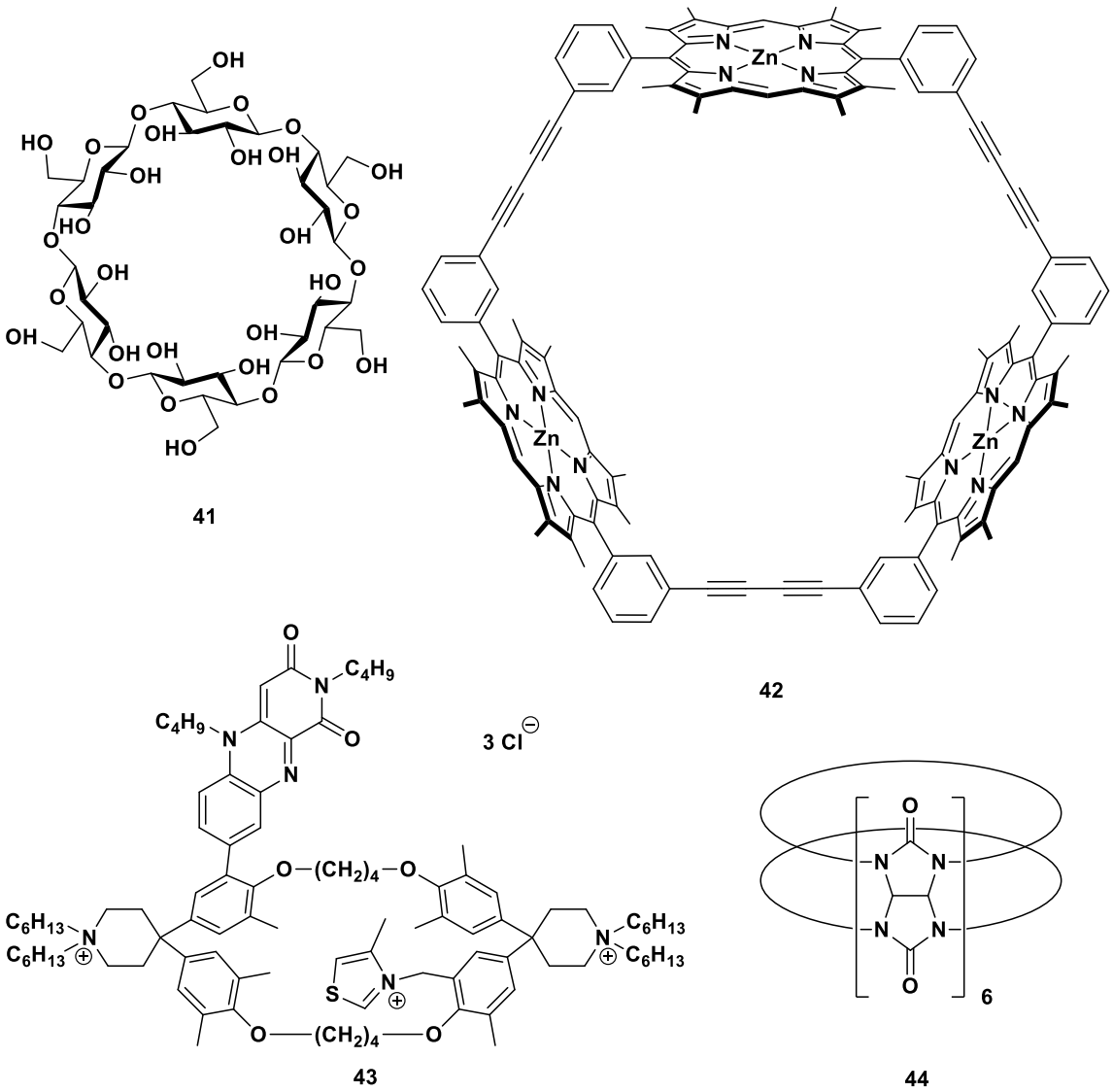

Figure 3: Different types of macrocyclic molecules that have been applied in enzyme mimetic catalysis: α-Cyclodextrin (**41**), porphyrin based structure **42**, cyclophane **43** and cucurbit[6]uril **44**.

Due to their bowl-shape, cavitand molecules such as calixarene **45** and the related resorcinarenes **46**, and pyrogallolarenes **47** are of considerable interest for supramolecular chemistry (Figure 4).[59] These macrocycles are generally easily accessible by acid-catalyzed condensation of the phenolic units with the corresponding aldehydes. In case of pyrogallol and resorcinol this yields quite selectively the resorcin[4]- or pyrogallol[4]arenes (**46** and **47**), although larger oligomers have also been isolated.[60-62] Due to their bowl shape and the polar functional groups these macrocycles are good candidates for the formation of supramolecular complexes. Their properties can be adapted for specific guests and applications relying on numerous synthetic modifications that have been reported.[63-64]

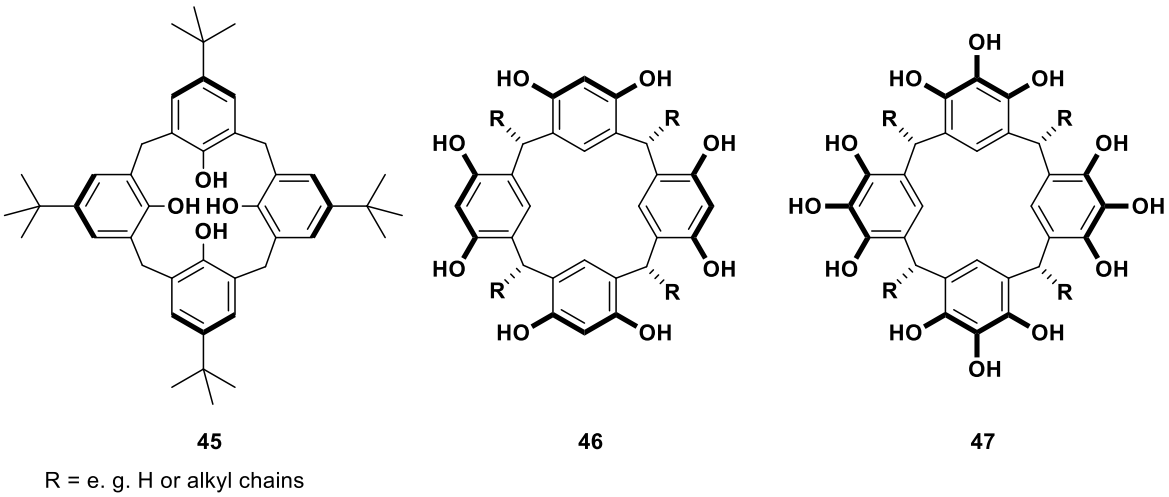

Figure 4: Bowl-shapped macrocycles: calix[4]arene **45**, resorcin[4]arene **46** and pyrogallol[4]arene **47**.

REBEK and coworkers pioneered the utilization of resorcinarene **46** as a platform to synthesize water-soluble deep cavitands (e.g., **48**, Scheme 5a).[65] Within their large hydrophobic interior, these molecules are able to accommodate long alkyl chains, while the hydrophilic head groups remain exposed to the aqueous medium and thereby enable for example macrolactamization reactions (Scheme 5b).[66] Derivatives of **48** have also been employed as supramolecular protection group allowing the selective monohydrolysis of diesters.[67] Upon hydrolysis of one of the esters the product adopts a conformation, where the second ester moiety remains deep within the cavity protecting it from reacting further, while the more polar carboxyl group is exposed to the aqueous medium. This concept has been applied to other transformations, all of them requiring **48** in stochiometric amounts.

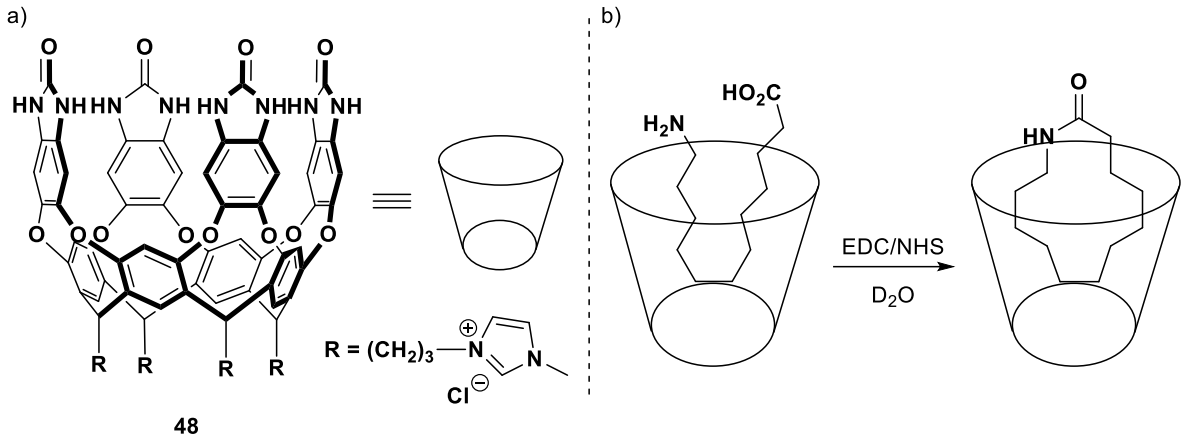

Scheme 5: a) Resorcin[4]arene-derived deep cavitand **48**. b) Application of **48** for selective intramolecular macrolactamization.

Today covalently linked host systems offer a great structural variety and have been utilized in various contexts. In absolute terms the cavities remained rather small and an increase in size is normally associated with significant synthetic effort. Additionally, most cavities are relatively open and guest molecules are still exposed to the bulk solution. While this can be advantageous in some cases, it limits the applicability of open, covalently linked host structures for enzyme mimetic catalysis. Nonetheless, the field is still very active and new macrocycles (e.g., catecholarene,[68] pillararene,[69] beltarene[70]) are reported frequently, opening up new opportunities for the practical application of supramolecular chemistry across different disciplines.

1.2.3 Assemblies Based on Metal-Ligand Interactions

Albeit the impressive diversity of covalently linked host systems and their successful applications, another class of self-assembled host systems based on metal-ligand interactions has received considerable attention.[71-76] The self-assembling nature of these host structures based on, in many cases quite simple precursors, provides access to large assemblies with relative synthetic ease and additionally introduces some modularity. This is in contrast to the more conventional approach using covalent chemistry, where increasing size is usually associated with considerable synthetic effort. The largest structure based on metal-ligand interactions to date with an internal cavity volume of 153,000 Å^3 has been reported by the FUJITA group and self-assembles from 144 components.[77] Regarding supramolecular catalysis somewhat smaller systems such as assembly **I** (Figure 5) or structure **IIIa** (Figure 6a) and its derivatives reported by RAYMOND, BERGMANN and TOSTE have been shown to be of interest.[75, 78]

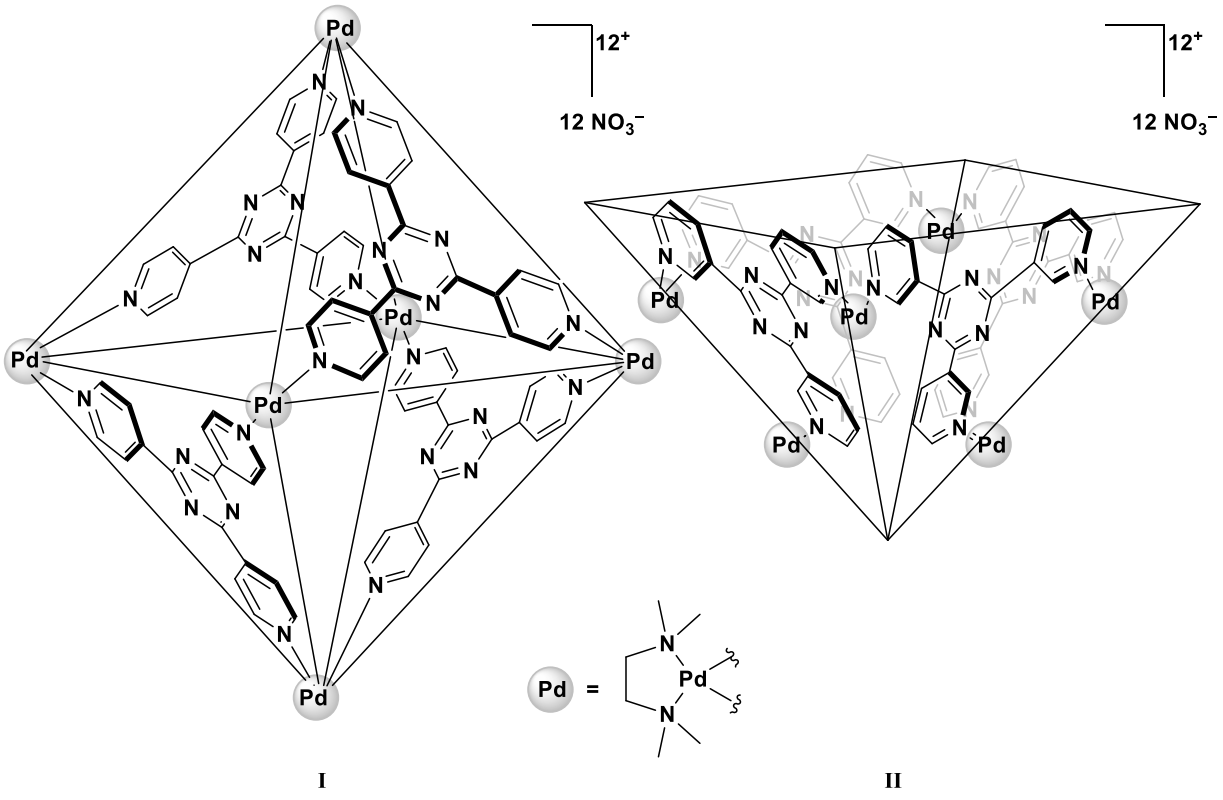

Figure 5: Self-assembled structures **I** and **II** reported by FUJITA.

Structure **I** self-assembles from two components: a cationic, capped (en)Pd^{2+} fragment (en = ethylenediamine) and 1,3,5-tris(4-pyridyl)triazine acting as a rigid ligand.[79] These building blocks combine in a 6:4 stoichiometry to form octahedral structure **I**, which features a discrete

cavity capable of accommodating small organic guest molecules. Modulating the building blocks allows for adaption of the geometry (i.e., square-pyramidal structure **II**) and the size of the supramolecular host as well as the size of the apertures. Substituting ethylenediamine with an optically active diamine renders **I** optically active. **I** and **II** have been shown to accelerate a DIELS-ALDER reaction of aromatic substrates due to favorable π-stacking interactions.[80] The chiral derivative of **I** was found to induce a modest chiral induction in a [2+2] photocycloaddition. Recently, the group could apply a platinum-based derivative of **I** for a biomimetic, base mediated amide cleavage successfully mimicking the activation mechanism of enzymes by inducing a mechanical strain on the amide and thereby altering its reactivity.[81]

Another system from the family of M_4L_6 hosts that has been studied in detail and has found numerous applications in catalysis is the water-soluble structure **IIIa** first reported by RAYMOND in 1998 (Figure 6a and b). Tetrahedral assembly **IIIa** is spontaneously formed by combining a gallium(III) salt with the ditopic ligands featuring catecholate moieties separated by planar, aromatic spacers, in a 4:6 stoichiometry.[82] Compared to the related structure **I**, assembly **IIIa** has much smaller apertures shielding the interior more strictly from the bulk solvent. Due to the negative charge of the host, cationic guests are well encapsulated by **IIIa** due to favorable coulombic interactions. The encapsulation of neutral, organic molecules, while enthalpically disfavored, is driven by entropic gains through expulsion of solvent molecules from the cavity upon encapsulation.[83]

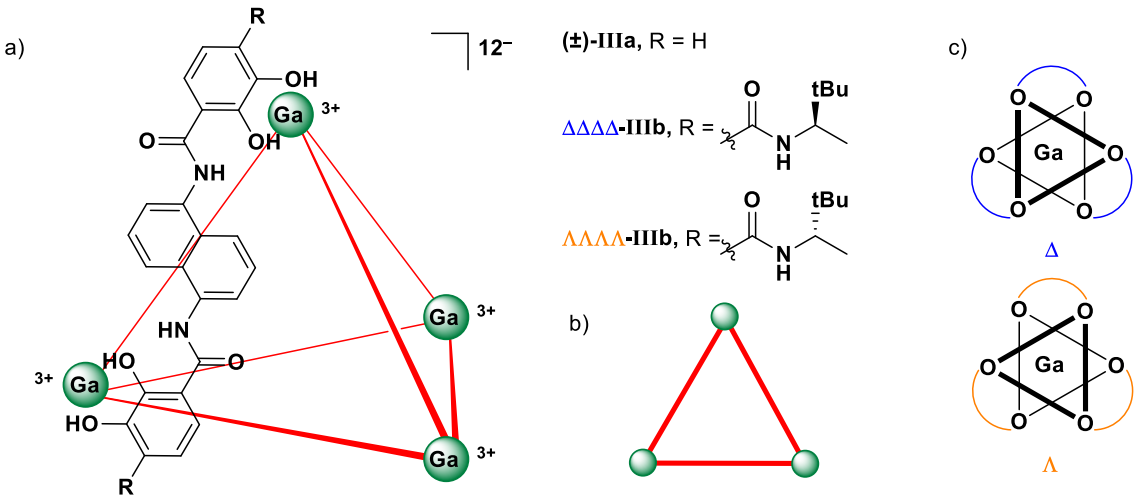

Figure 6: a) Self-assembled capsule **IIIa** reported by RAYMOND. b) Schematic representation of structure **IIIa**, c) Schematic representation of the two enantiomers ΔΔΔΔ-**IIIb** and ΛΛΛΛ-**IIIb** with helical chirality.

With a cavity volume of 250 to 400 Å^3 and a wide array of guests encapsulated, structure **IIIa** highlights the potential of metal-ligand assemblies as supramolecular host systems. An interesting feature of structure **IIIa** is its inherent chirality even though all building blocks are achiral (Figure 6c). The trivalent binding of the catecholate ligands to the metal center induces a geometry resulting either in the formation of a right-handed (Δ) or left-handed (Λ) helix. Thanks to mechanical coupling between the metal centers only one pair of enantiomers, the ΔΔΔΔ– and the ΛΛΛΛ-structures, is observed. The addition of chiral guest molecules to the racemate allows the chiral resolution and subsequently the isolation of the enantiopure host.[84] Another approach leading to more stable capsules is the use of chiral ligands dictating which enantiomer is formed.[85] Numerous examples have been reported using the Ga_4L_6 cages as supramolecular catalysts in reactions involving cationic intermediates and transition states. The applications include the acid-catalyzed hydrolysis of orthoesters[86] as well as an aza-COPE electrocyclization of allylenammonium salts[87] within **IIIa**. An example that combines these approaches to realize large rate enhancements with cage **IIIa** is the NAZAROV cyclization (Scheme 6a) of pentamethylcyclopentdiol (**49**): firstly, the required protonation of substrate **49** is favored upon encapsulation and secondly, the cage forms a constrained environment which favors the intramolecular electrocyclization.[88] This synergistic mode of action led to for supramolecular catalysis unprecedented rate enhancements of up to 2.1 million-fold.

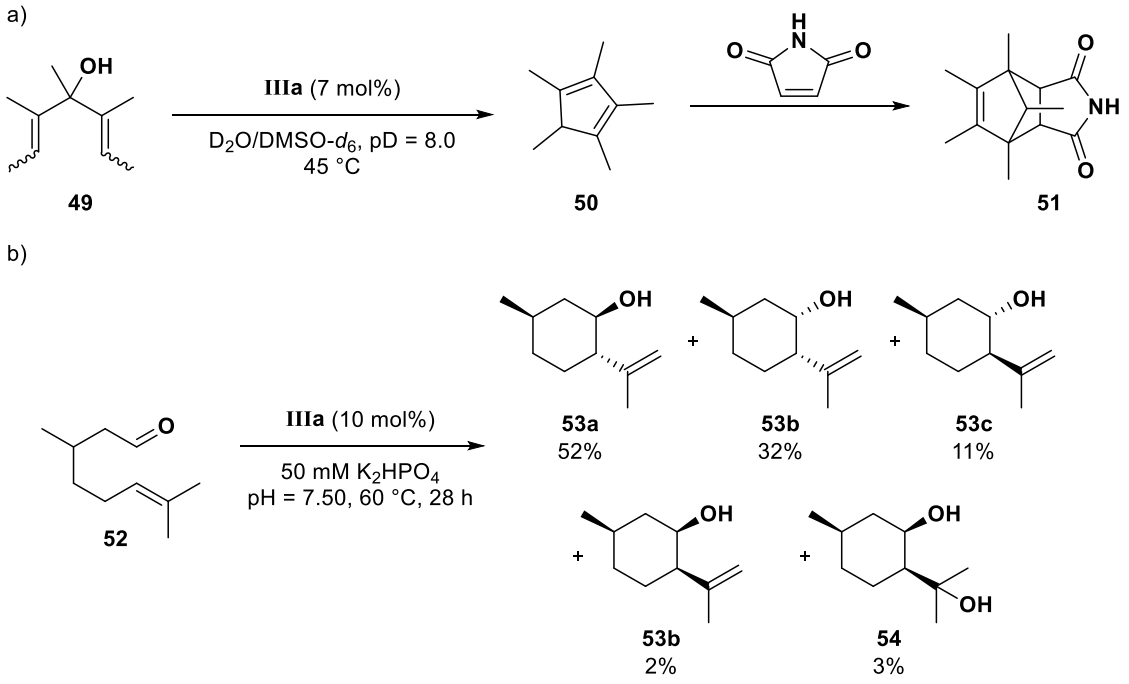

Scheme 6: Applications of **IIIa** in catalysis: a) NAZAROV cyclization followed by DIELS-ALDER reaction of the resulting cyclopentadiene (**50**) b) Terpene cyclization of citronellal (**52**).

Acid-catalyzed reactions with **IIIa** have also been expanded to the PRINS-type cyclization of monoterpenes such as citronellal (**52**) (Scheme 6b).[89] Under acidic conditions **52** usually cyclizes to form diol **54**, whereas in presence of **IIIa** the cyclization is followed by elimination rather than hydration to give the four different diastereomeric products **53a** − **d**. This highlights the effect of the encapsulation within the defined nanoenvironment inside the cavity of **IIIa**. The chiral derivatives **IIIb** of **IIIa** have been successfully employed for chiral discrimination of guest molecules and yielded considerable enantiomeric excess (up to 78% ee) in the aza-COPE rearrangement of enammonium salts **55** (Scheme 7).[90] The efficacy of the chirality transfer from ΔΔΔΔ- **IIIb** onto the substrates was found to be highly dependent on size and shape of the substrate as well as the temperature under which experiments were conducted.

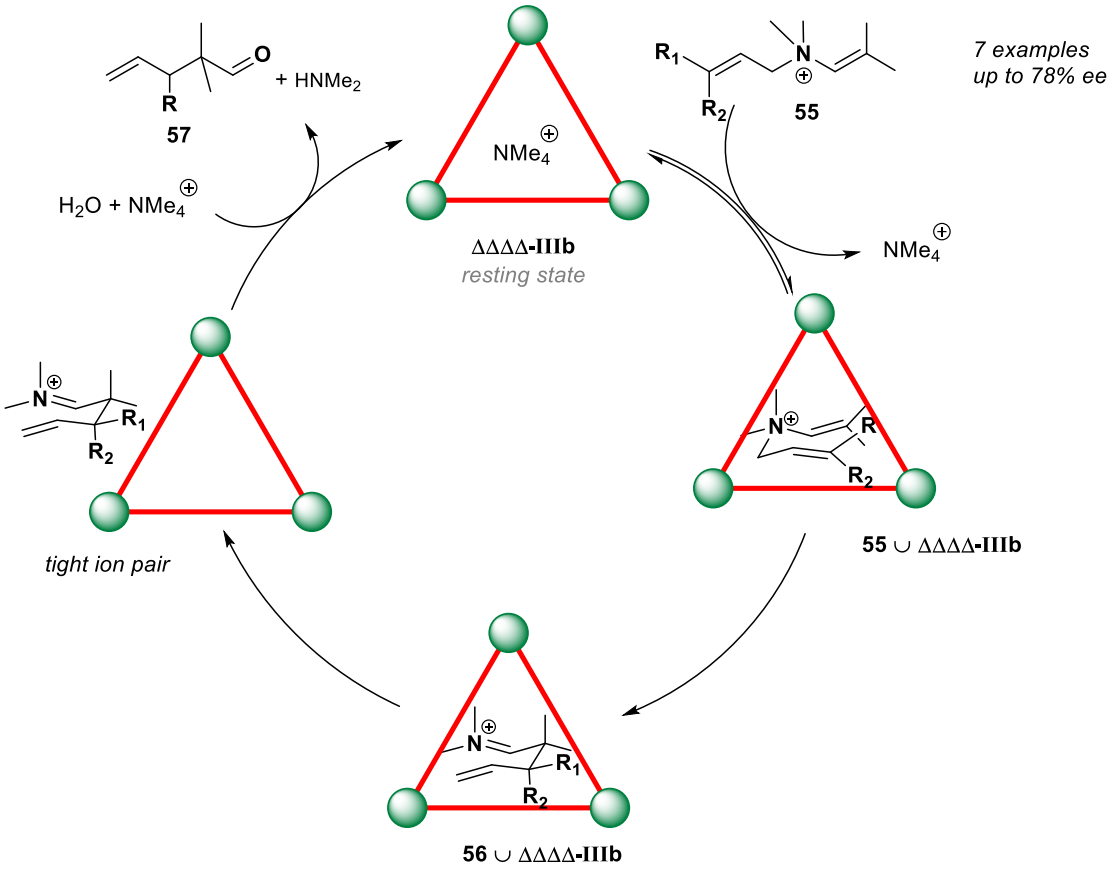

Scheme 7: Chirality induction in the aza-COPE rearrangement of enammonium salts **55** using enantiopure catalyst ΔΔΔΔ-**IIIb**.

Structurally closely related M_4L_6 cages have been reported and applied in catalysis by the NITSCHKE group. Tetrahedral cage **IVa** self-assembles from iron(II) ions and imine ligands formed *in situ* from 4,4'-diaminobiphenyl-2,2'-disulfonic acid and 2-formylpyridine (Scheme 8a).[91] Structure **IVa** features a cavity enclosing 141 Å^3 capable of hosting small

neutral, organic molecules (e.g., cyclohexane) based on the hydrophobic effect in aqueous solution. Its catalytic applications are relatively limited due to the small cavity size which restricts the number of suitable substrates and the acid labile imine ligands. The diminished affinity for cationic guest compared to structure **IVa** is attributed to the lesser overall charge of the assembly and therefore weaker coulombic interactions. The racemic cage can also be accessed in its optically active form **IVb** by employing optically active ligands which also leads to a bigger cavity volume of 418 Å^3 (Scheme 8b).

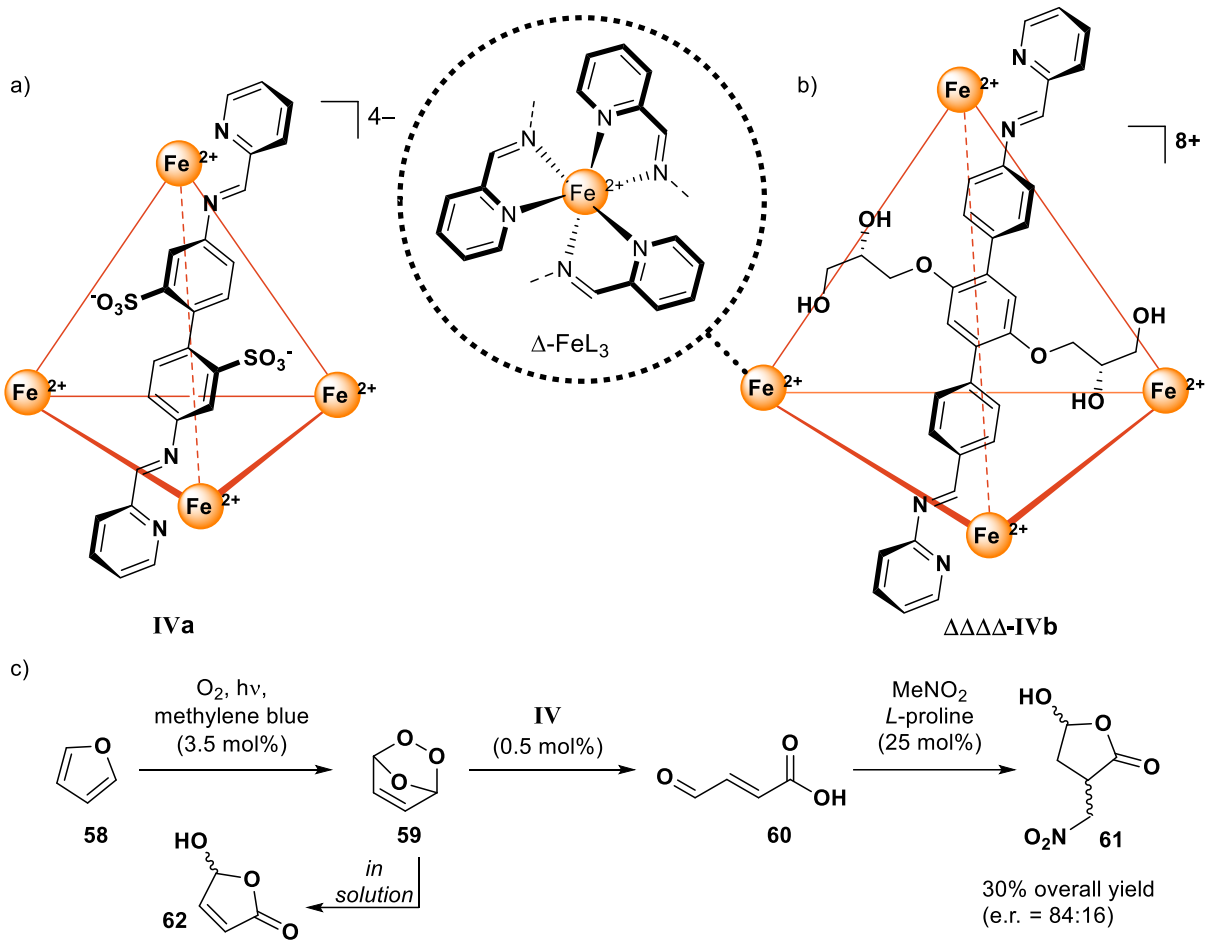

Scheme 8: a) Cage **IVa** reported by NITSCHKE. b) Chiral derivative **IVb**. c) Multicatalytic tandem reaction employing cage **IVa**.

The robust self-assembly process of structure **IVa** tolerating the presence of other catalysts allowed its application in a remarkable multicatalytic tandem reaction.[45] The first step of this sequence involves the formation of the endoperoxide **59** *via* DIELS-ALDER reaction between furan (**58**) and singlet oxygen. **59** is then hydrolyzed by catalyst **IVa** yielding α,β-unsaturated aldehyde **60**, which is then further converted in a 1,4-addition of nitromethane catalyzed by L-

proline to give the final product **61**. In contrast, when structure **IVa** is absent, hydroxyfuranone (**62**) is formed rather than the desired product **61** (Scheme 8c).

Inspired by naturally occurring metalloenzymes REEK employed a promising approach merging supramolecular chemistry with homogenous transition metal catalysis to create a defined nanoenvironment around the metal catalyst. This was achieved using ligands such as porphyrins which feature an additional binding site for an active metal complex.[92] In the case of self-assembled structure **V** three zinc(II) tetraphenylporphyrins (**63**) and a phosphine ligand **64**, which can then bind to a catalytically active [RhH(CO)$_3$] complex, form a supramolecular catalyst (Scheme 9a). Structure **V** was shown to catalyze the hydroformylation of internal alkenes (e.g., **65**) with high regioselectivity induced by the specific environment (Scheme 9c) created by the second coordination sphere around the catalytic center (Scheme 9b).[93] A second generation of catalysts based on bis-(Zn-salphen) phosphoramidite ligands yielded a chiral structure capable of inducing high enantioselectivities in the hydroformylation reaction accessing the enantioenriched aldehydes **66a** and **66b**.[94]

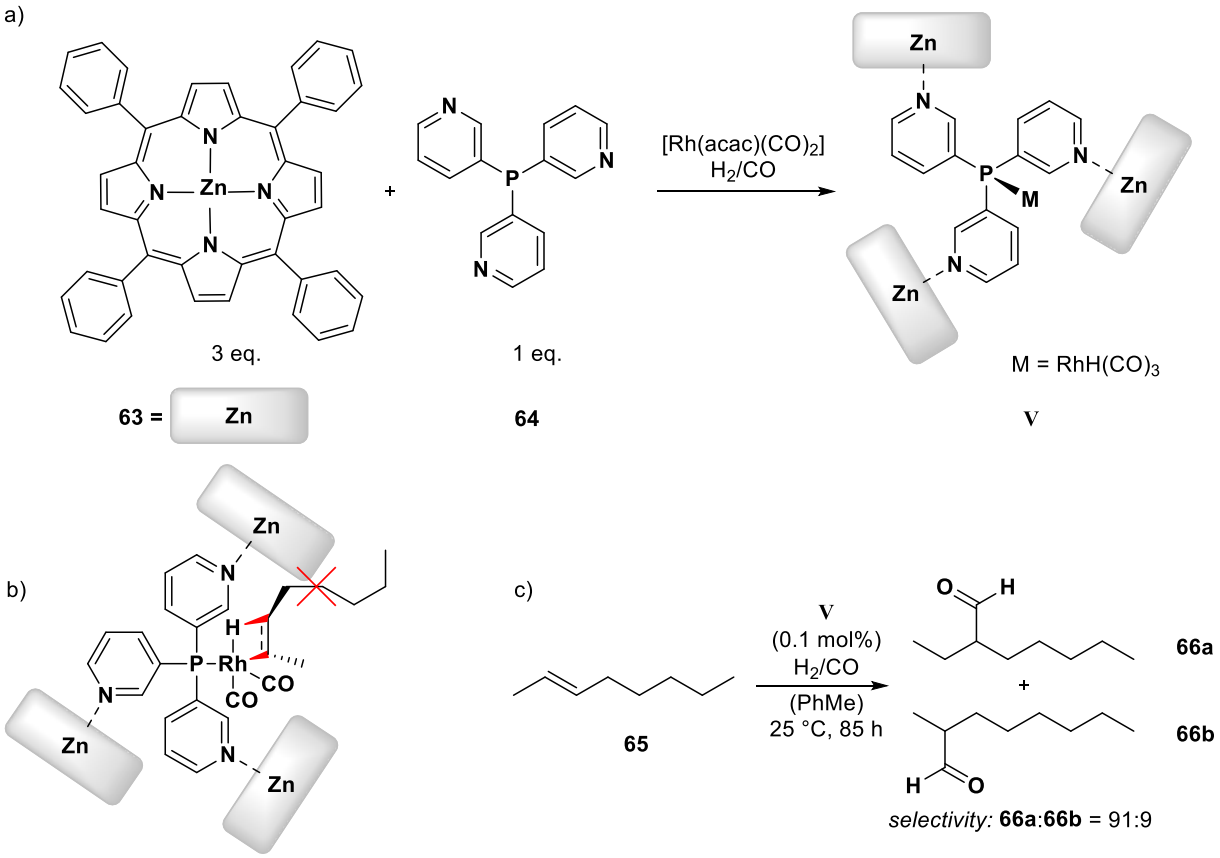

Scheme 9: a) Supramolecular catalyst **V** reported by REEK. b) Catalyst–substrate complex showing the steric hindrance disfavoring the formation of **66b**. c) Regioselective hydroformylation employing catalyst **V**.

1.2.4 Assemblies Based on Hydrogen Bonding

Similar to metal-ligand assemblies, structures self-assembled based on hydrogen bonding have contributed significantly to enzyme mimetic, supramolecular catalysis.[95-99] The total number of structures and especially their size remained quite limited compared to metal-ligand based assemblies. This can be in part assigned to the nature of hydrogen bonding: while in principle a linear binding mode is preferred, large deviations are tolerated and even different binding motives (e.g., bifurcation) are possible. Furthermore, the desired linearity requires a large degree of curvature and preorganization of the individual building blocks. The prediction of hydrogen bond based self-assembly is therefore complicated compared to metal-ligand self-assembly where the binding motives around the metal centre and the angle between the ligands can be simulated quite accurately. For these reasons dimeric systems based on hydrogen bonds are more abundant than multimeric assemblies. Another striking difference to metal-ligand assemblies is the increased dynamic flexibility caused by the weaker binding motif. Guest exchange in hydrogen bonded systems occurs *via* a portal mechanism[100] and partial disassembly rather than *via* diffusion through the openings of the assembly observed in metal-ligand assemblies.[83]

One of the earliest examples for hydrogen bond based self-assembly resulting in a discrete, molecular capsule was reported by REBEK. The 'softball'-like structure **VI** was found to assemble in apolar solvents from building block **67** containing two glycouril units connected by a tether (Scheme 10a).[101] The cavity formed has a volume of about 320 $Å^3$ and shows reversible guest encapsulation. Guest binding occurs *via* hydrogen bonding to the capsule walls or alternatively by van der Waals interactions in the case of hydrophobic guests (e.g., adamantane). The process of encapsulation is additionally entropy driven when two solvent molecules are expelled from the cavity upon encapsulation of a single guest molecule. A consecutive study utilizing structure **VI** and other dimeric assemblies based on similar building blocks found that the guest encapsulation is highly dependent on host and guest volume. The ideal packing coefficient was found to be 0.55, with higher values (up to 0.7) possible when strong intermolecular forces (e.g., hydrogen bonds) play a role.[102]

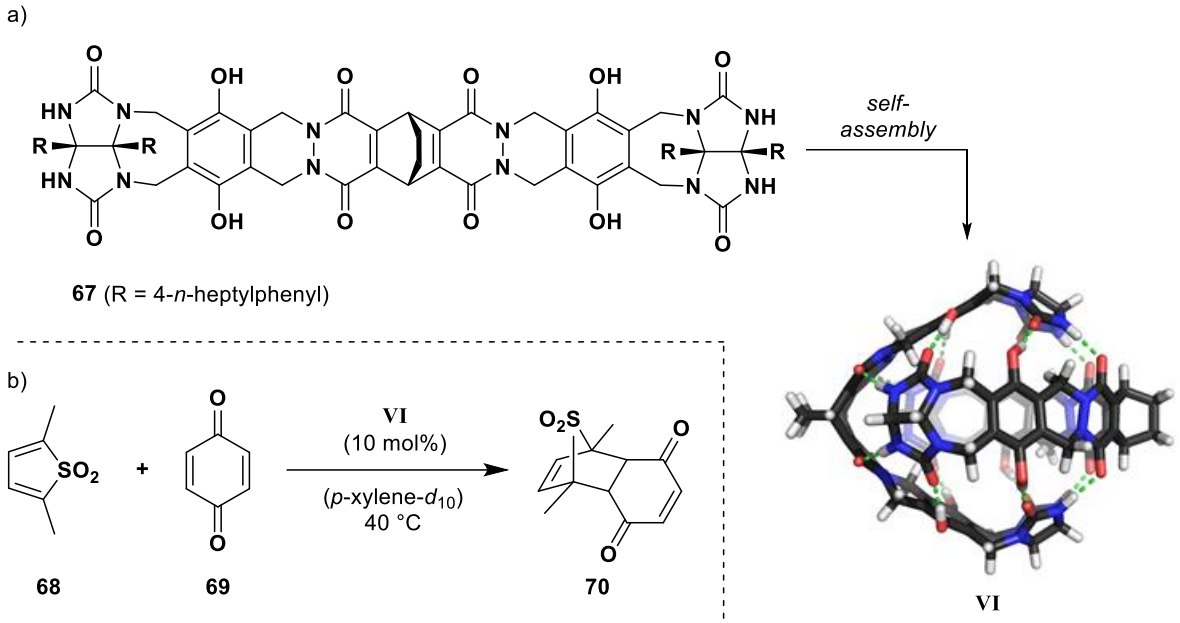

Scheme 10: a) Self-assembly of 'softball'-capsule **VI**. b) DIELS-ALDER reaction catalyzed within **VI** forming **70**.

With the 'softball'-capsule **VI** able to encapsulate multiple solvent molecules such as xylene, it was further investigated concerning its catalytic abilities in bimolecular reactions. In a proof-of-concept study it was found that 10 mol% of **VI** accelerate the DIELS-ALDER reaction between thiophene **68** and *p*-benzoquinone (**69**) by a factor of 10 compared to the bulk solution (Scheme 10b).[103] Due to the simultaneous encapsulation of the reaction partners, the local concentration is increased which leads to the rate enhancement. Other dienes showed significantly higher rate accelerations but suffered from severe product inhibition. A similar concept was applied in another study by the REBEK group utilizing the dimeric structure **VII** (Scheme 11a) for a 1,3-dipolar cycloaddition reaction between phenyl azide (**72**) and phenylacetylene (**73**) (Scheme 11b).[104] While in bulk solution the 1,2- and the 1,4-adducts are obtained in almost equal quantities, the encapsulation of the reaction partners favours the 1,4-regioisomer. The orientation of the two polar functionalities near the seam of hydrogen bonds dictates the regioselectivity. Although high rate accelerations were observed the reaction suffers again from severe product inhibition. This highlights a general problem of catalyzing bimolecular reactions, where transition state and final product are very similar and are therefore competing for binding within the supramolecular catalyst structure. Strategies to circumvent this problem include the *in situ* conversion of the product to a species with a lower binding affinity or modification of the substrate.

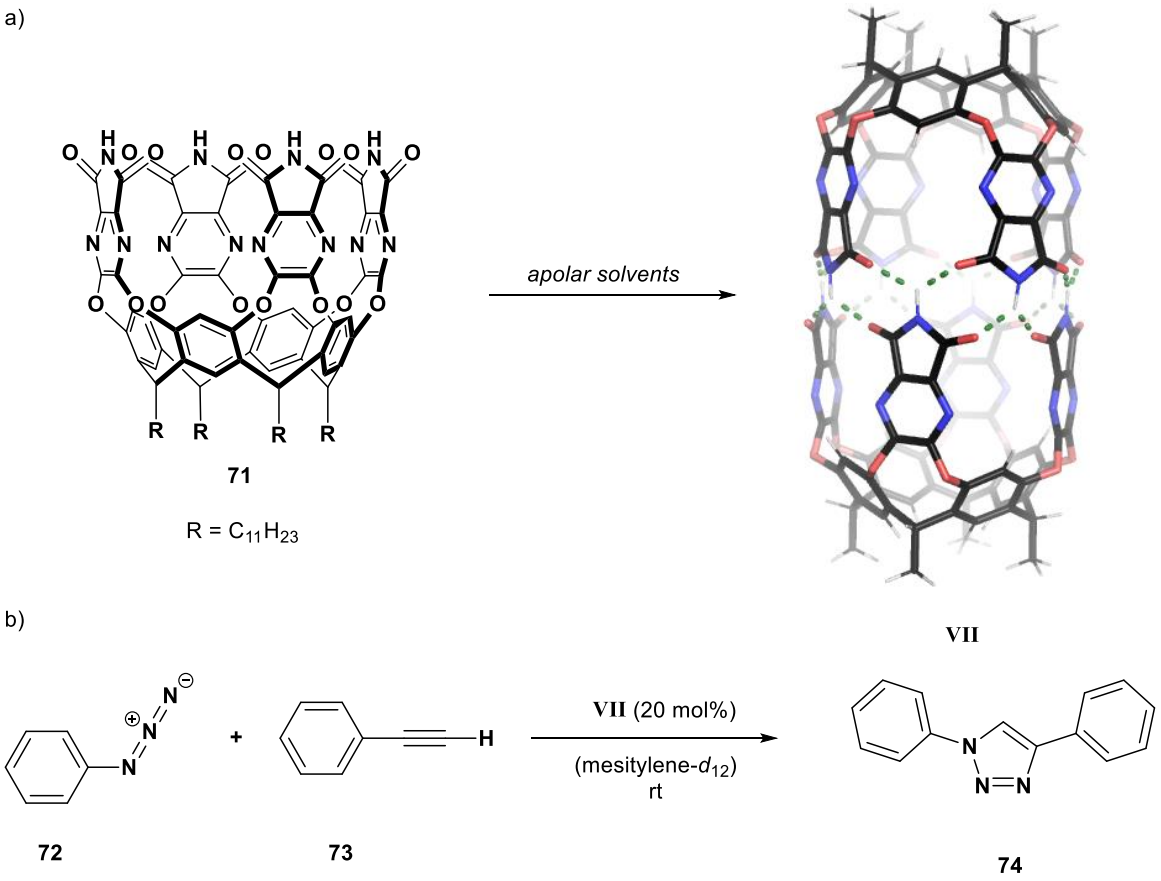

Scheme 11: a) Formation of dimer **VII** form building block **71**. b) Regioselective 1,3-dipolar cycloaddition yielding **74** catalyzed by **VII**.

A multitude of dimeric hydrogen bonded systems has been developed and applied in guest binding and catalysis. Among them are several examples forming such strong hydrogen bond networks that even competing solvents such as water or DMSO are tolerated, as long as there is a suitable guest present templating the assembly. REBEK for instance reported the formation of structure **VIII** based on the dimerization of macrocycle **75** in the presence of hydrophobic guest molecules (e. g., stilbene **76**, Scheme 12a).[65] Similar observations were reported by SZUMNA showcasing the templating effect of C_{60} to assemble structure **IX** from modified resorcinarene macrocycles **77** with polar amino acids attached at the upper rim (Scheme 12b).[105]

While dimeric systems based on hydrogen bonding represent an important development in supramolecular chemistry, their relatively small size limits their application in catalysis to some degree. Since larger building blocks often require more synthetic effort, multimeric assemblies represent an attractive alternative to form larger, molecular capsules.

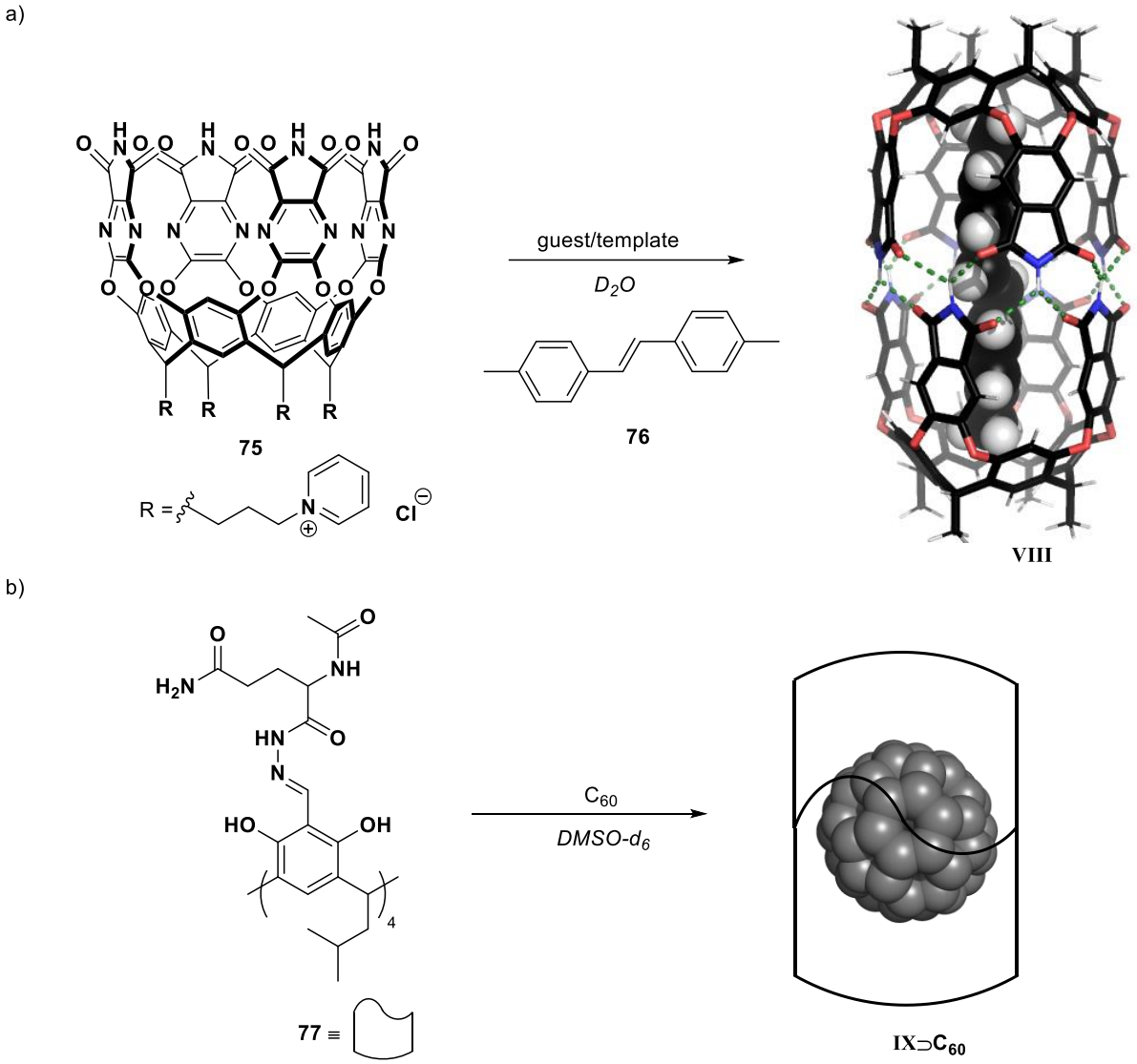

Scheme 12: a) Templated self-assembly of **VIII** in water. Feet were omitted for clarity. b) Self-assembly of dimer **IX** in DMSO in presence of C_{60}.

This particular research area was kickstarted by the report of a hexameric assembly in 1997 by ATWOOD and MACGILLIVRAY based on the C-methyl resorcinarene macrocycle **46a** in the solid state.[106] The resorcinarene hexamer **X** self-assembles *via* 60 hydrogen bonds and incorporates eight water molecules at each corner of the cube-like structure (Scheme 13a). The cavity volume was determined to be 1400 Å^3. Shortly after, MATTAY and coworkers reported the hexameric crystal structure of the closely related C-*iso*-butyl pyrogallolarene macrocycle **47a** (Scheme 13b).[107] Forming a completely saturated hydrogen bond network due to the additional hydroxy groups, the pyrogallolarene hexamer **XI** self-assembles *via* 72 hydrogen bonds under exclusion of water. Ensuing studies, most notably by REBEK and COHEN, indicated that the reported solid-state structures are also present in solution when lipophilic derivatives of resorcinarene and pyrogallolarene with longer alkyl 'feet' (residues denoted with R in Scheme

13) are dissolved in apolar, organic solvents.[108-110] The ease of synthetic availability of the building blocks add to the attractiveness of these systems and their enzyme mimetic properties are subject of ongoing research.

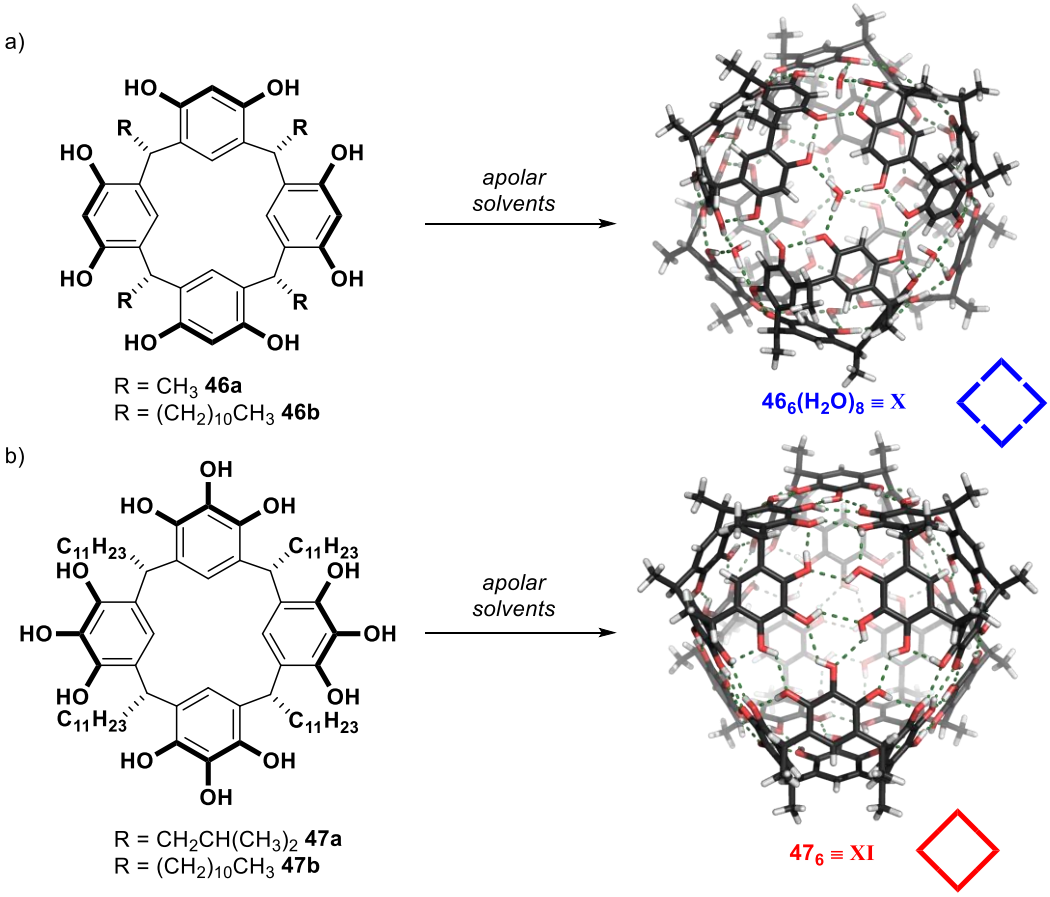

Scheme 13: a) Self-assembly of the resorcinarene hexamer **X** under incorporation of eight water molecules in apolar solvents. b) Self-assembly of the pyrogallolarene hexamer **XI** in apolar solvents. Feet were omitted for clarity. Scheme was partly reproduced from reference[111] with permission of 'American Chemical Society'.

Initially, the hexameric structures **X** and **XI** were investigated concerning their abilities to encapsulate guest molecules in $CDCl_3$. In particular, the resorcinarene hexamer **X** was found to readily encapsulate tetraalkyl ammonium salts and tetraalkyl phosphine salts due to favourable cation-π interactions.[112] The encapsulation of ammonium salts can be easily investigated using ^{1}H-NMR. Interactions with the aromatic moieties of the hexamer **X** cause anisotropy effects which lead to a strong upfield shift of the signals of encapsulated guests compared to 'free' guest molecules. Guest exchange is believed to occur by (partial) disassembly of the hexamer – termed portal mechanism – *via* a pentameric intermediate.[100] If this process is slow on the NMR timescale a second set of signals corresponding to the encapsulated guest is observed in

the upfield region of the NMR spectrum. In general, guest affinity is determined by steric and electronic parameters. While larger guests are often encapsulated at a slower rate, the formed host-guest complex is often more stable. If guest molecules become too large, uptake is no longer observed.

Another valuable tool to study supramolecular systems in solution is DOSY-NMR spectroscopy allowing the determination of diffusion coefficients of multiple species present at the same time. Using this technique COHEN and coworkers were able to show that the hexameric structures **X** and **XI** self-assemble in apolar solvents even in absence of suitable guest molecules.[110] The results indicate that around six solvent molecules of $CDCl_3$ occupy the cavity. By analysing the diffusion coefficient of water in chloroform solutions of **X** and **XI**, the group was furthermore able to determine the amount of water needed to form the respective capsule.[113-114] In case of the pyrogallolarene capsule **XI** the water signal and the corresponding diffusion coefficient was virtually unaffected by the overall water content of the solution indicating that similar to the solid state structure water is not part of the hydrogen bond network. In contrast, the water signal in ^{1}H-NMR spectra of **X** in $CDCl_3$ experiences a significant downfield shift. The magnitude of the shift depends on the total amount of water present in solution. Due to fast exchange on the NMR time scale between water being part of the hexamer and 'free' water, a low overall water content leads to a strong shift, whereas a high water content means more 'free' water and results in a smaller shift. A similar trend was observed for the diffusion coefficient of water in chloroform solutions. If the water content is very low, namely only the eight equivalents necessary to form the resorcinarene hexamer **X**, the diffusion coefficient of water is similar to the value observed for the hexamer, while with increasing water content the diffusion coefficient of water also increases towards the values obtained for 'free' water. The stability of the hexameric structures **X** and **XI** regarding polar media was also investigated using this protocol. Upon titration with competitive solvents such as methanol and DMSO the diffusion coefficient increases, indicating the disassembly of the hexameric structure. Presumably due to its fully saturated hydrogen bond network the pyrogallolarene hexamer **XI** was found to be more stable towards polar solvents compared to hexamer **X**.

Interestingly, the encapsulation behavior of the resorcinarene and the pyrogallolarene hexamers **X** and **XI** differ quite significantly. Hexamer **X** shows affinity for a range of guest molecules including neutral amines,[115] ammonium salts,[112] oxygenated species (i.e., alcohols,[116] carboxylic acids[117] and sugars[117]), metal complexes[118] and radical species.[119] In contrast, the pyrogallolarene hexamer **XI** is able to encapsulate neutral amines[115] but was found to be

incapable of binding ammonium salts in $CDCl_3$. A recent study suggests that while cations are stabilized well within **XI**, the encapsulation of a cationic ammonium salt leads to an unfavorable charge separation with the corresponding anion remaining outside, resulting overall in minute uptake.[120] Hexamer **X** on the other hand stabilizes the complete ion pair within its cavity avoiding the unfavorable charge separation. COHEN and coworkers reported that ammonium salts can be encapsulated in pyrogallolarene hexamer **XI** to some degree when benzene is employed as a solvent.[121] This suggest a high affinity of chloroform solvent molecules for the cavity of **XI**, potentially hindering encapsulation. To circumvent the issue of solvent competition PURSE reported methods to obtain kinetic host-guest complexes by melting[122] or ball-milling[123] host **XI** in the presence of neutral hydrocarbons (e.g., anthracene and pyrene). An explanation for the broader guest range observed for the resorcinarene hexamer **X** compared to the pyrogallolarene hexamer **XI** could be related to the incorporated water molecules. Four of these are not fully saturated within the hydrogen bond network of **X** resulting in potential binding sites based on hydrogen bonds that are lacking in the fully saturated hydrogen bond network of **XI**. The exact requirements for efficient guest uptake in multimeric systems based on hydrogen bonding are still matter of debate though, and recent results show that also assemblies with a fully saturated hydrogen bond network can encapsulate guest molecules (e.g., ammonium salts) to some degree.[124]

The first successful utilization of the resorcinarene capsule **X** in a catalytic context was reported by SCARSO, REEK and coworkers.[125] Capsule **X** readily encapsulates cationic gold complexes with *N*-heterocyclic carbene (NHC) ligands. The encapsulation of the metal catalyst strongly influences the outcome of the catalysis and leads to a change in product distribution.

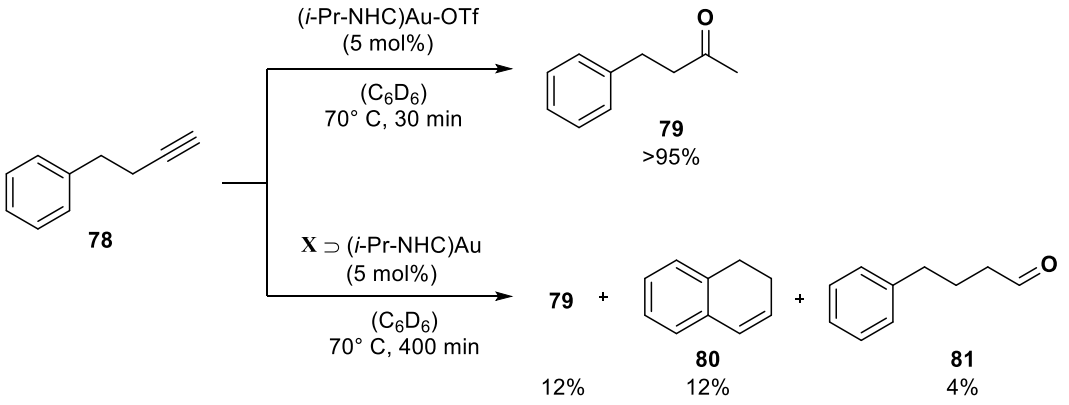

Scheme 14: Regioselective alkyne hydration catalyzed by a gold complex encapsulated within **X**.

While the free catalyst in solution produces mainly the MARKOVNIKOV product **79**, in the presence of the hexamer **X** significant amounts of the *anti*-MARKOVNIKOV product **81** and dihydronaphtalene (**80**) are observed (Scheme 14).[126] This is believed to be a direct consequence of the confined space available within the cavity. However, the encapsulation of the catalyst also causes a significant rate reduction. The influence of size and shape effects was demonstrated by an ensuing study using competition experiments with substrates with varying bulkiness and flexibility.[127] Indeed, significant changes in selectivity were observed compared to solution chemistry, which is governed rather by electronic requirements. Using a dinuclear gold complex that is split into monomers and thereby deactivated by encapsulation within **X**, REEK and coworkers were able to realize a switchable catalyst system. Reactivity of the dinuclear complex can be restored by adding a competitive guest and expelling the mononuclear complex from capsule **X**.[128] Similar results for a switchable catalyst system by encapsulation were obtained for a $[Ru(bpy)_3]^{+2}$ photocatalyst utilized for aerobic oxidation of aliphatic sulfides.[129]

In 2013, SCARSO and STRUKUL reported that hexamer **X** efficiently catalyzes the hydrolysis of nitriles **82** *via* protonation of the substrate and subsequent attack of a water molecule leading to formylamides **83** (Scheme 15a).[130]

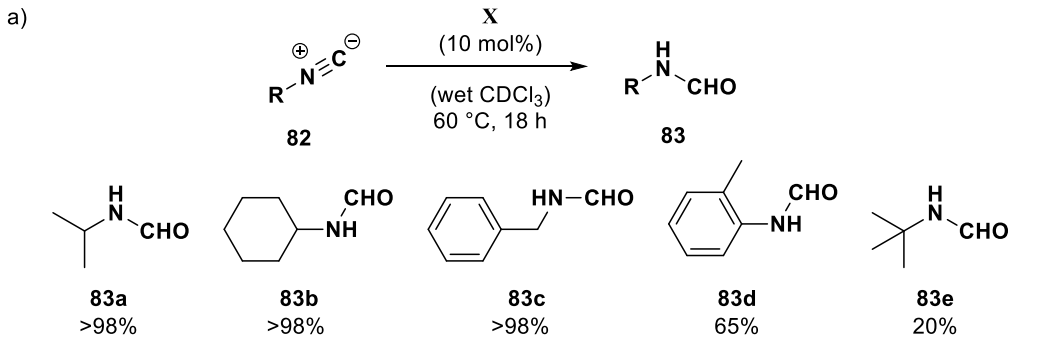

b)

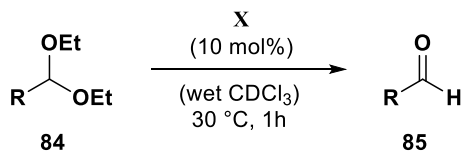

acetal	conversion (60 min)	acetal	conversion (60 min)
84a (R = CH_3)	85%	**84e** (R = n-C_5H_{11})	30%
84b (R = n-C_2H_5)	86%	**84f** (R = n-C_7H_{15})	13%
84c (R = n-C_3H_7)	62%	**84g** (R = n-$C_{11}H_{23}$)	3.4%
84d (R = n-C_4H_9)	44%	**84a** + Bu_4NBr	1%

Scheme 15: a) Hydrolysis of nitriles **82** catalyzed by hexamer **X**. b) Size-selective acetal hydrolysis catalyzed by **X**.

This report was followed by a study from the TIEFENBACHER group concerning the hydrolysis of acetals **84** to aldehydes **85** with a good substrate selectivity concerning size (Scheme 15b).[131] Detailed NMR investigations indicated that the hexameric resorcinarene capsule **X** has an unexpectedly low pK_a of 5 – 6 and is indeed acting as a BRØNSTED acid in these transformations. A later study by the same group showed that the acetal hydrolysis actually requires traces of external acid (HCl).[132] Regardless, these early results led to a number of follow-up reports utilizing the resorcinarene hexamer **X** in catalysis. The favorable encapsulation properties of nitriles for instance were exploited for a [3+2] cycloaddition with trimethylsilyl azides to construct a series of 1*H*-tetrazoles.[133] A similar approach was utilized for the catalysis of a 1,3-dipolar addition of electron-poor alkenes (i.e., **86**) and diazoacetate ester **87** forming 4,5-dihydro-1*H*-pyrazoles **88** (Scheme 16).[134] The reaction displayed modest substrate selectivity for smaller substrates and enabled the transformations of substrate combinations that were unreactive in bulk solution. The rate enhancement and activation of substrates likely stems from interactions with the electron-rich cavity and the increased effective concentration inside **X**.

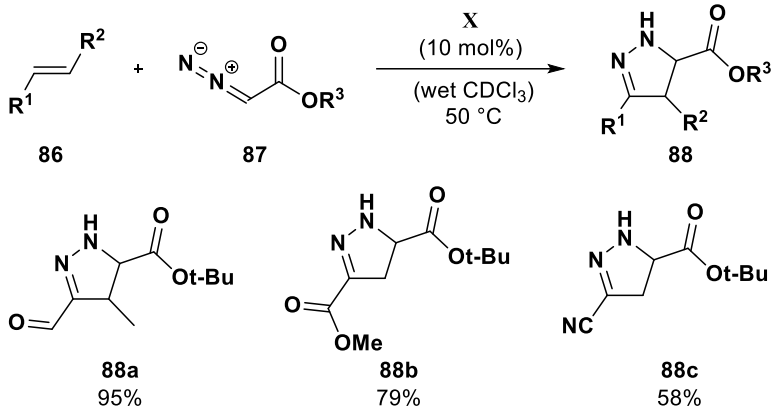

Scheme 16: 1,3-dipolar addition between electron-poor alkenes **86** and diazoacetate esters **87** forming 4,5-dihydro-1*H*-pyrazoles **88** catalyzed by resorcinarene hexamer **X**.

The ability of hexamer **X** to stabilize positively charged intermediates has been utilized for a number of acid-catalyzed reactions including an intramolecular hydroalkoxylation,[135] a cyclodehydration-rearrangement cascade,[136] the hydration of alkynes with HBF_4[137] or the isomerization of epoxides.[138] Of significant importance are the reports by TIEFENBACHER and coworkers demonstrating that the resorcinarene capsule **X** is able to mimic terpene cyclases and effectively catalyzes the cyclization of monoterpenes in a tail-to-head fashion.[15, 139] Due to the cationic intermediates involved, THT cyclizations in bulk solution often suffer from premature attacks of nucleophiles (e.g., water) resulting in acyclic side products. The resorcinarene hexamer **X** in contrast, was shown to activate monoterpenes such as nerol (**21**) or geranyl

acetate (**27**) and induce the formation of cyclic terpenes under mild conditions. The cyclization of nerol (**21**) for instance in presence of 10 mol% of **X** and 3 mol% HCl at 30 °C yields eucalyptol (**13**) in 39 % yield as the major product among other cyclic monoterpenes (Scheme 17a). The reaction proceeds *via* the α-terpinyl cation (**6**) which reacts with the previously cleaved leaving group to form α-terpineol (**12**) and subsequent hydroalkoxylation (Scheme 17c). To prevent the quenching of the intermediate cation **6** acetate was introduced as a less nucleophilic leaving group. Indeed, geranyl acetate (**27**) reacts under the same conditions to form selectively α-terpinene (**9**) in good selectivity and up to 40% yield (Scheme 17b).

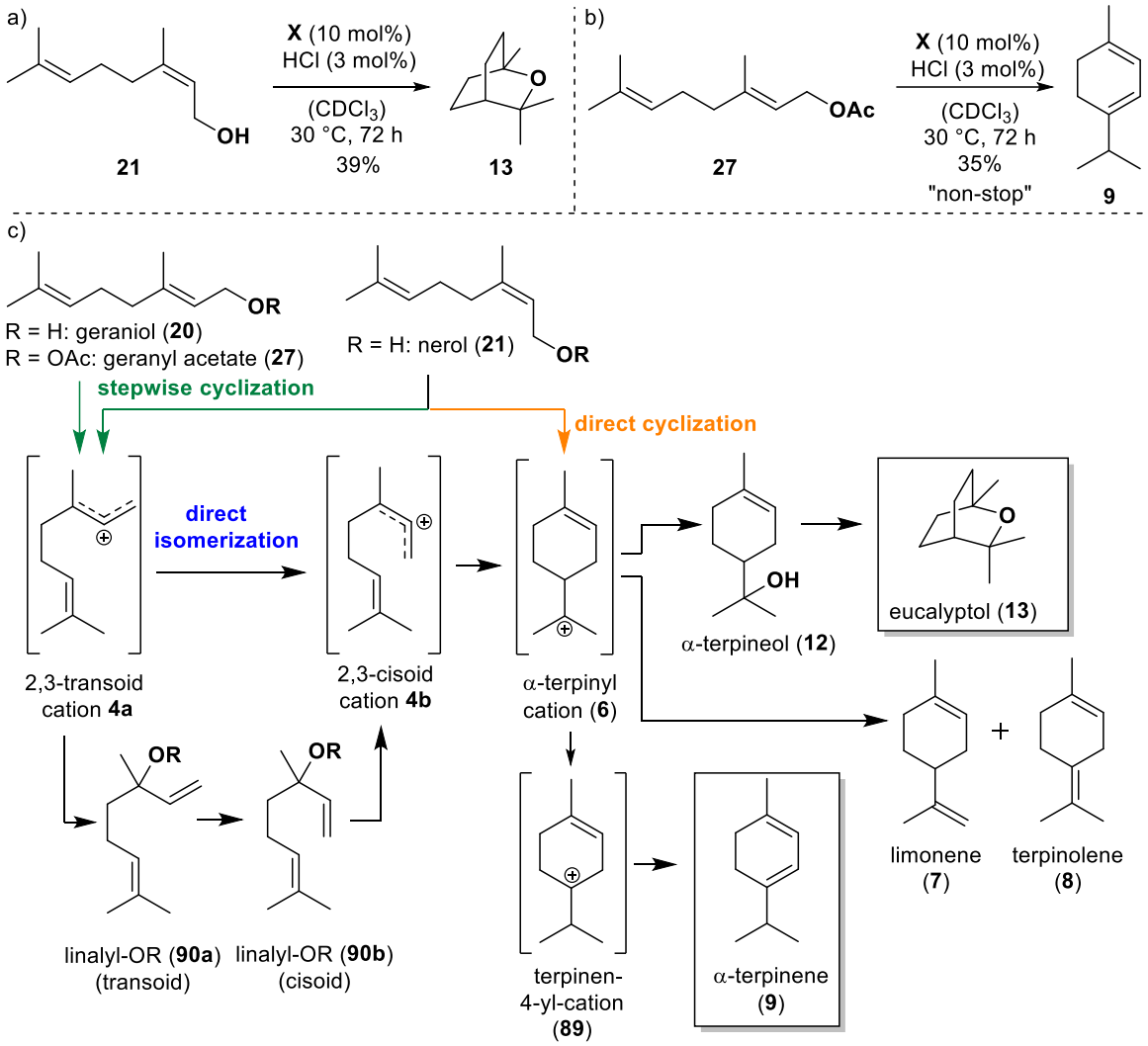

Scheme 17: a) Cyclization of nerol (**21**) forming eucalyptol (**13**) as the major product. b) Cyclization of geranyl acetate (**27**) forming α-terpinene (**9**) as the major product. c) Substrate dependent reaction pathways of the THT cyclization catalyzed by capsule **X**.

The absence of any intermediates also observed for the cyclization of geraniol (**20**) indicates a true non-stop cyclization mechanism likely involving the formation of cation **89** *via* 1,2-hydride

shift from intermediate **6**. The hexameric structure **X** stabilizes the cationic intermediates *via* cation-π interactions and protects them from outside nucleophiles, although especially in case of geranyl acetate (**27**) some alkylation of the capsule **X** was observed. Interestingly, the results obtained for the cyclization of geranyl acetate (**27**) in a non-stop fashion also implied the feasibility of the direct isomerization from the *transoid* cation **4a** to the *cisoid* cation **4b,** rather than *via* the linalyl derivatives **90a** and **90b**. This pathway had previously been considered unlikely in the context of terpene biosynthesis. Detailed kinetic analysis led to a proposal for the catalytic cycle (Scheme 18). Crucial steps for efficient catalysis within hexamer **X** are: 1) encapsulation of the substrate; 2) protonation of the encapsulated substrate, 3) cleavage of the leaving group (rate determining step) and stabilization of the resulting ion pair within the cavity.

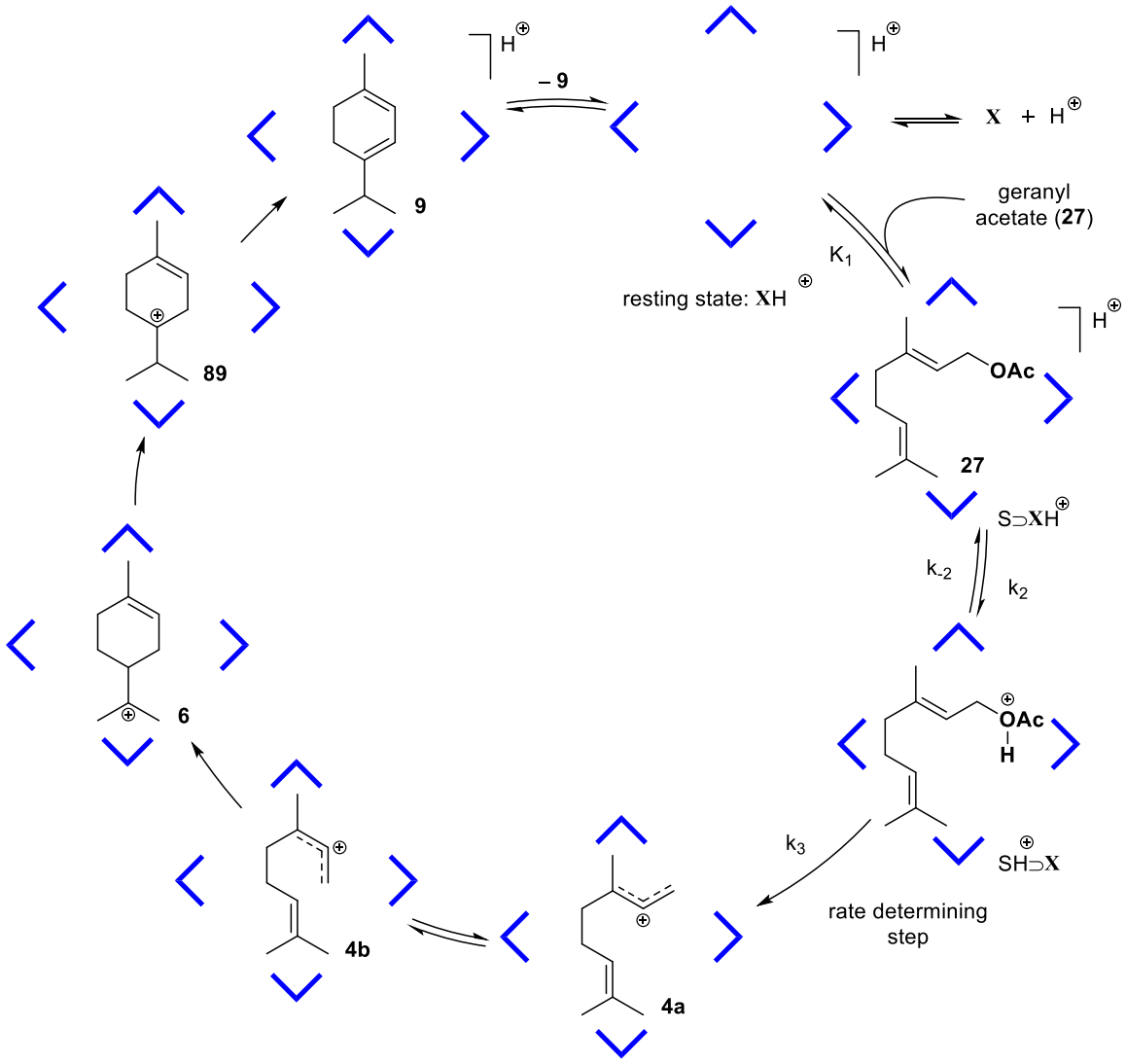

Scheme 18: Proposed mechanistic cycle for the acid-catalyzed cyclization of geranyl acetate (**27**) within the resorcinarene capsule **X**. The scheme is reproduced in slightly modified form from reference[139] with permission from 'American Chemical Society'.

The ability of **X** to catalyze the cyclization of terpenes in a tail-to-head fashion has since been utilized also in the context of larger substrates leading to more complex carbon frameworks.[140] Of practical relevance is the total synthesis of isolongifolenone (**91**) in a mere five steps starting from **92** (Scheme 19a).[141] Ketone **92** is transformed into the cyclization substrate cyclofarnesylacetate (**93**) which is then converted in presence of capsule **X** to give isolongifolene (**94**) in 24%. Another interesting application was shown to be the four-step synthesis of (−)-presilphiperfolan-1β-ol (**95**) starting from caryophyllene oxide (**96**) *via* the cyclization precursor **97** (Scheme 19b).[142] The methodology also allowed access to some unnatural analogues. These results highlight the advantages of supramolecular catalysis, simplifying the synthesis of natural products while also providing access to unnatural derivatives.

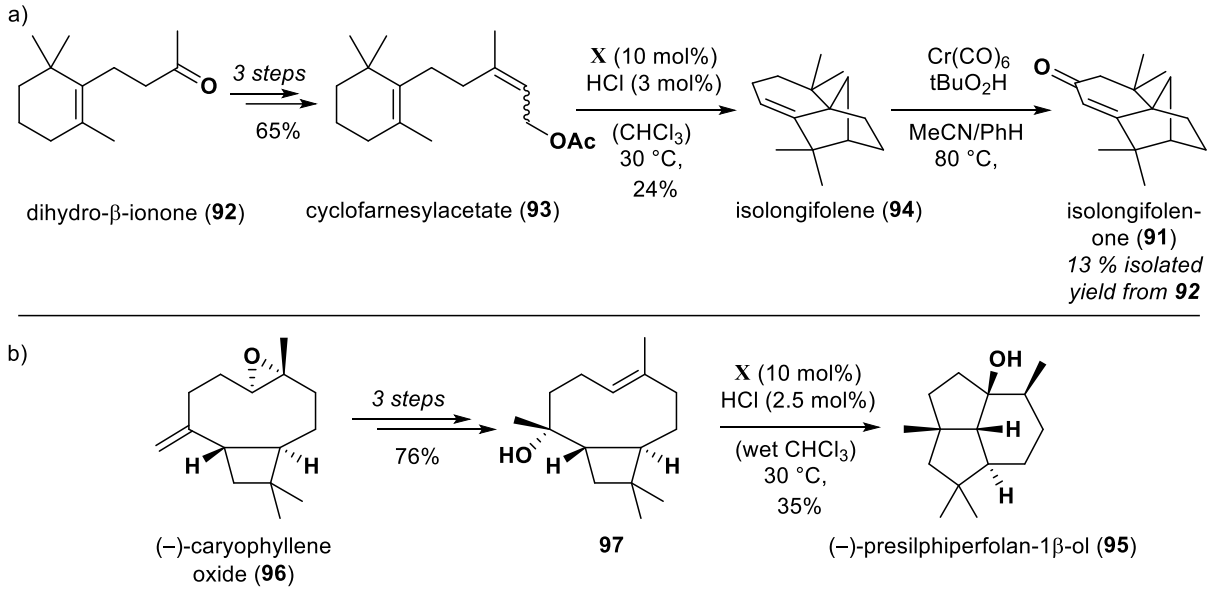

Scheme 19: Total synthesis of isolongifolenone (**91**) including a key step using supramolecular catalysis. b) 4-Step total synthesis of (–)-presilphiperfolan-1β-ol (**95**) starting from caryophyllene oxide (**96**) utilizing capsule **X** for the final cyclization step.

TIEFENBACHER and coworkers also demonstrated the ability of supramolecular structure **X** to modulate the stereochemical outcome of iminium-catalyzed reactions.[143-144] The 1,4-reduction of α,β-unsaturated cinnamaldehyde derivatives **98** catalyzed by chiral proline derivatives was found to be more enantioselective when conducted in presence of **X**, in contrast to bulk solution (Scheme 20a). Upon formation of the iminium ion the intermediate is readily encapsulated within **X** and subsequently attacked by the HANTZSCH ester (**99**) forming aldehyde **100** (Scheme 20b). The complexation inside the cavity not only enhances the reactivity, but also

effectively shields one side forcing the attack from the top side (Scheme 20c) and favouring the (*S*)-product (up to 78% ee). In solution the (*S*)-product (9% ee) is slightly favoured with lower overall yields. This hypothesis is strengthened by experiments using proline derivatives unable to form hydrogen bonds with the capsule walls showing a lower enantiomeric excess.

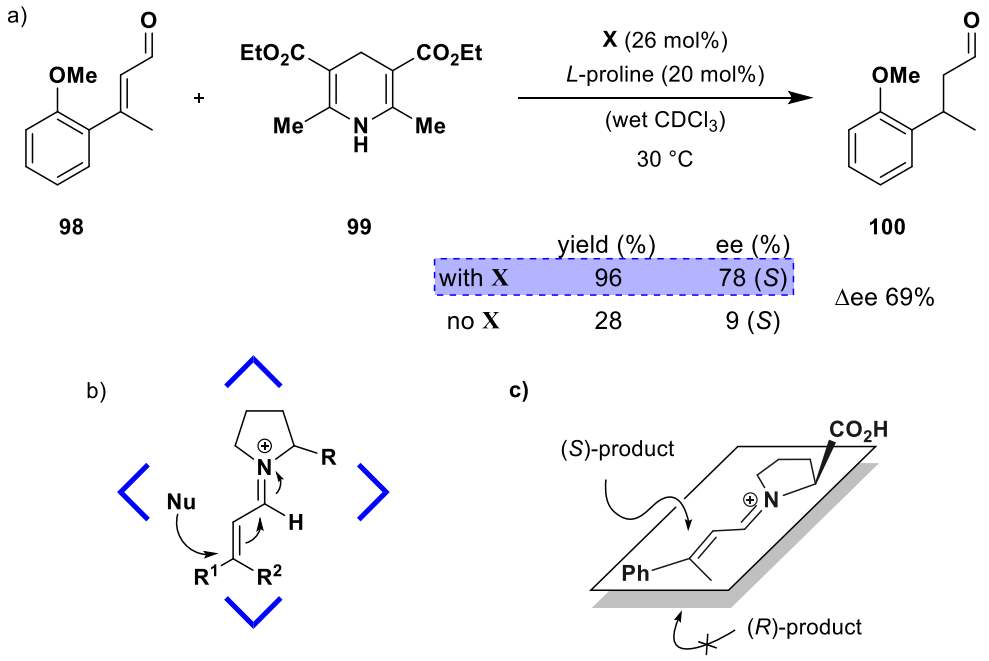

Scheme 20: a) Enantioselective iminium catalysis within hexamer **X**. b) Encapsulation of the reactive iminium species within structure **X**. c) Chiral induction caused by the shielding of the bottom face by the capsule walls. Partly reproduced from reference[144] with permission of 'American Chemical Society'

The resorcinarene hexamer **X** was furthermore found to catalyze an intramolecular carbonyl-olefin metathesis which usually requires strong LEWIS acids (i.e., $FeCl_3$).[145] Several substrates were effectively converted in presence of 10 mol% of host **X** and HCl as a co-catalyst with up to 98% yield, albeit with long reaction times (up to 17 days). NERI and coworkers recently reported the application of **X** as a supramolecular catalyst in acid-catalyzed MICHAEL-type FRIEDEL-CRAFTS reactions[146] using pyrroles and indoles as nucleophiles and a number of variations with different co-catalyst[147] and electrophiles.[148]

The number of applications utilizing hexamer **X** in a catalytic context certainly highlights the importance of hydrogen bonded supramolecular capsules in enzyme mimetic catalysis. However, apart from the related pyrogallolarene capsule **XI**, which was found to be catalytically inactive in several transformations[120] (i.e., THT cyclization, acetal hydrolysis) there is a distinct lack of structures based on hydrogen bonds with comparable size and

complexity. Among the notable exceptions[149] is the chiral octameric capsule **XII** reported by MASTALERZ in 2016 (Scheme 21a).[124] Structure **XII** self-assembles in apolar solvents from enantiopure tris(isatin) **101** forming a cavity with a volume of 2300 Å^3. The racemic building block was found to form ill-defined aggregates rather than a discrete assembly. The assembly is held together by a total of 72 NH−O and CH−O bonds forming a 'closed-shell' hydrogen bond network. Formation of structure **XII** was indicated by DOSY-NMR and additionally by MALDI-TOF mass spectroscopy showing the octameric ions. Cationic guests such as tetraalkylammonium salts, but also neutral molecules (i.e., pyrene) are readily encapsulated by **XII**. Slow exchange on the NMR time scale allowed for determination of in most cases moderate binding constants. Another remarkable example is the enantiopure nanocapsule **XIII** described by STEFANKIEWICZ (Scheme 21b).[150] Based on a simple trisubstituted benzene building block **102** functionalised with amino acids, eight molecules self-assemble *via* 48 hydrogen bonds to form structure **XIII** (V = 1700 Å^3).

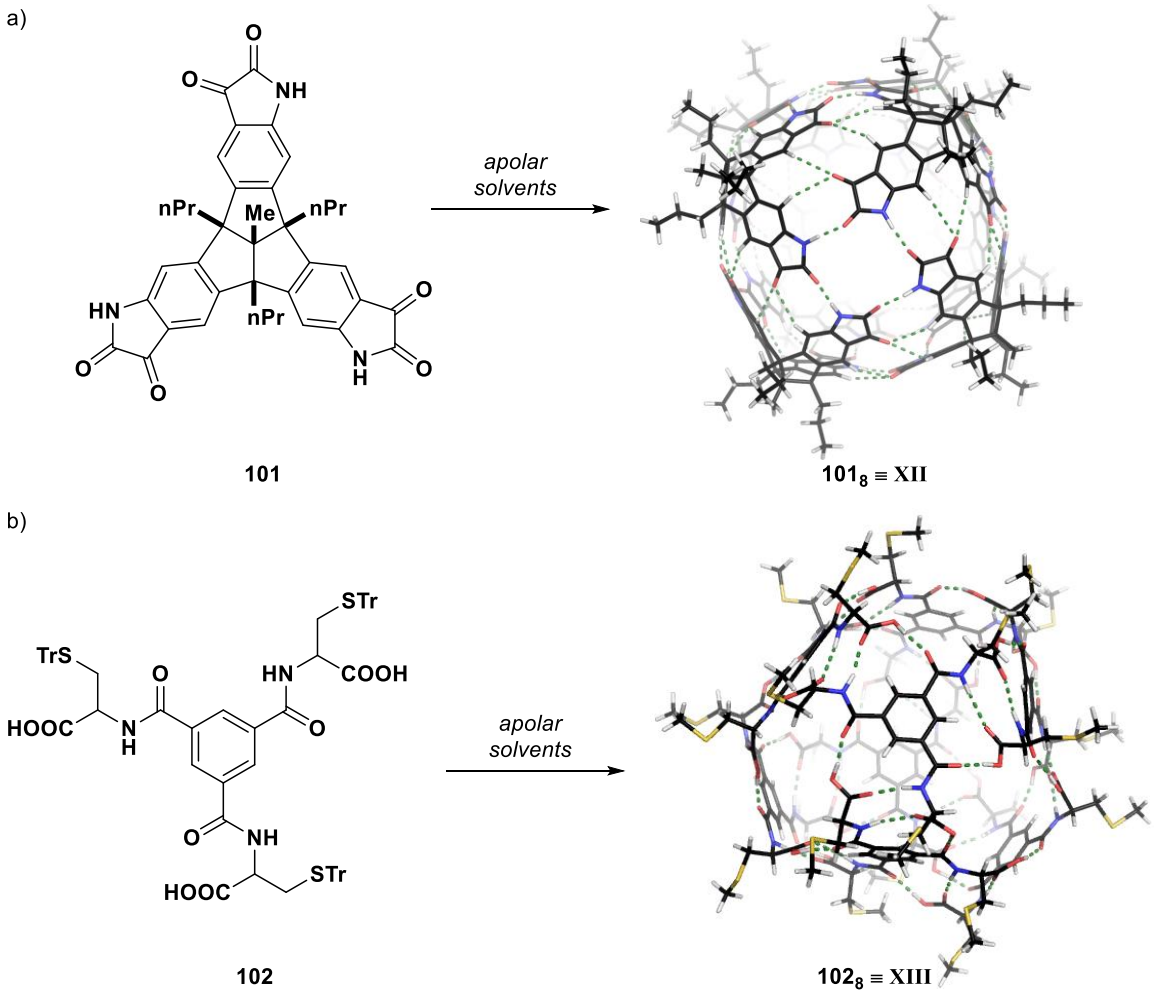

Scheme 21: a) Self-assembly of octameric structure **XII** form enantiopure **101**. b) Formation of chiral, octameric structure **XIII** based on building block **102**.

The capsule was found to be stable at high and low temperatures and tolerates large amounts of base (i.e., NEt_3). Capsule **XIII** selectively encapsulates fullerenes C_{60} and C_{70} with a preference for C_{70}. Interesting is also the case of the pyridinearene **103**, a macrocycle closely resembling resorcinarene **46** with a pyridine moiety instead of a benzene moiety. Synthesis of pyridinearenes **103a** and **103b** is easily achieved by acid-catalyzed condensation of 2,6-dihydroxypyridine and the corresponding aldehyde.[151] Solid state structures showed the formation of head-to-head dimers and also in $CDCl_3$ two species were observed initially assigned to the monomeric and the dimeric species.[152] COHEN and coworkers later revised those results showing with detailed DOSY-NMR studies, that most likely the two species correspond to a dimeric and a hexameric species.[153] In 2019 the solid state structure for a hexameric assembly **XIV** was reported (Scheme 22a).[154] The results of ESI-MS spectroscopy indicated that cationic tris(bipyridine)ruthenium(II) complexes stabilize hexamer **XIV** in the gas phase. In solution it was found that while initially the dimeric species is formed (kinetic product) over time the hexameric species prevails (thermodynamic product). The binding motif is based on the tautomerization of the macrocycle favouring the hydroxy-oxo tautomer (Scheme 22b) forming a relatively simple and highly symmetric hydrogen bond network (24 hydrogen bonds) for hexamer **XIV** (V = 1160 Å^3).

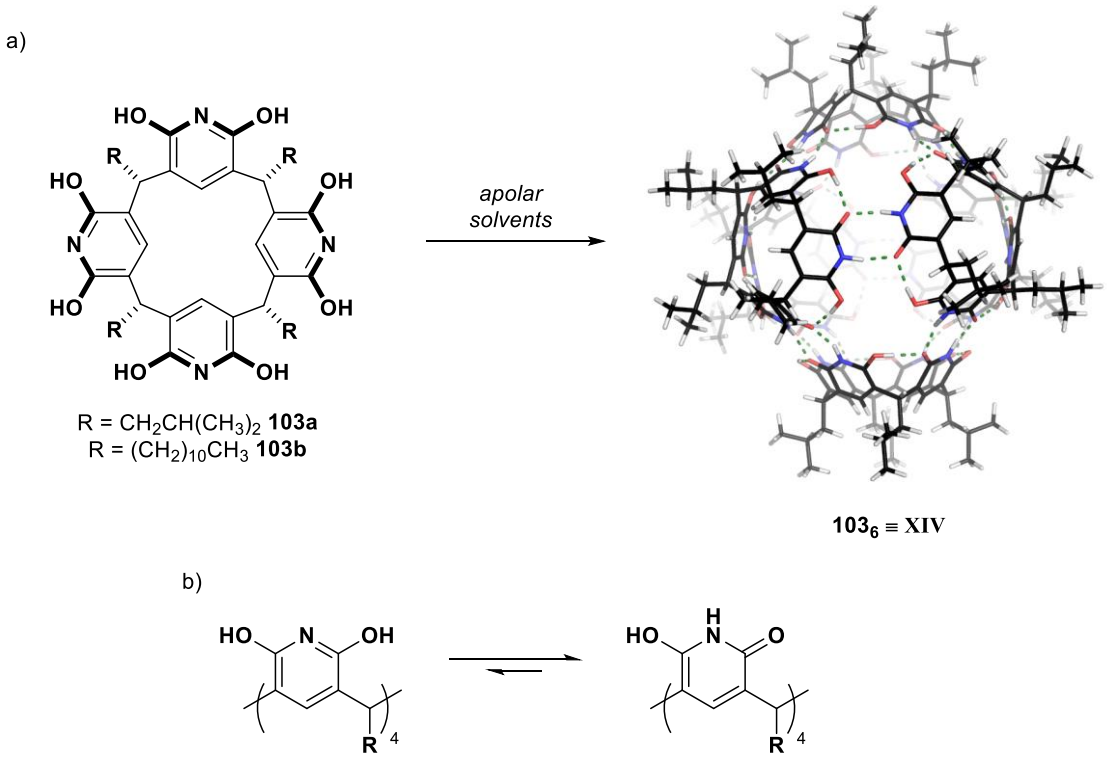

Scheme 22: a) Self-assembly of the pyridinearene hexamer **XIV** (*iso*-butyl feet pictured here). b) Tautomeric forms of pyridinearenes.

1.2.4 Assemblies Based on the Hydrophobic Effect

Supramolecular structures can also be assembled utilizing the hydrophobic effect.[155] A prominent example is the dimeric structure **XV** reported by GIBB (Scheme 23).[156] It is based on the resorcinarene derived deep cavitand **104**, which can be readily synthesized in large quantities. Due to the carboxylic acid moieties cavitand **104** is well soluble in basic, aqueous solution (pH = 10) and is present mainly in its monomeric form. As soon as a suitable guest (e.g., butane) is added as a template, structure **104** forms due to the hydrophobic effect.[157] Dimer **XV** has been applied in photochemical reactions with interesting changes in product selectivity,[158] however catalytic applications have yet to be reported.

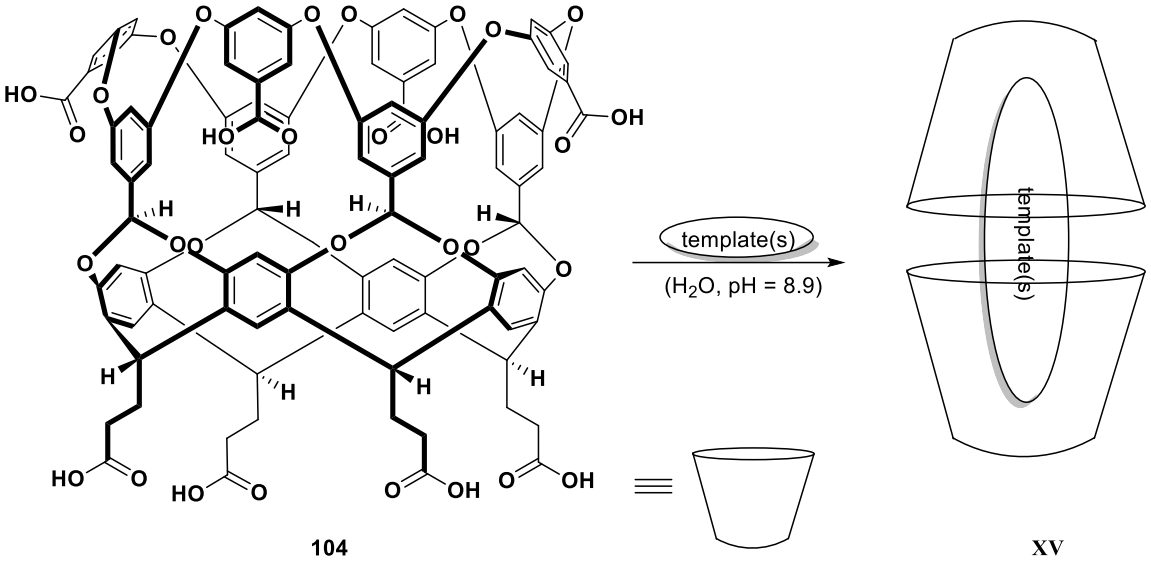

Scheme 23: Templated assembly of dimer **XV** from building block **104** relying on the hydrophobic effect.

Inspired by naturally occurring micelles YOSHIZAWA and coworkers designed micellar capsules composed of bent, polyaromatic frameworks.[76] These π-stacking capsules are aptly named 'aromatic micelles'. The initial study reports the synthesis of amphiphilic building block **105** with two trimethylammonium groups linked to two anthracene panels.[159] **105** was found to assemble in water forming spherical capsules **XVI** with on average five units of **105** and an average core diameter of about 1 nm (Scheme 24a). Ensuing reports demonstrated that similar capsules can be formed modulating either the anthracene panels or the hydrophilic part of the molecule.[160-161] Capsule **XVI** was found to encapsulate a variety of hydrophobic aromatic molecules (e.g., fluorescent dyes, fullerenes, nanographenes) based on the hydrophobic effect and favourable π–π-stacking.[162] Additionally, it was found that capsule **XVI** incorporates

various metal-complexes[163] among them manganese tetraphenylporphyrins (Scheme 24b) that are otherwise insoluble in water.[164] Such a 1:1 host-guest complex with a perfluorinated derivative (MnPrF) of the manganese complex was utilized for the catalytic epoxidation of 2-chlorostyrene **106** forming the corresponding epoxide **107** in 81% yield (Scheme 24c).

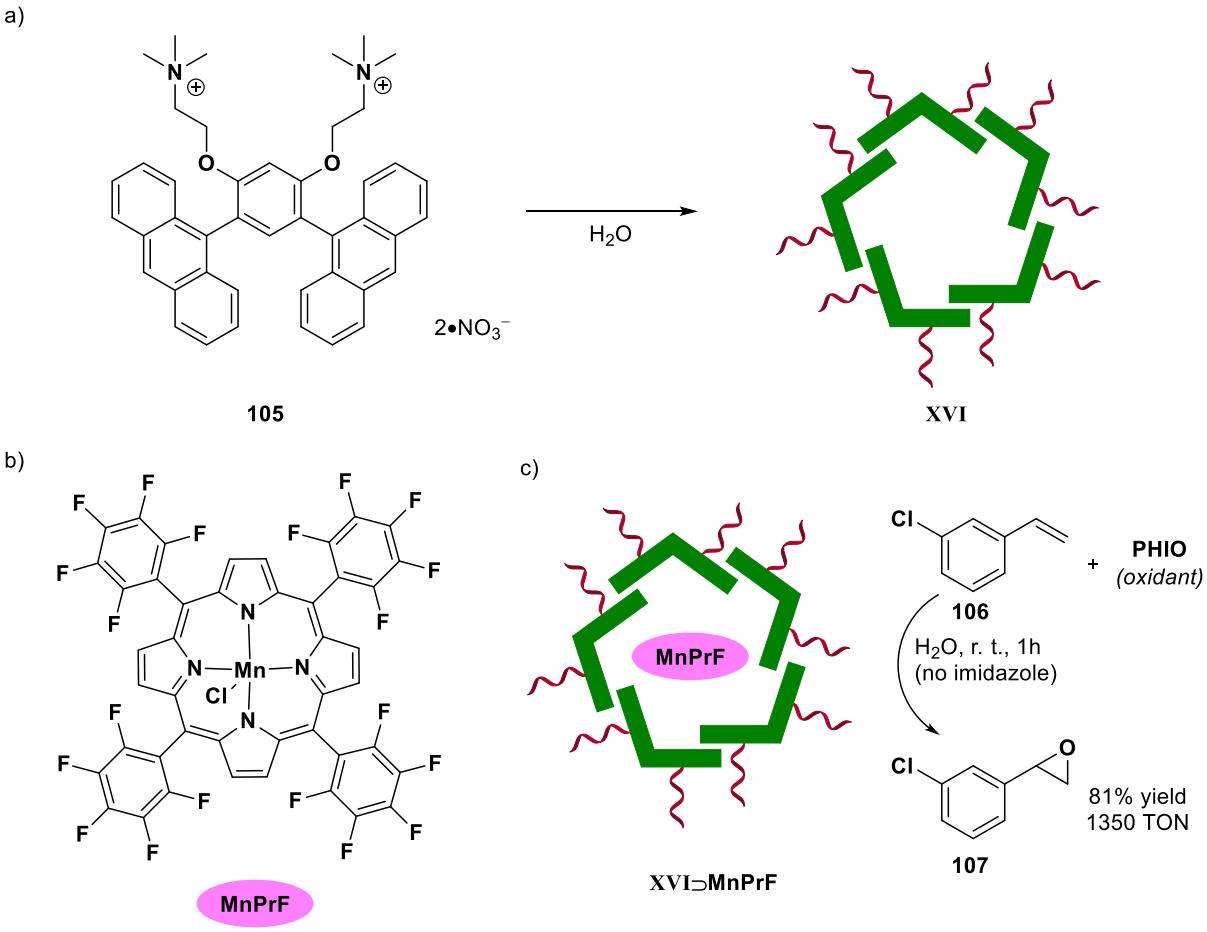

Scheme 24: a) Formation of micellar capsule **XVI**. b) Manganese complex **MnPrF**. c) Catalytic epoxidation using a **MnPrF** complex encapsulated by **XVI**.

Another modification of the initial building block such as the substitution with acridine panels **108** allows the formation of stimuli responsive (pH-value) capsules (Scheme 25a).[165] Photoresponsive guest encapsulation was achieved by using derivatives **109** with *ortho*-dianthrylbenzene units (Scheme 25b).[166] While under normal conditions π-stacking capsules and the corresponding host-guest complexes are formed, the irradiation with light leads to a structural conversion of building block **109** and thereby to disassembly and guest release. Regeneration can be achieved either by photoirradiation or heating.

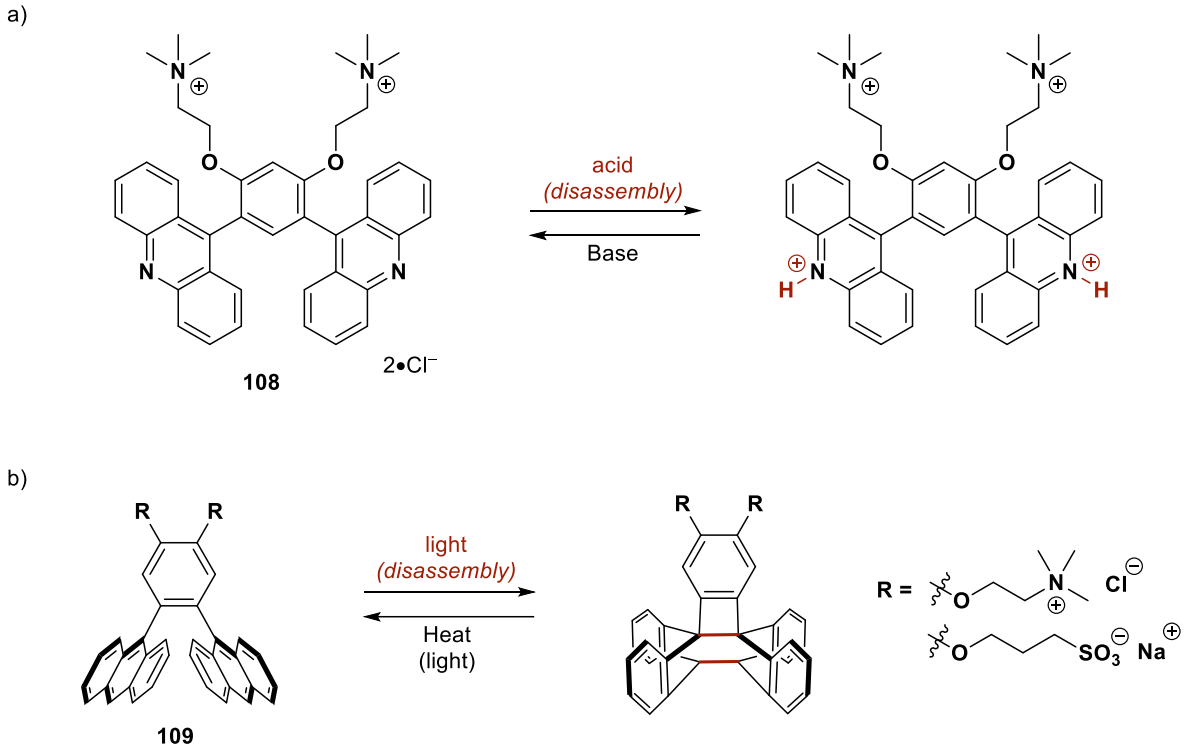

Scheme 25: a) Building block **108** forming pH-responsive capsules, b) Building block **109** forming photoresponsive capsules.

1.2.5 Assemblies Based on Halogen Bonding

In recent years the interest in halogen bonding as a means to construct discrete, molecular assemblies has increased. Halogen bonding relies on the interaction between a halide and a usually LEWIS basic acceptor.[167] Covalently bonded halides are known to have an anisotropic charge distribution with a local electron deficiency opposite to the covalent bond which is often referred to as σ-hole and can interact with a halogen bond acceptor.

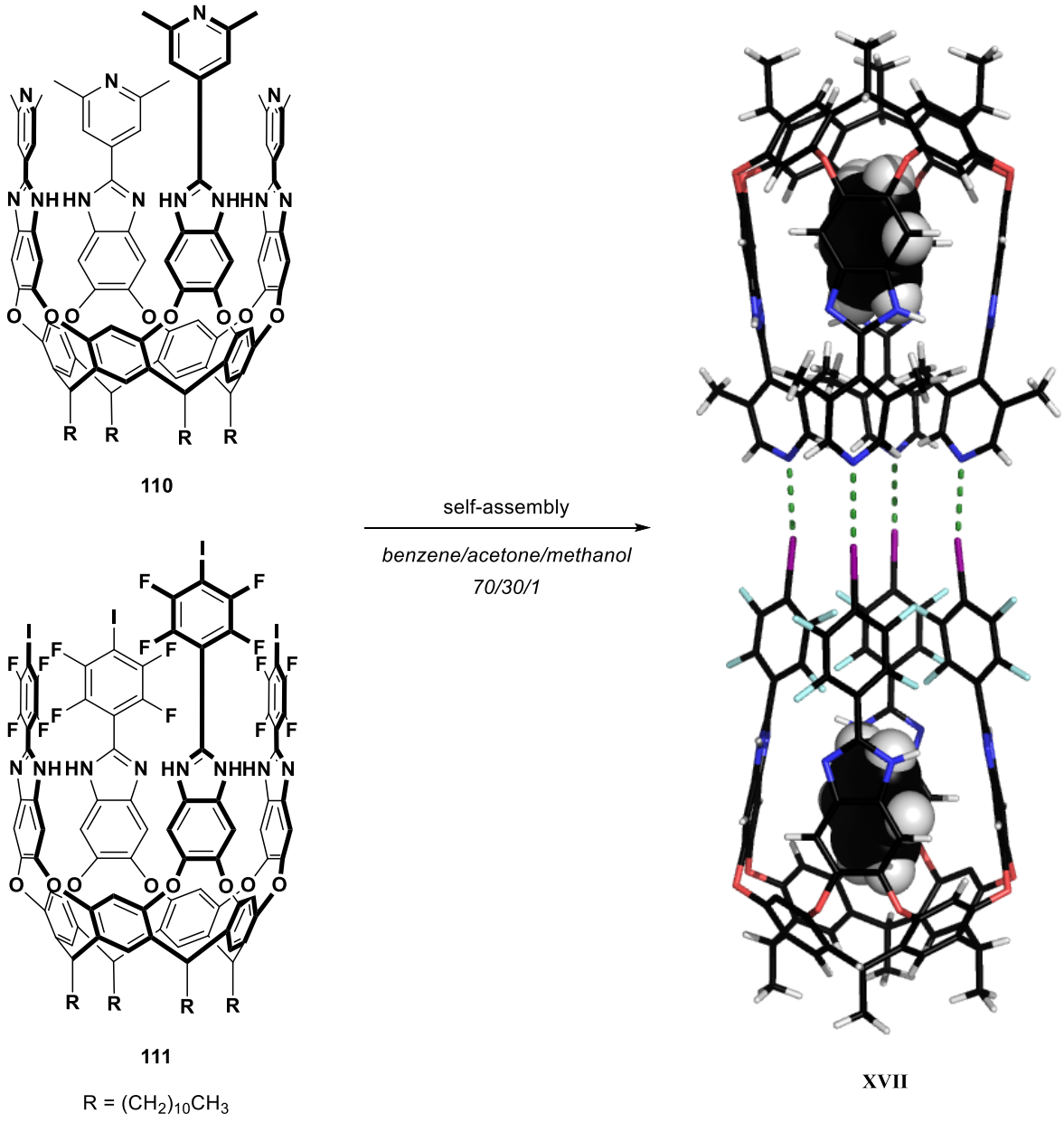

Scheme 26: Halogen-bonded dimer **XVII** (including two benzene molecules) assembled from building blocks **110** and **111**. Feet and additional solvent molecules were omitted.

This characteristic explains the high directionality (bond angle = 180°) of halogen bonds and is also the reason why in most cases iodides due to higher polarizability form stronger halogen bonds compared to bromides, chlorides or even fluorides. While this results in a high degree of predictability, it also limits the use of halogen bonds for the construction of large non-covalently bonded assemblies. Building blocks for self-assembly require a high degree of preorganization and carefully arranged functionalities in order to fulfil the strict requirements for halogen bond based self-assembly. An interesting contribution to the field was reported by DIEDERICH and coworkers. Based on earlier work by PILATI,[168] the group showed the self-assembly of dimeric structure **XVII** from two complimentary functionalized resorcinarene subunits **110** and **111** (Scheme 26).[169] Evidence for the formation of dimers similar to structure **XVII** in the solid state, in solution and in the gas-phase was presented in an ensuing study.[170] Optimization of both the halogen bond acceptor and the donor allowed for high binding constants (K_a = 2.11 × 10^5 M^{-1}) in competitive solvent (benzene/acetone/methanol 70/30/1) for related derivatives. Structure **XVII** has two separated binding sites for small guests such 1,4-dioxane or 1,4-dithiane.

The group of RISSANEN employed a different strategy using molecular iodine as halogen bond donor to create multimeric assemblies. An initial report utilizes a modified resorcinarene building block, two of which are linked by iodine.[171] The concept was then further expanded to multimeric system based on building block **112**.[172] When **112** is exposed to a silver salt (i.e., $AgPF_6$) it forms a tetrameric structure linked by Ag^+-ions. These can then be replaced with halonium ions (i.e., I^+) by reaction with molecular iodine to form structure **XVIII** (Scheme 27).

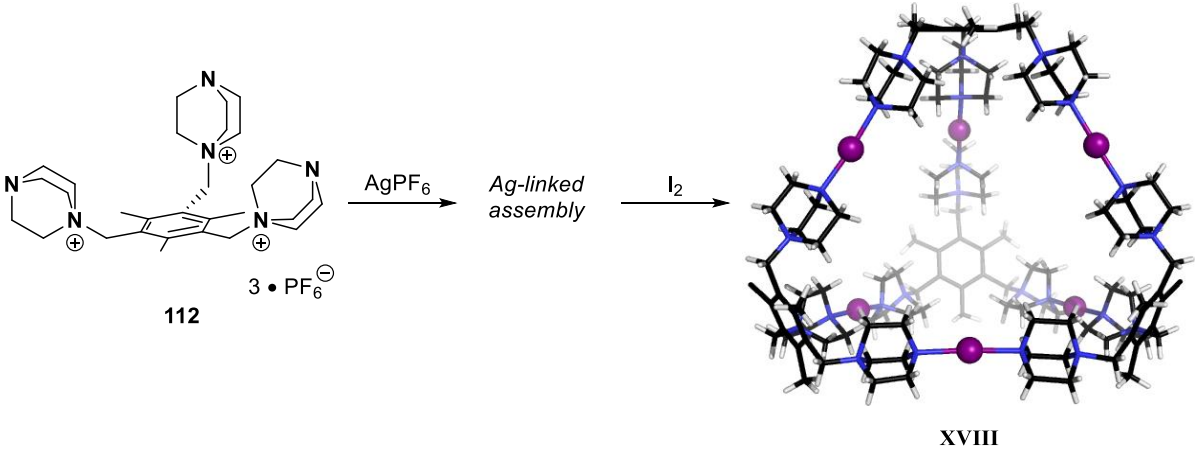

Scheme 27: Silver templated self-assembly of tetrameric **XVIII** from **112**. I^+-ions are represented as spheres (purple). Solvent molecules and counterions were omitted for clarity.

Assembly **XVIII** and related structures were characterized by solid state X-ray structures as well as in solution by NMR spectroscopy demonstrating the robust nature and predictability of the [N−I^+−N] binding motif.

Recently, also chalcogen bonding has been exploited for catalysis[173] and was investigated regarding its potential for self-assembly of cyclic structures.[174] While these studies mark important steps, the assembly of larger systems based on this specific interaction and their applications remains a challenge for the future.

1.2.6 Assemblies Based on Resorcinarene Using Dynamic Covalent Chemistry

A rapidly evolving field of research is the assembly of shape-persistent organic cages and materials utilizing dynamic covalent chemistry (DCC).[175-177] Approaches using DCC circumvent the synthetic effort often required to construct large covalently linked three-dimensional structures by exploiting reversible reactions (e.g., imine formation, disulfide formation, boronic ester formation, metathesis reactions, etc.). If building blocks with complimentary functionalities (e.g., carbonyl and amine) are mixed and allowed to equilibrate, the thermodynamic product is formed. When using appropriately designed building blocks complex, molecular 3D-architechtures can be accessed in a highly modular way. A complete overview of the vast number of structures and approaches reported would be beyond the scope of this introduction. The following paragraph will therefore focus on the concepts applied for the synthesis of hexameric structures based on the resorcinarene macrocycle **46** that are of particular relevance to the structures presented in this thesis.

In 1991 the first structure using imine condensation of resorcinarene derivatives was published by QUAN and CRAM.[178] The assembly is comprised of two tetraaldehyde resorcinarene units (**113** with different 'feet') fused together by imine condensation with 1,3-diaminobenzene. The resulting hemicarcerand was found to encapsulate a number of guest molecules (e.g., menthol, camphor, ferrocene) upon heating. It took another 15 years until WARMUTH and coworkers realized the potential of this approach and in a series of reports combined a similar resorcinarene building block **113** with several different diamines (Scheme 28).[179]

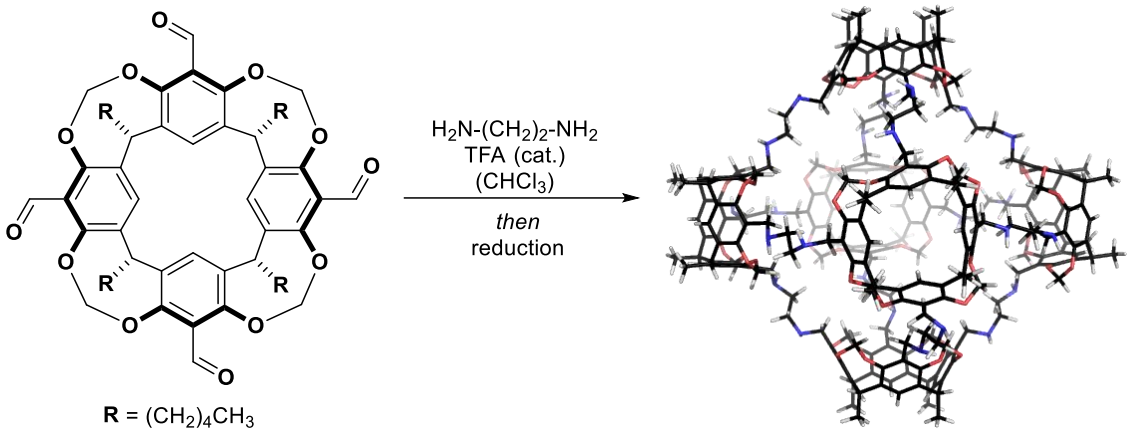

113 **XIX**

Scheme 28: Cage **XIX** synthesized from building block **113** using imine formation and subsequent reduction. Feet were omitted for clarity.

Depending on the linker unit[180-181] and the specific conditions for the imine condensation[182] this led to the formation of several large assemblies of different form (e.g., cage **XIX** with six resorcinarene units) incorporating up to eight resorcinarene units. These assemblies generally feature large openings which allow small molecules (e.g., solvents or tetraalkyl ammonium salts) to enter the cavity *via* these pores.[180] Exceptionally large cavity volumes (up to 13 000 $Å^3$)[181] have been reported highlighting the feasibility of this approach for the synthesis of large, organic cage molecules.

Recently, the SZUMNA group expanded the concept to form inherently chiral cages (Scheme 29).[183] In contrast to the cages reported by WARMUTH using macrocylces with bridged phenol groups, SZUMNA and coworkers utilized tetraaldehyde building block **114** based on resorcinarene with unprotected phenol groups. A stepwise reaction process with hydrazine led to the formation of chiral cage **XX** proven by X-ray crystallography. The chirality stems from the directional arrangement of the hydrazone groups while the phenol groups additionally stabilize the structure *via* hydrogen bonds. The two enantiomers could be partially resolved using HPLC and were characterized with CD spectroscopy.

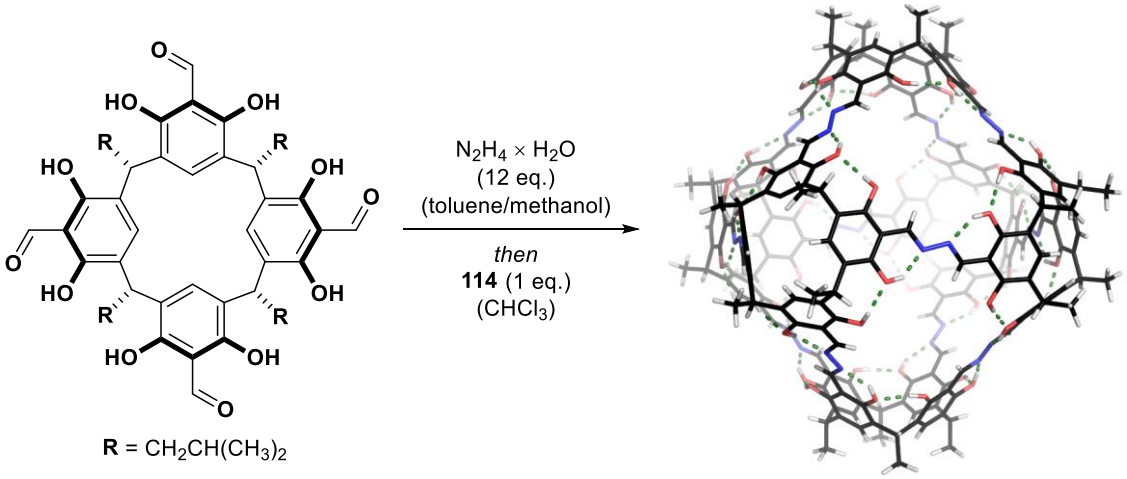

114 **XX**

Scheme 29: Chiral Cage **XX** assembled using tetraaldehyde **114**. Feet were omitted for clarity.

When compared to the hydrogen bonded resorcinarene hexamer **X** two differences are immediately apparent: 1) Bonding type: The covalent nature of the organic cages **XIX** and **XX** changes the dynamic of the system entirely. This has implications for the mechanism of guest uptake which cannot take place anymore by partial disassembly. On the other hand, the covalently linked cages are expected to be much less prone to disassembly in polar solvents and should tolerate e.g., water as a solvent, given they can be synthesized in a soluble form (possibly

different ‘feet’). 2) Structural differences: While the hydrogen bonded hexamer **X** forms a rather ‘closed-shell’ hydrogen bond network effectively isolating guests from bulk solution, the cages **XIX** and **XX** feature large, porous openings through which small guest molecules can diffuse in and out.

So far applications of these and similar covalently linked organic cages in the context of classical homogenous catalysis have not yet been reported. However, due to their exceptionally high surface area and defined pore size structures assembled using DCC have been proven to be extremely potent as porous materials for selective gas sorption.[175, 177] Additional applications include gravimetric sensoring,[184] molecular sieving[185] or as stationary phases for gas chromatography.[186-187]

2. Objective of This Thesis

The hexameric resorcinarene capsule **X** has been shown to be an effective supramolecular catalyst. Several interesting transformations using **X** have been published in recent years including the first biomimetic tail-to-head terpene (THT) cyclization using a man-made catalyst.[15] In contrast, the closely related pyrogallolarene hexamer **XI** has been found catalytically inactive under identical conditions.[120] Even though certain structural differences such as the incorporation of eight water molecules in **X** are obvious, and other factors such as guest uptake, intrinsic acidity of the assemblies and influence of the electrostatic potential surface (ESP) were investigated, the underlying cause for the catalytic inactivity of **XI** remains unknown. A better understanding of the current catalytic system is highly desirable to overcome the current limitations concerning product selectivity and also relevant for the design of new catalytically active systems. The primary goal of this work is therefore the elucidation of the specific requirements for efficient catalysis inside hexamer **X**. Initially, we will attempt to devise a concise synthetic route accessing macrocycles **115** – **117** in pure form. These compounds can be described as the 'missing-link' between the resorcinarene and the pyrogallolarene macrocycles (Figure 7a). Upon isolation these compounds will be characterized concerning their self-assembling behaviour. If assemblies comparable to hexameric structures **X** and **XI** are formed, these will be investigated concerning their catalytic activity in the THT cyclization of monoterpenes.

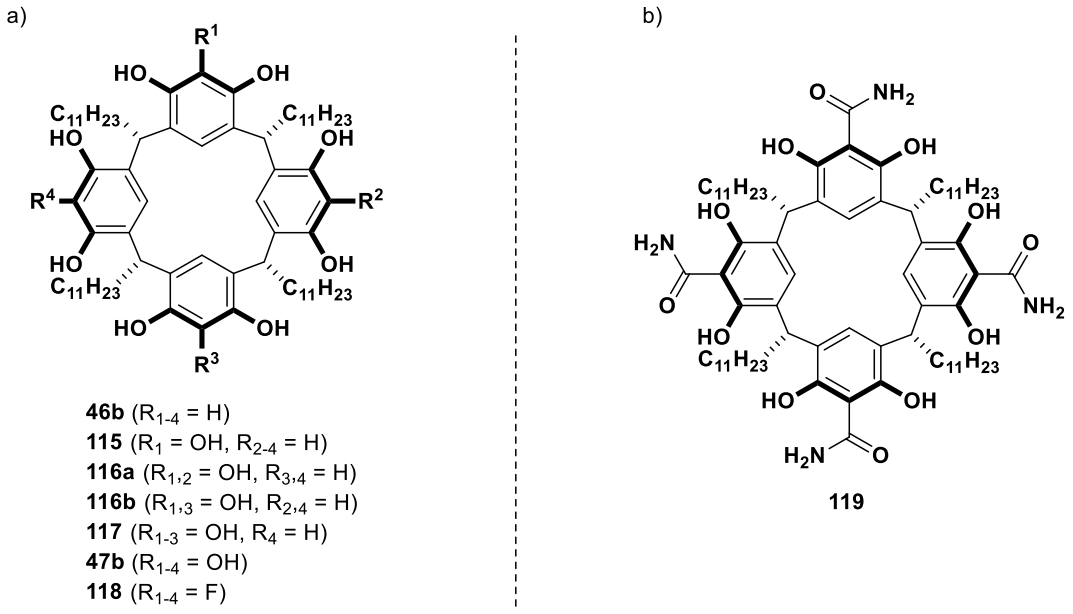

Figure 7: a) Macrocycles **46b, 47b** and **115** – **118** with varying ratios of resorcinol and pyrogallol units. b) Resorcinarene-derived macrocycle **119** with additional amide moieties.

Subsequently, the corresponding assemblies will be compared with regards to different properties (i.e., guest uptake, protonation by external acid, water being part of the hydrogen bond network) to establish a correlation with the catalytic activity. In order to investigate the influence of the ESP we will additionally seek to synthesize the tetra fluoro compound **118**.

The second objective of this thesis will be the development of a new, large assembly based on hydrogen bonding. We envisioned that decorating the resorcinarene macrocycle **119** with additional groups capable of hydrogen bonding (Figure 7b) could lead to new hexameric assemblies. Molecular modelling indicated that tetraamide compound **119** could indeed form different hexameric structures including a porous cage – unusual for hydrogen bonded assemblies. Again, we will attempt to establish a reliable synthetic route accessing macrocycle **119** in sufficient quantities. With **119** in hand, we will subsequently investigate self-assembly, potential for guest uptake and applications in supramolecular catalysis.

3. Results and Discussion

The following pages of this chapter function as a summary of the publications that were prepared over the course of these PhD studies.

3.1 Publication summaries

3.1.1 Requirements for Terpene Cyclizations inside the Supramolecular Resorcinarene Capsule: Bound Water and Its Protonation Determine the Catalytic Activity

Based on earlier results from our group comparing the resorcinarene hexamer **X** with the closely related, but catalytically inactive pyrogallolarene hexamer **XI**, we set out to elucidate the specific requirements for efficient catalysis within **X**. To this end, we designed an efficient synthesis to access several new macrocycles containing varying amounts of pyrogallol and resorcinol units **115** – **117**. Synthesis of macrocycles **115** – **118** was achieved by a two-step sequence from tetrabromo compound **120a** involving lithium-halogen exchange followed by *in situ* hydroxylation (yielding **121** – **124**) and finally deprotection of the phenol groups (Scheme 30a). Using a similar approach, we were also able to access an electron-deficient tetra fluorinated resorcinarene derivative **118** to investigate the influence of the electrostatic potential surface (ESP) on the catalytic efficiency. Starting material **120a** is available *via* literature procedures and was synthesized on decagram scale. Apart from compound **116b** with two *distal* hydroxy groups, all obtained macrocycles dissolved well in chloroform. DOSY-NMR experiments provided diffusion coefficients very close to the values of the known assemblies **X** and **XI**, indicating the formation of hexameric assemblies. Assemblies **X**, **XI** and **XXI** – **XXIV** were subsequently investigated concerning their catalytic activity in the THT cyclization of monoterpenes. The cyclization of geranyl acetate (**27**) had been shown previously to proceed within hexamer **X** in a 'non-stop'-fashion forming α-terpinene (**9**) and was chosen as a suitable test reaction. The addition of traces of HCl, while unable to catalyze the reaction itself, is crucial for efficient catalysis acting as cocatalyst in a synergistic fashion with hexamer **X**. As previously reported, in presence of the pyrogallolarene hexamer **XI** no conversion of geranyl acetate (**27**) was observed, while the resorcinarene hexamer **X** catalyzed the formation of α-terpinene (**9**) with 30 − 35% yield. Assembly **XXI** based on monomer **115** featuring one additional hydroxy group showed a similar catalytic efficiency forming α-terpinene (**9**) as the main product, albeit with lower yield.

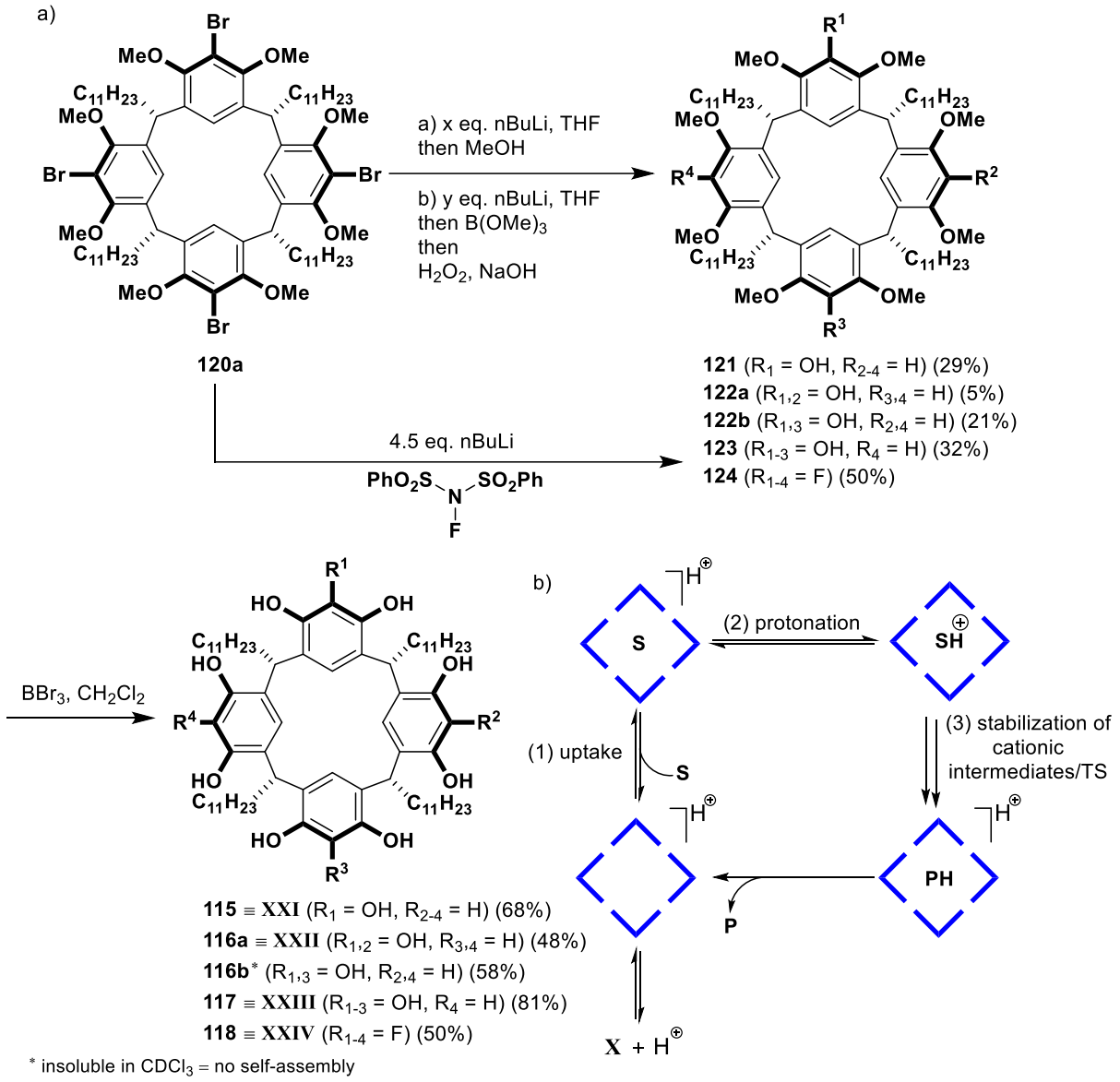

Scheme 30: a) Synthesis of compounds **115** – **118** corresponding to the respective assemblies **XXI** – **XXIV**. b) Potentially decisive steps of the catalytic cycle.

Assembly **XXII** still showed significant conversion, but product formation decreased notably. This is most likely due to a side reaction in which the highly reactive cationic intermediates are quenched by phenol groups leading to alkylation of the assembly. In contrast, assembly **XXIII** showed no significant conversion of geranyl acetate (**27**) after five days, while the reaction in presence of **XXIV** proceeds very slowly. Largely similar results were obtained with intrinsically more reactive nerol (**21**) as the substrate for assemblies **X**, **XI** and **XXI** – **XXIV**. Surprisingly, in the presence of assembly **XXIII** nerol (**21**) was converted quite efficiently (up to 60%). Control experiments and careful analysis of the product profile indicated that in this case the reaction takes place mostly outside of the cavity. Possibly due to defects in the hydrogen bond network and the inherently more reactive nature of nerol (**21**) limonene (**7**) is

formed as the main product. Several other substrates showed only minor conversion (≤ 15% after 72 h) indicating that assembly **XXIII** cannot be considered an effective catalyst for the THT cyclization of monoterpenes (Table 1).

As mentioned above three distinct events of the catalytic cycle (Scheme 30b) can be considered decisive for efficient catalysis: 1) Encapsulation of substrate within the cavity; 2) Protonation of the encapsulated substrate; 3) Stabilization of the ion pair formed upon cleavage of the leaving group.

The ability for guest uptake is crucial for catalysis and was confirmed in all cases using a saturated analogue of geranyl acetate (**27**), which shows no conversion in presence of HCl and the respective assemblies **X**, **XI** and **XXI** – **XXIV**. Encapsulation was indicated by the gradual appearance of upfield shifted signals in the ^{1}H-NMR spectra and a decrease of the amount of nonencapsulated substrate analogue determined by ^{1}H-NMR analysis.

While assembly **X** has been shown to readily encapsulate ammonium salts as ion pairs, the encapsulation of anions within assembly **XI** was found to be energetically unfavourable. Since the catalytic cycle involves the formation of an ion pair upon protonation and cleavage of the leaving group the ability to stabilize these within the cavity is considered decisive. To investigate the abilities of assemblies **X**, **XI** and **XXI** – **XXIV** to encapsulate anions a fluorine containing anion (i.e., triflate) was chosen. This allowed analysis with ^{19}F-NMR spectroscopy where encapsulation is associated with a shift and a broadening of the fluorine signal of the triflate anion. The results indicated the stabilization of ion pairs inside all assemblies except for **XI**. Since assembly **XXIII** was found to stabilize ion pairs but was found to be catalytically inactive, a clear correlation could not be established in that respect.

During our experiments we noticed that upon addition of HCl, the ^{1}H-NMR of assembly **X** changed notably, while in case of **XI** the signals corresponding to the assembly remained unaffected. Specifically, we found that the addition of external acid led to a broadening of signals associated with the phenol groups of assemblies **X, XXI, XXII** and **XIV**. This can be attributed to the protonation of these assemblies, while in case of assemblies **XI** and **XXIII** the phenol signals remain unaffected and only the water signal experiences some broadening. Importantly, the protonation of the assemblies correlates well with the catalytic activity observed in the cyclization of monoterpenes.

The main structural difference between **X** and **XI** is the incorporation of eight water molecules into the hydrogen bond network of **X**, while **XI** self-assembles without water. This can also be

observed in the ^{1}H-NMR spectra of the assemblies. In case of the resorcinarene hexamer **X** the water signal is shifted downfield due to fast exchange between water molecules that take part in the formation of the hexameric structure **X** and water molecules that are in bulk solution.

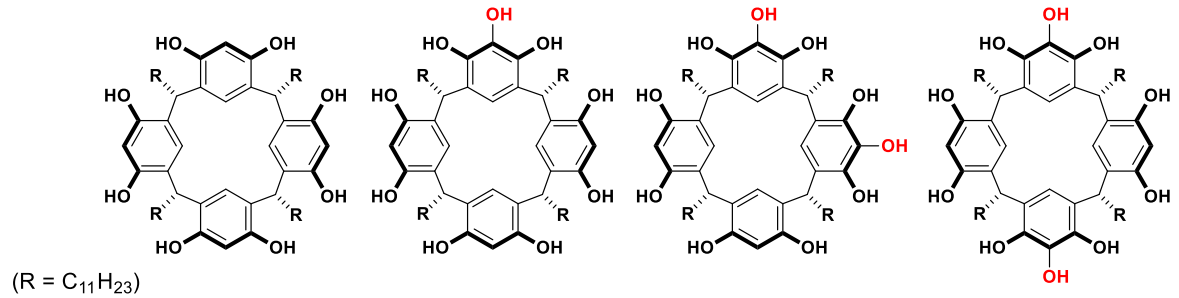

(R = $C_{11}H_{23}$)

	46b/X	**115/XXI**	**116a/XXII**	**116b**
catalysis	✓	✓	✓	n. d.[a]
anion binding	✓	✓	✓	n. d.[a]
water	✓	✓	✓	n. d.[a]
HCl-exchange	✓	✓	✓	n. d.[a]

[a] Not determined. Insoluble in $CDCl_3$.

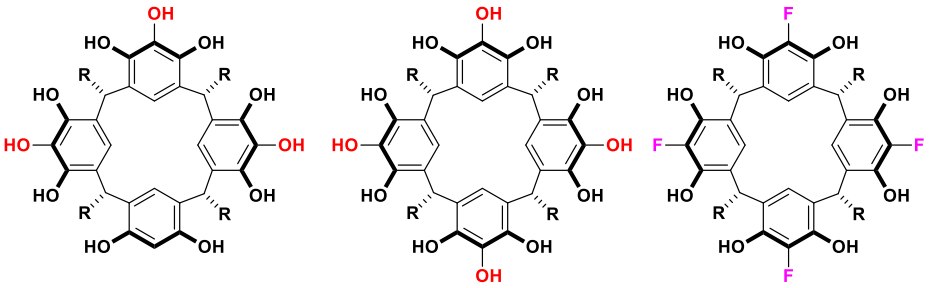

	117/XXIII	**47b/XI**	**118/XXIV**
catalysis	×	×	✓
anion binding	✓	×	✓
water	×	×	✓
HCl-exchange	×	×	✓

Table 1: Comparison of macrocycles **46b, 47b** and **115** – **118** and corresponding assemblies **X**, **XI** and **XXI** – **XXIV** indicating water being part of the hydrogen bond network as the distinct property enabling catalysis of the THT cyclization.

The magnitude of the shift depends on the total amount of water present in solution, resulting in increasing shifts with decreasing water content. In contrast, the water signal in presence of

assembly **XI** is unaffected. Determination of the amount of water incorporated into the hydrogen bond network is possible utilizing DOSY-NMR spectroscopy. At low overall water content, corresponding to the minimal amount necessary to form the assembly (i.e., eight equivalents in case of **X**) the diffusion value determined for water is very close to the value found for the assembly itself, indicating that most of the water present is part of the assembly. With increasing overall water content, the amount of 'free' water increases and so does the diffusion coefficient of water. If water is not part of the assembly (i.e., assembly **XI**) the diffusion coefficient of water remains unaffected by the total amount of water in the solution. Using this methodology, we were able to show that assemblies **X, XXI, XXII** and **XIV** incorporate water within their hydrogen bond network to some degree, while assemblies **XI** and **XXIII** assemble without water. Since these results correlate well with the protonation studies and the catalytic activity of the respective assemblies. We concluded that water incorporated into the hydrogen bond network must play a significant role for the protonation of the encapsulated substrate.

To gain more insight into these processes molecular dynamics (MD) simulations were conducted. For this purpose, the resorcinarene hexamer **X** in presence of HCl as cocatalyst and geranyl acetate (**27**) as substrate were submitted to quantum mechanics/molecular mechanics (QM/MM) MD simulations.

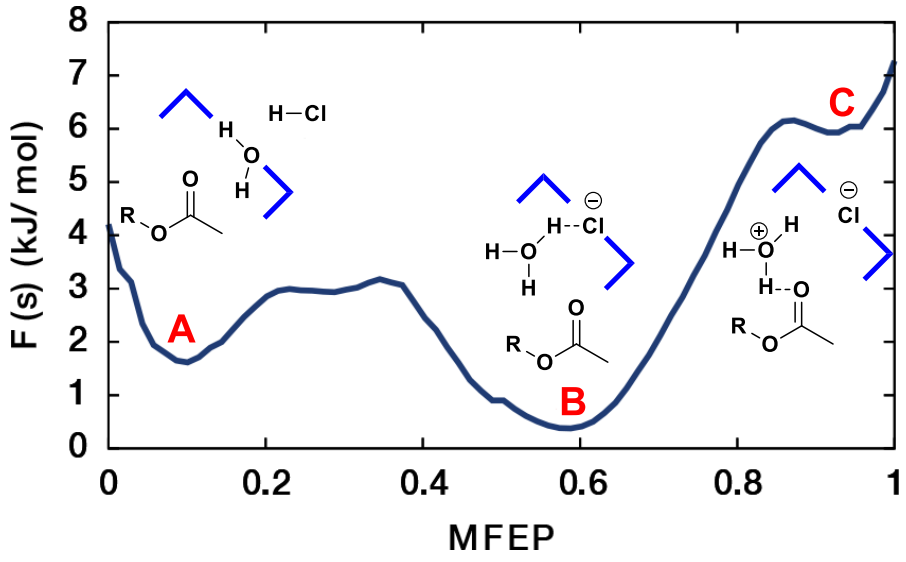

Figure 8: The minimum free energy path (MFEP) along the free energy surface highlighting the importance of water incorporated into the hydrogen bond network for protonation of the encapsulated substrate.

The results indicated that indeed water incorporated into the hydrogen bond network is protonated by HCl, while the alternative pathway involving the protonation of a phenol, followed by proton migration to a water molecule is energetically unfavorable. The formed ion pair H_3O^+/Cl^- is stabilized within the hydrogen bonding network by the surrounding phenol groups (Figure 8). Interestingly, the chloride anion replaces the hydronium ion, which moves inside the cavity to form a carbonyl/hydronium complex, in the hydrogen bonding network. This could also help explain the surprising observation that HCl or the resulting chloride anion do not interfere with the cationic cyclization cascade, an effect often observed in solution.

In conclusion we report in this publication the synthesis and characterization of four new macrocycles **115** – **117** with different resorcinol/pyrogallolarene ratios as well as a tetra fluorinated derivative **118**. Apart from compound **116b** all macrocycles were found to assemble forming hexameric capsules **XXI** – **XXIV**. Detailed investigations of the new assemblies concerning their catalytic activity in the THT cyclization of monoterpenes, guest uptake, ability to stabilize ion pairs and water content were conducted (summarized in Table 1). The results revealed a correlation between the ability for efficient catalysis and water incorporated into the hydrogen bond network of the corresponding assemblies. Protonation studies and MD simulations indicated a proton shuttle mechanism, where water within the hydrogen bond network plays a crucial role for the protonation of the encapsulated substrate. These findings shine light on the requirements for catalysis within hexamer **X** and finally elucidate the exact mode of activation. Since this model is most likely transferable to other related systems, we expect these results to significantly impact the design of future supramolecular catalyst systems.

3.1.2 Concentration-dependent Self-assembly of an Unusually Large Hexameric Hydrogen-bonded Molecular Cage

In this study we report our attempt to design a building block that is expected to show self-assembling behaviour to construct a new, large assembly based on hydrogen bonding. The decoration of the upper rim of the well-known resorcinarene macrocycle **46** with four additional amide moieties, capable of hydrogen bonding was found to be a promising approach. Based on our initial molecular modelling attempts two hexameric structures, a cage-like structure **XXV** with large openings (commonly observed for related structures formed using dynamic covalent chemistry, compare Section 1.2.6), and the more conventional 'closed-shell' structure **XXVI** seemed possible using building block **119** (Scheme 31).

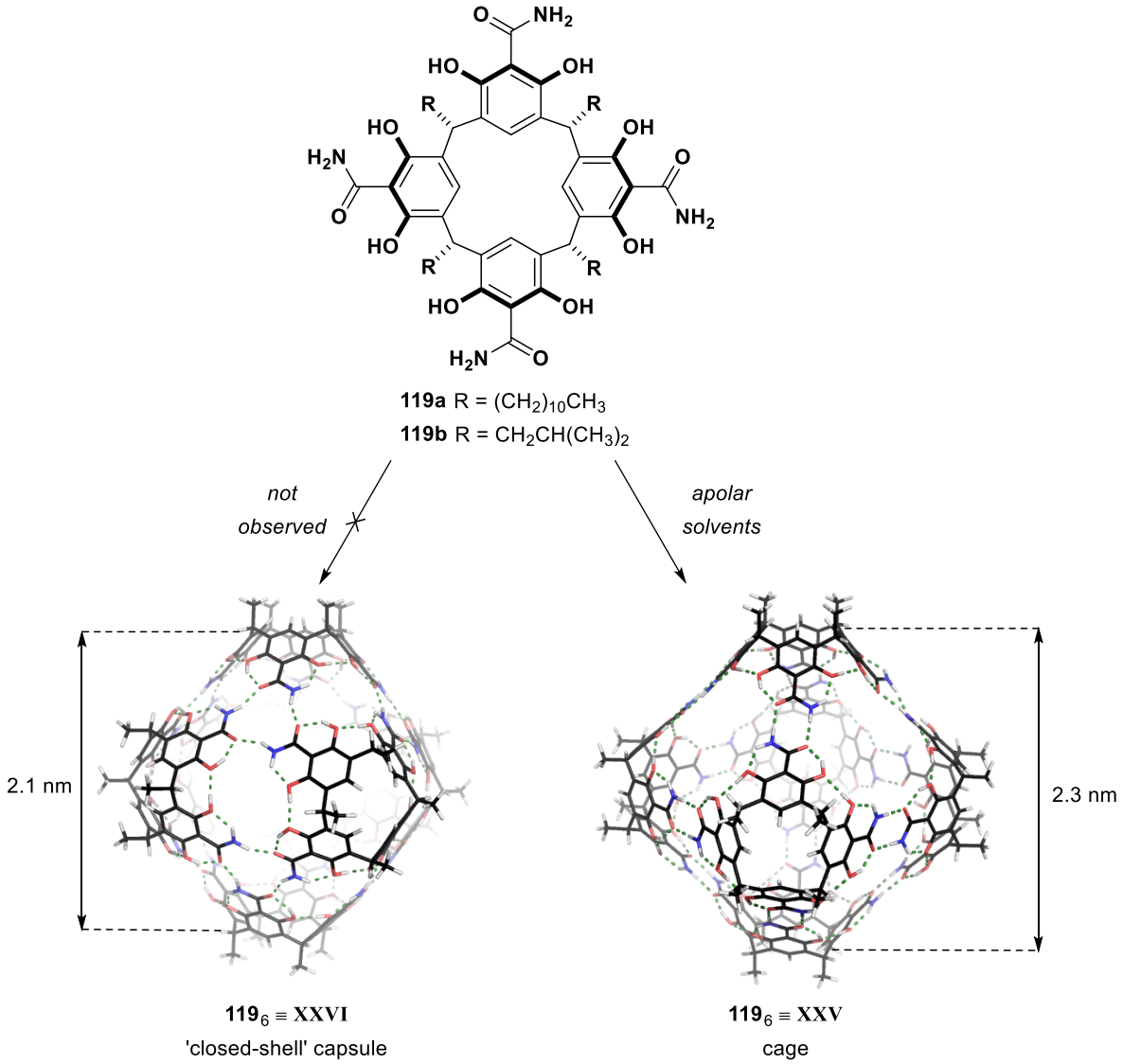

Scheme 31: Molecular models of the possible hexameric structures **XXV** (Cage) and **XXVI** ('closed-shell') based on macrocycle **119**.

A synthetic route was developed that allowed to access macrocycle **119a** in significant quantities (Scheme 32a). Starting from literate known compound **120a** a halogen-lithium exchange followed by addition of trimethylsilyl isocyanate (TMSNCO) as the electrophile gave **125a** and subsequent deprotection with trimethylsilyl iodide led to compound **119a**. Derivative **119b** featuring shorter *iso*-butyl 'feet' for crystallization was synthesized along the same route. The solid-state structure obtained for **119b** showed the expected dimerization for the amide−amide interaction associated with structure **XXV** (Scheme 32b). A second crystal conformation of **119b** with a much larger unit cell remained unsolved likely due to unordered solvent molecules within the cavity.

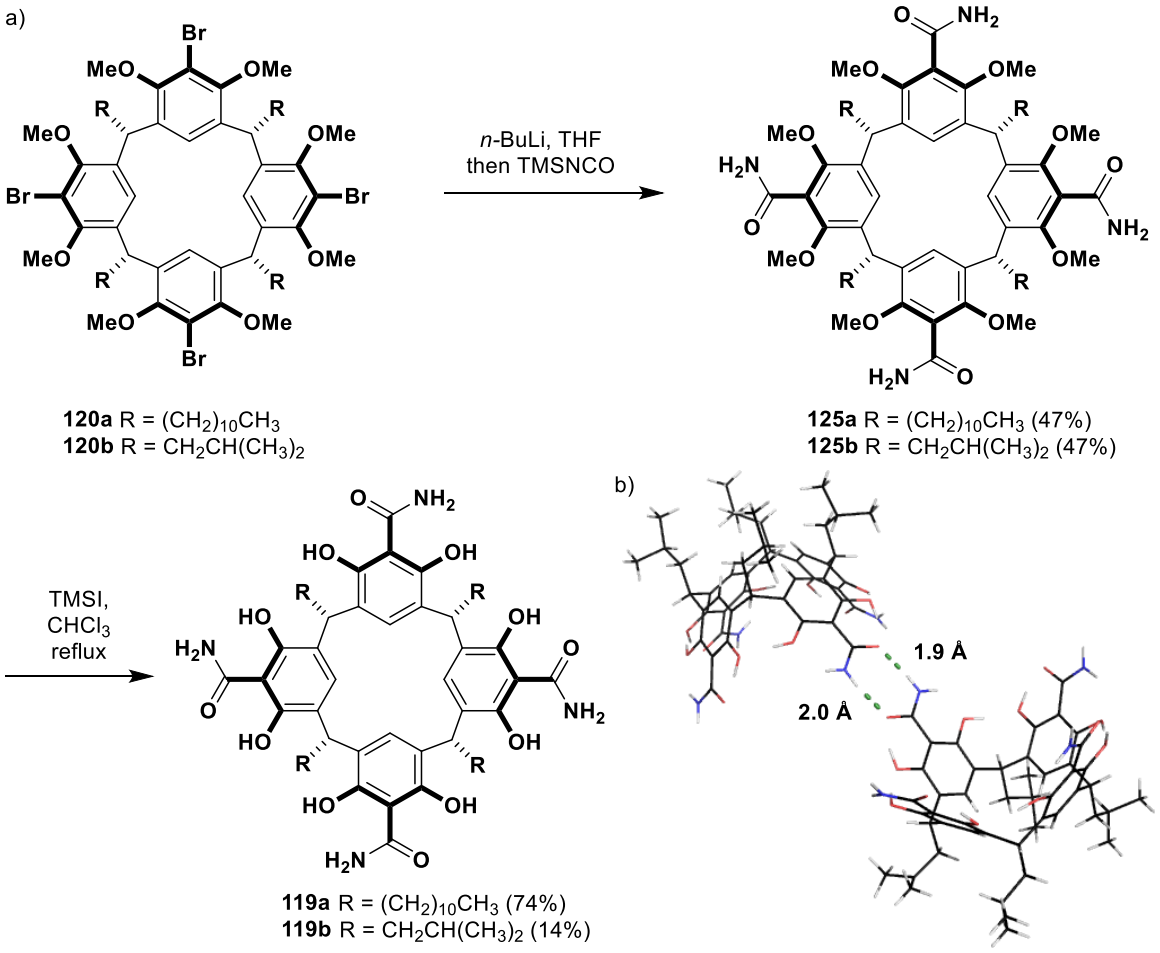

Scheme 32: a) Synthesis of **119a** and **119b** starting from compound **120a** and **120b**, respectively. b) X-ray structure of **119b**.

Macrocycle **119a** was found to be well soluble in several apolar solvents and DOSY-NMR spectroscopy indicated the formation of a hexameric species. Interestingly, the self-assembly was found to be highly concentration dependent with the monomeric species **119a** prevailing at low concentrations (Scheme 33a). The self-assembly of **XXV** can be considered cooperative

with a critical aggregation concentration of around 3 mM (Scheme 33b). Detailed DOSY-NMR studies and comparison with the well-known hexameric resorcinarene and pyrogallolarene capsules **X** and **XI** (Scheme 33c) indicated the formation of the larger cage-like structure **XXV** based on the dimerization binding motif which was also found in the solid-state structure. DFT calculations revealed an energy preference of 1.8 – 17.2 kcal/mol for the formation of cage-like structure **XXV** over the 'closed-shell' structure **XXVI** depending on the basis set.

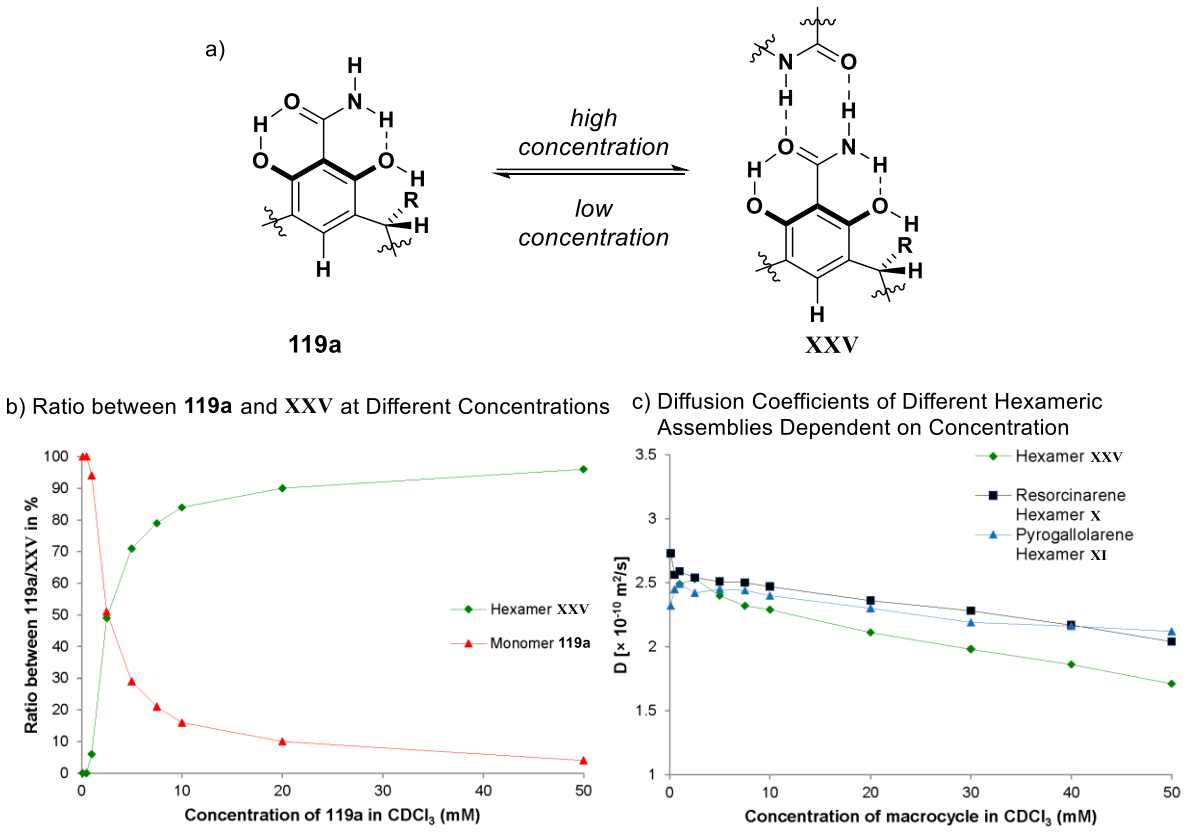

Scheme 33: a) Concentration dependent self-assembly of **XXV** from **119a**. b) Ratio between monomer **119a** and hexamer **XXV** depending on concentration. c) Diffusion coefficients of hexameric assemblies **X**, **XI** and **XXV** at different concentrations compared.

Additionally, assembly **XXV** was investigated concerning guest uptake. Fullerenes (C_{60} and C_{70}) were found to be suitable guest molecules based on characteristic shifts in ^{13}C-NMR spectra. Due to the low solubility of these fullerenes in $CDCl_3$ and the low concentrations required for UV/Vis-spectroscopy, hindering the self-assembly of **XXV** the determination of binding constants proved challenging. To gain some insight into the encapsulation process four well soluble ethyl and *tert*-butyl malonyl derivatives of C_{60} and C_{70} were synthesized. These compounds showed slow exchange allowing the determination of binding constants by comparing the integrals of 'free' and encapsulated guest in the ^{1}H-NMR spectra. Binding

constants were found to be modest (750 – 2200 M^{-1}) and generally higher for the C_{60}-derivatives.

In summary, we present here the design and synthesis of a new, large hexameric cage structure self-assembled from macrocycle **119a**. Structure **XXV** has large openings often observed for structures assembled using dynamic covalent chemistry but unusual for hydrogen bonded assemblies, most of which rather form a 'closed-shell' hydrogen bond network. Furthermore, structure **XXV** has an internal cavity volume of around 2800 $Å^3$ rendering it to the best of our knowledge the largest structure to date based exclusively on hydrogen bonding. While the porous openings could allow for modifications and/or provide an additional binding site, the overall simplification of the hydrogen bond network is believed to aid the rational design of future assemblies. We expect that the results presented here will inspire the development of new structures to overcome the current limitations concerning guest uptake and size of hydrogen bonded assemblies.

4. Summary and Outlook

The first enzyme mimetic tail-to-head terpene cyclization catalyzed using a man-made catalyst, namely the resorcinarene hexamer **X**, represents an important milestone for supramolecular catalysis. However, the exact mode of action of acid catalysis within **X** remained elusive for some time, while the closely related pyrogallolarene hexamer **XI** was found to be catalytically inactive. To investigate the prerequisites for catalysis within **X**, we present here the synthesis of several new macrocycles bearing close resemblance to resorcinarene. The macrocycles **115** − **118** were shown to self-assemble forming hexameric capsules and were subsequently investigated concerning their catalytic activity in the acid-catalyzed THT cyclization of monoterpenes. The obtained assemblies were additionally characterized concerning their abilities to encapsulate substrate molecules, stabilize ion pairs in the cavity and the amount of water incorporated into the hydrogen bond network. By correlation with the catalytic activity, we were able to establish a correlation between water being part of the assemblies and efficient catalysis (Figure 9). We found that only assemblies where water takes part in the hydrogen bond network are protonated by external acid (HCl).

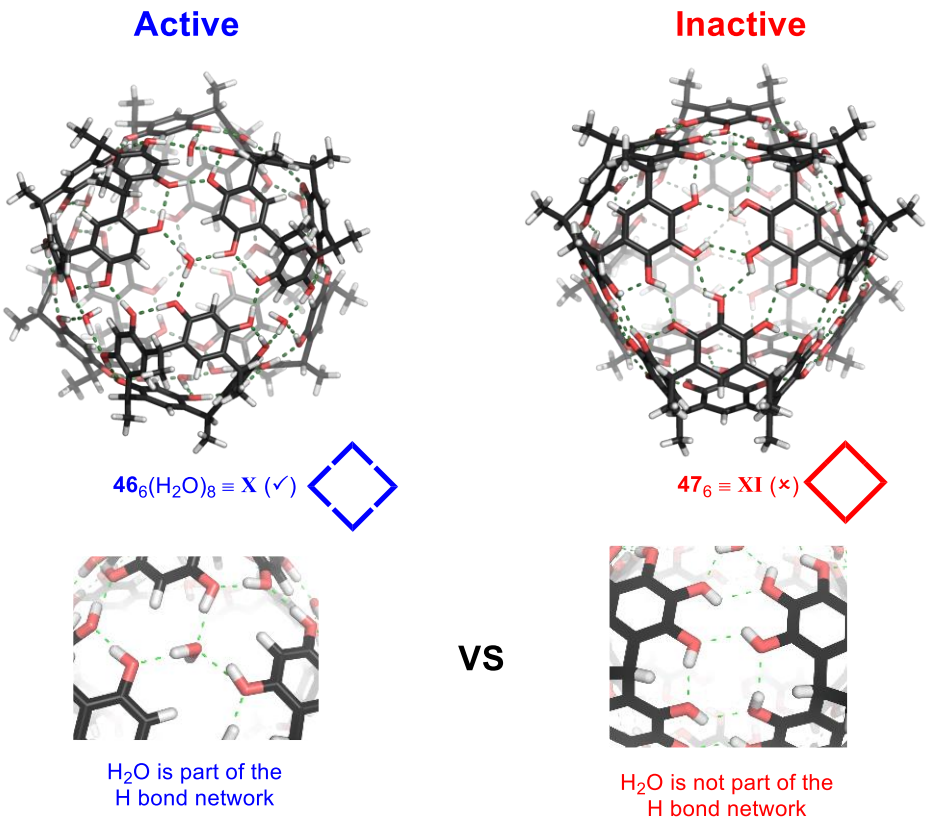

Figure 9: The incorporation of water within the hydrogen bond network was found to be the crucial prerequisite enabling the enzyme mimetic catalysis of the THT cyclization within **X**.

Computational studies indicated a proton shuttle mechanism where the water within the hydrogen bond network of the assembly effectively transfers a proton onto the encapsulated substrate initiating the cyclization reaction. The study presented here highlights the role water incorporated into the hydrogen bond network of **X** plays for efficient catalysis and shows how relatively subtle structural variations can cause a large difference in catalytic activity.

Furthermore, the design and synthesis of a completely novel assembly is presented (Figure 10). The derivatization of resorcinarene **46** with four additional amide groups proved to be sufficient to form a large hexameric cage **XXV** based exclusively on hydrogen bonds. Cage **XXV** features large openings in contrast to other assemblies reported in literature forming rather 'closed-shell' capsules. Results from DOSY-NMR and computational studies indicated the formation of the larger cage-like structure **XXV**, rather than the formation of an alternative smaller hexameric structure **XXVI** suggested by molecular modelling. Crystallographic data of the macrocycle was obtained using derivative **119b** with shorter alkyl chains, also showing the amide−amide dimerization binding motif. A second crystal structure with a large unit cell could not be solved presumably due to unordered solvent molecules within the cavity.

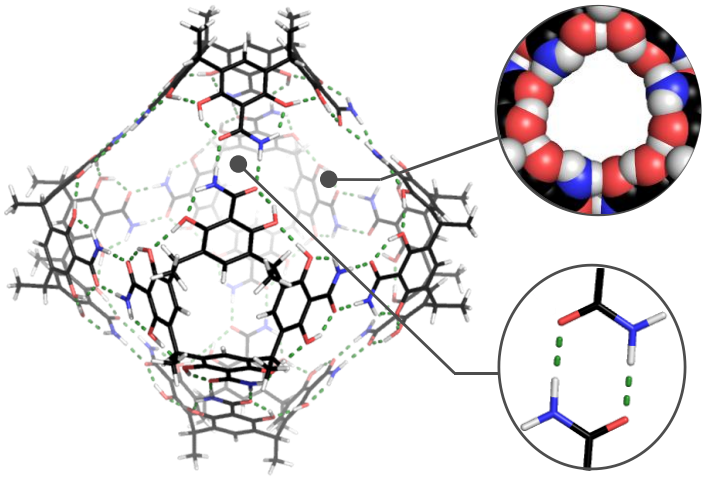

Figure 10: Large, hexameric cage **XXV** with an internal cavity volume of 2800 $Å^3$ based on amide−amide dimerization

The self-assembly of cage **XXV** was found to be highly concentration dependent and was investigated in detail using ^{1}H-and DOSY-NMR spectroscopy. Fullerenes (C_{60} and C_{70}) are suitable guest molecules for **XXV** and several derivatives of C_{60} and C_{70} were found to be encapsulated within **XXV**. With a cavity volume of 2800 A^3 cage **XXV** represents the largest assembly to date based purely on hydrogen bonds.

The results presented in this work are expected to aid the development of new systems in order to overcome the current limitations of man-made supramolecular catalyst systems, concerning substrate and product selectivity as well as the overall size of hydrogen bonded assemblies. The need for the incorporation of water or at least functional groups capable of proton transfer should be one of the key parameters when designing new potentially catalytic supramolecular systems. Another challenge that needs to be addressed is the induction of chirality using supramolecular catalysis. A promising approach could be the use of inherently chiral building blocks for self-assembly of hydrogen bonded capsules. For instance, the introduction of chiral 'feet' using a chiral aldehyde for the condensation of the resorcinarene macrocycle would yield chiral macrocycles which would be expected to self-assemble to hexameric structures (Figure 11a). Since this would introduce the chiral centre quite far from the reactive site a promising alternative is an approach using monofunctionalization of resorcinarene **46**. The derivatization of one of the phenol groups allows the introduction of circular chirality that would additionally provide some modularity depending on what functional group is introduced in this position (Figure 11b). Upon separation of enantiomers these building blocks are expected to self-assemble forming enantiopure capsules, producing a chiral field possibly influencing the stereochemical outcome of reactions catalyzed within the cavity.

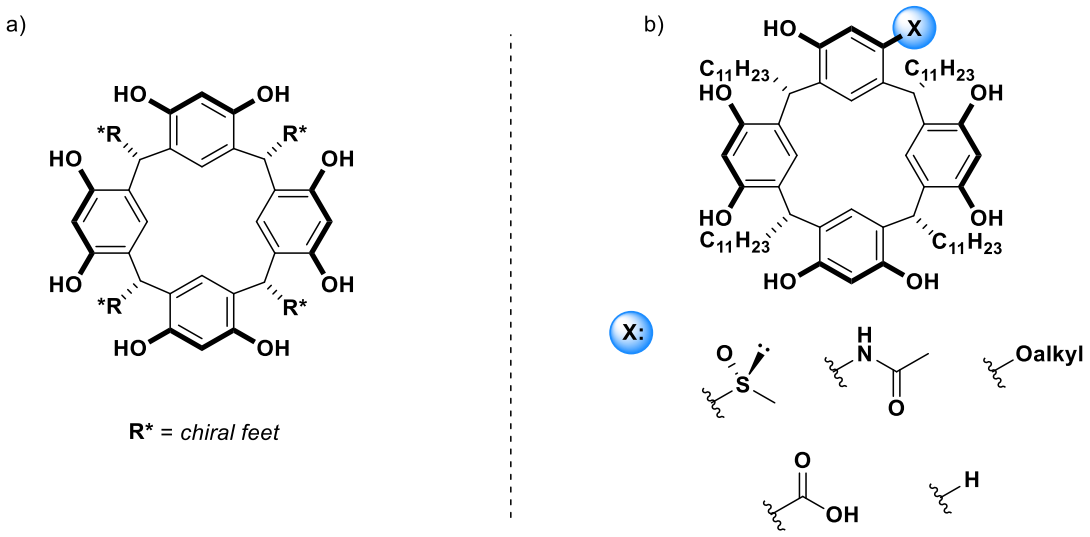

Figure 11: a) Resorcinarene macrocycle bearing chiral feet. b) Introduction of chirality by monofunctionalization of resorcinarene.

5. Index of Abbreviations

°C	degree Celsius
Å	Ångström
Ac	acetyl
δ	chemical shift
d	day
DBU	1,8-diazabicyclo[5.4.0]undec-7-ene
DFT	density functional theory
DMAP	4-(dimethylamino)-pyridine
DMF	*N*,*N*-dimethylformamide
DMSO	dimethylsulfoxide
DOSY	diffusion ordered spectroscopy
ESI	electrospray ionisation
Et	ethyl
et al.	et alii (and others)
eq.	equivalent
g	gram
GC	gaschromatography
GOAc	geranyl acetate
GOH	geraniol
h	hour
HPLC	high performance liquid chromatography
Hz	hertz
K	kelvin
L	liter
L	ligand
LOAc	linalyl acetate
LOH	linalool
µL	microliter
µmol	micromol
µg	microgram
M	molar
M	metal

Me	methyl
mg	milligram
MHz	Megahertz
min	minute
mL	milliliter
mm	millimeter
mmol	millimol
mol	mol
MS	mass spectroscopy
nmol	nanomol
n. a.	not analyzed
n-BuLi	*n*-butyllithium
ng	nanogram
NMR	nuclear magnetic resonance
NOESY	nuclear Overhauser effect spectroscopy
NOAc	neryl acetate
NOH	nerol
OAc	acetate
P	*n*-pentane
ppm	parts per million
R	organic residue
rt	room temperature
TBAB	tetrabutylammonium bromide
TMSNCO	trimethylsilyl isocyanate
TFA	trifluoroacetic acid
THF	tetrahydrofuran

6. References

1. Petrovska, B. B., Historical review of medicinal plants' usage. *Pharmacogn Rev* **2012,** *6* (11), 1-5.

2. Fischer, E., Einfluss der Configuration auf die Wirkung der Enzyme. *Ber. Dtsch. Chem. Ges.* **1894,** *27* (3), 2985-2993.

3. Morimoto, M.; Bierschenk, S. M.; Xia, K. T.; Bergman, R. G.; Raymond, K. N.; Toste, F. D., Advances in supramolecular host-mediated reactivity. *Nat. Catal.* **2020,** *3* (12), 969-984.

4. Zhang, X.; Houk, K. N., Why enzymes are proficient catalysts: beyond the Pauling paradigm. *Acc. Chem. Res.* **2005,** *38* (5), 379-85.

5. Garcia-Viloca, M.; Gao, J.; Karplus, M.; Truhlar, D. G., How enzymes work: analysis by modern rate theory and computer simulations. *Science* **2004,** *303* (5655), 186-95.

6. Degenhardt, J.; Kollner, T. G.; Gershenzon, J., Monoterpene and sesquiterpene synthases and the origin of terpene skeletal diversity in plants. *Phytochemistry* **2009,** *70* (15-16), 1621-37.

7. Dickschat, J. S., Bacterial terpene cyclases. *Nat. Prod. Rep.* **2016,** *33* (1), 87-110.

8. Christianson, D. W., Structural biology and chemistry of the terpenoid cyclases. *Chem. Rev.* **2006,** *106* (8), 3412-42.

9. Mahizan, N. A.; Yang, S. K.; Moo, C. L.; Song, A. A.; Chong, C. M.; Chong, C. W.; Abushelaibi, A.; Lim, S. E.; Lai, K. S., Terpene Derivatives as a Potential Agent against Antimicrobial Resistance (AMR) Pathogens. *Molecules* **2019,** *24* (14).

10. Jordan, M. A.; Wilson, L., Microtubules as a target for anticancer drugs. *Nat. Rev. Cancer.* **2004,** *4* (4), 253-65.

11. Kingston, D. G., Recent advances in the chemistry of taxol. *J. Nat. Prod.* **2000,** *63* (5), 726-34.

12. Christianson, D. W., Structural and Chemical Biology of Terpenoid Cyclases. *Chem. Rev.* **2017,** *117* (17), 11570-11648.

13. Wendt, K. U.; Schulz, G. E., Isoprenoid biosynthesis: manifold chemistry catalyzed by similar enzymes. *Structure* **1998,** *6* (2), 127-33.

14. Pronin, S. V.; Shenvi, R. A., Synthesis of highly strained terpenes by non-stop tail-to-head polycyclization. *Nat. Chem.* **2012,** *4* (11), 915-20.

15. Zhang, Q.; Tiefenbacher, K., Terpene cyclization catalysed inside a self-assembled cavity. *Nat. Chem.* **2015,** *7* (3), 197-202.

16. Yoder, R. A.; Johnston, J. N., A case study in biomimetic total synthesis: polyolefin carbocyclizations to terpenes and steroids. *Chem. Rev.* **2005,** *105* (12), 4730-56.

17. McCormick, J. P.; Barton, D. L., Studies in 85% H3PO4—II. *Tetrahedron* **1978,** *34* (3), 325-330.

18. Yu, W.; Wen, M.; Yang, L.; Liu, Z. L., Ferric chloride catalyzed isomerization and cyclization of geraniol, linalool and nerol. *Chin. Chem. Lett.* **2002,** *13* (6), 495-496.

19. Tsangarakis, C.; Stratakis, M., Biomimetic Cyclization of Small Terpenoids Promoted by Zeolite NaY: Tandem Formation of α-Ambrinol from Geranyl Acetone. *Adv. Synth. Catal.* **2005,** *347* (9), 1280-1284.

20. Yu, W.; Bian, F. L.; Gao, Y.; Yang, L.; Liu, Z. L., Y-zeolite-catalyzed cyclizations of terpenols. *Adv. Synth. Catal.* **2006,** *348* (1-2), 59-62.

21. Raptis, C.; Lykakis, I. N.; Tsangarakis, C.; Stratakis, M., Acid-catalyzed cyclization of terpenes under homogeneous and heterogeneous conditions as probed through stereoisotopic studies: a concerted process with competing preorganized chair and boat transition states. *Chem. Eur. J.* **2009,** *15* (44), 11918-27.

22. Polovinka, M. P.; Korchagina, D. V.; Gatilov, Y. V.; Bagrianskaya, I. Y.; Barkhash, V. A.; Shcherbukhin, V. V.; Zefirov, N. S.; Perutskii, V. B.; Ungur, N. D.; Vlad, P. F., Cyclization and Rearrangements of Farnesol and Nerolidol Stereoisomers in Superacids. *J. Org. Chem.* **1994,** *59* (6), 1509-1517.

23. Knowles, R. R.; Lin, S.; Jacobsen, E. N., Enantioselective thiourea-catalyzed cationic polycyclizations. *J. Am. Chem. Soc.* **2010,** *132* (14), 5030-2.

24. Kutateladze, D. A.; Strassfeld, D. A.; Jacobsen, E. N., Enantioselective Tail-to-Head Cyclizations Catalyzed by Dual-Hydrogen-Bond Donors. *J. Am. Chem. Soc.* **2020,** *142* (15), 6951-6956.

25. Lehn, J. M., Supramolecular chemistry: receptors, catalysts, and carriers. *Science* **1985,** *227* (4689), 849-56.

26. Muller-Dethlefs, K.; Hobza, P., Noncovalent interactions: a challenge for experiment and theory. *Chem. Rev.* **2000,** *100* (1), 143-68.

27. Wood, P. A.; Allen, F. H.; Pidcock, E., Hydrogen-bond directionality at the donor H atom-analysis of interaction energies and database statistics. *Crystengcomm* **2009,** *11* (8), 1563-1571.

28. Bissantz, C.; Kuhn, B.; Stahl, M., A medicinal chemist's guide to molecular interactions. *J. Med. Chem.* **2010,** *53* (14), 5061-84.

29. Schneider, H. J., Binding mechanisms in supramolecular complexes. *Angew. Chem. Int. Ed.* **2009,** *48* (22), 3924-77.

30. Persch, E.; Dumele, O.; Diederich, F., Molecular recognition in chemical and biological systems. *Angew. Chem. Int. Ed.* **2015,** *54* (11), 3290-327.

31. Pedersen, C. J., Cyclic polyethers and their complexes with metal salts. *J. Am. Chem. Soc.* **1967,** *89* (26), 7017-7036.

32. Dougherty, D. A., The cation-pi interaction. *Acc. Chem. Res.* **2013,** *46* (4), 885-93.

33. Mecozzi, S.; West, A. P., Jr.; Dougherty, D. A., Cation-pi interactions in aromatics of biological and medicinal interest: electrostatic potential surfaces as a useful qualitative guide. *Proc. Natl. Acad. Sci. U.S.A.* **1996,** *93* (20), 10566-71.

34. Tsuzuki, S.; Honda, K.; Uchimaru, T.; Mikami, M.; Tanabe, K., Origin of attraction and directionality of the pi/pi interaction: model chemistry calculations of benzene dimer interaction. *J. Am. Chem. Soc.* **2002,** *124* (1), 104-12.

35. Dawson, R. E.; Hennig, A.; Weimann, D. P.; Emery, D.; Ravikumar, V.; Montenegro, J.; Takeuchi, T.; Gabutti, S.; Mayor, M.; Mareda, J.; Schalley, C. A.; Matile, S., Experimental evidence for the functional relevance of anion-pi interactions. *Nat. Chem.* **2010,** *2* (7), 533-8.

36. Lopez-Andarias, J.; Frontera, A.; Matile, S., Anion-pi Catalysis on Fullerenes. *J. Am. Chem. Soc.* **2017,** *139* (38), 13296-13299.

37. Paraja, M.; Matile, S., Primary Anion-pi Catalysis of Epoxide-Opening Ether Cyclization into Rings of Different Sizes: Access to New Reactivity. *Angew. Chem. Int. Ed.* **2020,** *59* (15), 6273-6277.

38. Hillyer, M. B.; Gibb, B. C., Molecular Shape and the Hydrophobic Effect. *Annu. Rev. Phys. Chem.* **2016,** *67* (1), 307-29.

39. Rablen, P. R.; Lockman, J. W.; Jorgensen, W. L., Ab initio study of hydrogen-bonded complexes of small organic molecules with water. *J. Phys. Chem. A.* **1998,** *102* (21), 3782-3797.

40. Rozas, I.; Alkorta, I.; Elguero, J., Bifurcated hydrogen bonds: Three-centered interactions. *J. Phys. Chem. A.* **1998,** *102* (48), 9925-9932.

41. Quiocho, F. A., Protein-Carbohydrate Interactions - Basic Molecular-Features. *Pure Appl. Chem.* **1989,** *61* (7), 1293-1306.

42. Dumele, O.; Wu, D.; Trapp, N.; Goroff, N.; Diederich, F., Halogen bonding of (iodoethynyl)benzene derivatives in solution. *Org. Lett.* **2014,** *16* (18), 4722-5.

43. Kolesnichenko, I. V.; Anslyn, E. V., Practical applications of supramolecular chemistry. *Chem. Soc. Rev.* **2017,** *46* (9), 2385-2390.

44. Catti, L.; Zhang, Q.; Tiefenbacher, K., Advantages of Catalysis in Self-Assembled Molecular Capsules. *Chem. Eur. J.* **2016,** *22* (27), 9060-6.

45. Salles, A. G., Jr.; Zarra, S.; Turner, R. M.; Nitschke, J. R., A self-organizing chemical assembly line. *J. Am. Chem. Soc.* **2013,** *135* (51), 19143-6.

46. Cram, D. J., The Design of Molecular Hosts, Guests, and Their Complexes (Nobel Lecture). *Angew. Chem. Int. Ed.* **1988,** *27* (8), 1009-1020.

47. Lehn, J.-M., Supramolecular Chemistry—Scope and Perspectives Molecules, Supermolecules, and Molecular Devices(Nobel Lecture). *Angew. Chem. Int. Ed.* **1988,** *27* (1), 89-112.

48. Pedersen, C. J., The Discovery of Crown Ethers (Noble Lecture). *Angew. Chem. Int. Ed.* **1988,** *27* (8), 1021-1027.

49. Dietrich, B.; Lehn, J. M.; Sauvage, J. P., Les Cryptates. *Tetrahedron Lett.* **1969,** *10* (34), 2889-2892.

50. Cram, D. J.; Lein, G. M., Host Guest Complexation .36. Spherand and Lithium and Sodium-Ion Complexation Rates and Equilibria. *J. Am. Chem. Soc.* **1985,** *107* (12), 3657-3668.

51. Chao, Y.; Cram, D. J., Catalysis and Chiral Recognition through Designed Complexation of Transition-States in Transacylations of Amino Ester Salts. *J. Am. Chem. Soc.* **1976,** *98* (4), 1015-1017.

52. Dietrich, B.; Fyles, T. M.; Lehn, J. M.; Pease, L. G.; Fyles, D. L., Anion Receptor Molecules - Synthesis and Some Anion Binding Properties of Macrocyclic Guanidinium Salts. *J. Chem. Soc., Chem. Commun.* **1978,** (21), 934-936.

53. Zhang, J.; Ma, P. X., Cyclodextrin-based supramolecular systems for drug delivery: recent progress and future perspective. *Adv. Drug. Deliv. Rev.* **2013,** *65* (9), 1215-33.

54. Breslow, R., Artificial enzymes. *Science* **1982,** *218* (4572), 532-7.

55. Mackay, L. G.; Wylie, R. S.; Sanders, J. K. M., Catalytic Acyl Transfer by a Cyclic Porphyrin Trimer - Efficient Turnover without Product Inhibition. *J. Am. Chem. Soc.* **1994,** *116* (7), 3141-3142.

56. Mattei, P.; Diederich, F., Catalytic Cyclophanes. Part XI. A flavo-thiazolio-cyclophane as a biomimetic catalyst for the preparative-scale electro-oxidation of aromatic aldehydes to methyl esters. *Helv. Chim. Acta* **1997,** *80* (5), 1555-1588.

57. Assaf, K. I.; Nau, W. M., Cucurbiturils: from synthesis to high-affinity binding and catalysis. *Chem. Soc. Rev.* **2015,** *44* (2), 394-418.

58. Mock, W. L.; Irra, T. A.; Wepsiec, J. P.; Manimaran, T. L., Cycloaddition Induced by Cucurbituril - a Case of Pauling Principle Catalysis. *J. Org. Chem.* **1983,** *48* (20), 3619-3620.

59. Espanol, E. S.; Villamil, M. M., Calixarenes: Generalities and Their Role in Improving the Solubility, Biocompatibility, Stability, Bioavailability, Detection, and Transport of Biomolecules. *Biomolecules* **2019,** *9* (3), 90.

60. Chwastek, M.; Szumna, A., Higher Analogues of Resorcinarenes and Pyrogallolarenes: Bricks for Supramolecular Chemistry. *Org. Lett.* **2020,** *22* (17), 6838-6841.

61. Purse, B. W.; Shivanyuk, A.; Rebek, J., Jr., Resorcin[6]arene as a building block for tubular crystalline state architectures. *Chem. Commun.* **2002,** (22), 2612-3.

62. Brown, P. O.; Enright, G. D.; Ripmeester, J. A., Pseudopolymorphism of ethylpyrogall[6]arene: Investigating the role of solvent in guiding self-assembly of 3D networks. *Cryst. Growth Des.* **2006,** *6* (3), 719-725.

63. Gajjar, J. A.; Vekariya, R. H.; Parekh, H. M., Recent advances in upper rim functionalization of resorcin[4]arene derivatives: Synthesis and applications. *Synth. Commun.* **2020,** *50* (17), 2545-2571.

64. He, Q.; Vargas-Zuniga, G. I.; Kim, S. H.; Kim, S. K.; Sessler, J. L., Macrocycles as Ion Pair Receptors. *Chem. Rev.* **2019,** *119* (17), 9753-9835.

65. Zhang, K. D.; Ajami, D.; Rebek, J., Hydrogen-bonded capsules in water. *J. Am. Chem. Soc.* **2013,** *135* (48), 18064-6.

66. Shi, Q.; Masseroni, D.; Rebek, J., Jr., Macrocyclization of Folded Diamines in Cavitands. *J. Am. Chem. Soc.* **2016,** *138* (34), 10846-8.

67. Shi, Q.; Mower, M. P.; Blackmond, D. G.; Rebek, J., Jr., Water-soluble cavitands promote hydrolyses of long-chain diesters. *Proc. Natl. Acad. Sci. U.S.A.* **2016,** *113* (33), 9199-203.

68. Nemat, S. J.; Jedrzejewska, H.; Prescimone, A.; Szumna, A.; Tiefenbacher, K., Catechol[4]arene: The Missing Chiral Member of the Calix[4]arene Family. *Org. Lett.* **2020,** *22* (14), 5506-5510.

69. Ogoshi, T.; Kanai, S.; Fujinami, S.; Yamagishi, T. A.; Nakamoto, Y., para-Bridged symmetrical pillar[5]arenes: their Lewis acid catalyzed synthesis and host-guest property. *J. Am. Chem. Soc.* **2008,** *130* (15), 5022-3.

70. Zhang, Q.; Zhang, Y. E.; Tong, S.; Wang, M. X., Hydrocarbon Belts with Truncated Cone Structures. *J. Am. Chem. Soc.* **2020,** *142* (3), 1196-1199.

71. Cook, T. R.; Zheng, Y. R.; Stang, P. J., Metal-organic frameworks and self-assembled supramolecular coordination complexes: comparing and contrasting the design, synthesis, and functionality of metal-organic materials. *Chem. Rev.* **2013,** *113* (1), 734-77.

72. Wiester, M. J.; Ulmann, P. A.; Mirkin, C. A., Enzyme mimics based upon supramolecular coordination chemistry. *Angew. Chem. Int. Ed.* **2011,** *50* (1), 114-37.

73. Leenders, S. H.; Gramage-Doria, R.; de Bruin, B.; Reek, J. N., Transition metal catalysis in confined spaces. *Chem. Soc. Rev.* **2015,** *44* (2), 433-48.

74. Zhang, D.; Ronson, T. K.; Nitschke, J. R., Functional Capsules via Subcomponent Self-Assembly. *Acc. Chem. Res.* **2018,** *51* (10), 2423-2436.

75. Hong, C. M.; Bergman, R. G.; Raymond, K. N.; Toste, F. D., Self-Assembled Tetrahedral Hosts as Supramolecular Catalysts. *Acc. Chem. Res.* **2018,** *51* (10), 2447-2455.

76. Yoshizawa, M.; Catti, L., Bent Anthracene Dimers as Versatile Building Blocks for Supramolecular Capsules. *Acc. Chem. Res.* **2019,** *52* (8), 2392-2404.

77. Fujita, D.; Ueda, Y.; Sato, S.; Mizuno, N.; Kumasaka, T.; Fujita, M., Self-assembly of tetravalent Goldberg polyhedra from 144 small components. *Nature* **2016,** *540* (7634), 563-566.

78. Brown, C. J.; Toste, F. D.; Bergman, R. G.; Raymond, K. N., Supramolecular catalysis in metal-ligand cluster hosts. *Chem. Rev.* **2015,** *115* (9), 3012-35.

79. Fujita, M.; Oguro, D.; Miyazawa, M.; Oka, H.; Yamaguchi, K.; Ogura, K., Self-assembly of ten molecules into nanometre-sized organic host frameworks. *Nature* **1995,** *378* (6556), 469-471.

80. Murase, T.; Peschard, S.; Horiuchi, S.; Nishioka, Y.; Fujita, M., Remote chiral transfer into [2+2] and [2+4] cycloadditions within self-assembled molecular flasks. *Supramol. Chem.* **2011,** *23* (3-4), 199-208.

81. Takezawa, H.; Shitozawa, K.; Fujita, M., Enhanced reactivity of twisted amides inside a molecular cage. *Nat. Chem.* **2020,** *12* (6), 574-578.

82. Caulder, D. L.; Powers, R. E.; Parac, T. N.; Raymond, K. N., The self-assembly of a predesigned tetrahedral M4L6 supramolecular cluster. *Angew. Chem. Int. Ed.* **1998,** *37* (13-14), 1840-1843.

83. Davis, A. V.; Fiedler, D.; Seeber, G.; Zahl, A.; van Eldik, R.; Raymond, K. N., Guest exchange dynamics in an M4L6 tetrahedral host. *J. Am. Chem. Soc.* **2006,** *128* (4), 1324-33.

84. Davis, A. V.; Fiedler, D.; Ziegler, M.; Terpin, A.; Raymond, K. N., Resolution of chiral, tetrahedral M4L6 metal-ligand hosts. *J. Am. Chem. Soc.* **2007,** *129* (49), 15354-63.

85. Zhao, C.; Sun, Q. F.; Hart-Cooper, W. M.; DiPasquale, A. G.; Toste, F. D.; Bergman, R. G.; Raymond, K. N., Chiral amide directed assembly of a diastereo- and enantiopure supramolecular host and its application to enantioselective catalysis of neutral substrates. *J. Am. Chem. Soc.* **2013,** *135* (50), 18802-5.

86. Pluth, M. D.; Bergman, R. G.; Raymond, K. N., Acid catalysis in basic solution: a supramolecular host promotes orthoformate hydrolysis. *Science* **2007,** *316* (5821), 85-8.

87. Fiedler, D.; Bergman, R. G.; Raymond, K. N., Supramolecular catalysis of a unimolecular transformation: aza-Cope rearrangement within a self-assembled host. *Angew. Chem. Int. Ed.* **2004,** *43* (48), 6748-51.

88. Hastings, C. J.; Pluth, M. D.; Bergman, R. G.; Raymond, K. N., Enzymelike catalysis of the Nazarov cyclization by supramolecular encapsulation. *J. Am. Chem. Soc.* **2010,** *132* (20), 6938-40.

89. Hart-Cooper, W. M.; Clary, K. N.; Toste, F. D.; Bergman, R. G.; Raymond, K. N., Selective monoterpene-like cyclization reactions achieved by water exclusion from reactive intermediates in a supramolecular catalyst. *J. Am. Chem. Soc.* **2012,** *134* (43), 17873-6.

90. Brown, C. J.; Bergman, R. G.; Raymond, K. N., Enantioselective catalysis of the aza-Cope rearrangement by a chiral supramolecular assembly. *J. Am. Chem. Soc.* **2009,** *131* (48), 17530-1.

91. Bolliger, J. L.; Belenguer, A. M.; Nitschke, J. R., Enantiopure water-soluble [Fe4L6] cages: host-guest chemistry and catalytic activity. *Angew. Chem. Int. Ed.* **2013,** *52* (31), 7958-62.

92. Slagt, V. F.; Reek, J. N. H.; Kamer, P. C. J.; van Leeuwen, P., Assembly of Encapsulated Transition Metal Catalysts. *Angew. Chem. Int. Ed.* **2001,** *40* (22), 4271-4274.

93. Slagt, V. F.; Kamer, P. C.; van Leeuwen, P. W.; Reek, J. N., Encapsulation of transition metal catalysts by ligand-template directed assembly. *J. Am. Chem. Soc.* **2004,** *126* (5), 1526-36.

94. Gadzikwa, T.; Bellini, R.; Dekker, H. L.; Reek, J. N., Self-assembly of a confined rhodium catalyst for asymmetric hydroformylation of unfunctionalized internal alkenes. *J. Am. Chem. Soc.* **2012,** *134* (6), 2860-3.

95. Koblenz, T. S.; Wassenaar, J.; Reek, J. N., Reactivity within a confined self-assembled nanospace. *Chem. Soc. Rev.* **2008,** *37* (2), 247-62.

96. Mouarrawis, V.; Plessius, R.; van der Vlugt, J. I.; Reek, J. N. H., Confinement Effects in Catalysis Using Well-Defined Materials and Cages. *Front. Chem.* **2018,** *6*, 623.

97. Adriaenssens, L.; Ballester, P., Hydrogen bonded supramolecular capsules with functionalized interiors: the controlled orientation of included guests. *Chem. Soc. Rev.* **2013,** *42* (8), 3261-77.

98. Raynal, M.; Ballester, P.; Vidal-Ferran, A.; van Leeuwen, P. W., Supramolecular catalysis. Part 2: artificial enzyme mimics. *Chem. Soc. Rev.* **2014,** *43* (5), 1734-87.

99. Liu, L. J.; Rebek, J., Hydrogen Bonded Capsules: Chemistry in Small Spaces. In *Hydrogen Bonded Supramolecular Structures*, Li, Z.-T.; Wu, L.-Z., Eds. Springer Berlin Heidelberg: Berlin, Heidelberg, 2015; pp 227-248.

100. Avram, L.; Cohen, Y.; Rebek, J., Jr., Recent advances in hydrogen-bonded hexameric encapsulation complexes. *Chem. Commun.* **2011,** *47* (19), 5368-75.

101. Meissner, R. S.; Rebek, J., Jr.; de Mendoza, J., Autoencapsulation through intermolecular forces: a synthetic self-assembling spherical complex. *Science* **1995,** *270* (5241), 1485-8.

102. Mecozzi, S.; Rebek, J., The 55% solution: A formula for molecular recognition in the liquid state. *Chem. Eur. J.* **1998,** *4* (6), 1016-1022.

103. Kang, J. M.; Santamaria, J.; Hilmersson, G.; Rebek, J., Self-assembled molecular capsule catalyzes a Diels-Alder reaction. *J. Am. Chem. Soc.* **1998,** *120* (29), 7389-7390.

104. Chen, J.; Rebek, J., Jr., Selectivity in an encapsulated cycloaddition reaction. *Org. Lett.* **2002,** *4* (3), 327-9.

105. Grajda, M.; Lewinska, M. J.; Szumna, A., The templation effect as a driving force for the self-assembly of hydrogen-bonded peptidic capsules in competitive media. *Org. Biomol. Chem.* **2017,** *15* (40), 8513-8517.

106. MacGillivray, L. R.; Atwood, J. L., A chiral spherical molecular assembly held together by 60 hydrogen bonds. *Nature* **1997,** *389* (6650), 469-472.

107. Gerkensmeier, T.; Iwanek, W.; Agena, C.; Frohlich, R.; Kotila, S.; Nather, C.; Mattay, J., Self-assembly of 2,8,14,20-tetraisobutyl-5,11,17,23-tetrahydroxyresorc[4]arene. *Eur. J. Org. Chem.* **1999,** *1999* (9), 2257-2262.

108. Atwood, J. L.; Barbour, L. J.; Jerga, A., Hydrogen-bonded molecular capsules are stable in polar media. *Chem. Commun.* **2001,** (22), 2376-7.

109. Shivanyuk, A.; Rebek, J., Jr., Hydrogen-bonded capsules in polar, protic solvents. *Chem. Commun.* **2001,** (22), 2374-5.

110. Avram, L.; Cohen, Y., Spontaneous formation of hexameric resorcinarene capsule in chloroform solution as detected by diffusion NMR. *J. Am. Chem. Soc.* **2002,** *124* (51), 15148-9.

111. Merget, S.; Catti, L.; Piccini, G.; Tiefenbacher, K., Requirements for Terpene Cyclizations inside the Supramolecular Resorcinarene Capsule: Bound Water and Its Protonation Determine the Catalytic Activity. *J. Am. Chem. Soc.* **2020,** *142* (9), 4400-4410.

112. Shivanyuk, A.; Rebek, J., Jr., Reversible encapsulation by self-assembling resorcinarene subunits. *Proc. Natl. Acad. Sci. U.S.A.* **2001,** *98* (14), 7662-5.

113. Avram, L.; Cohen, Y., The role of water molecules in a resorcinarene capsule as probed by NMR diffusion measurements. *Org. Lett.* **2002,** *4* (24), 4365-8.

114. Avram, L.; Cohen, Y., Hexameric capsules of lipophilic pyrogallolarene and resorcinarene in solutions as probed by diffusion NMR: one hydroxyl makes the difference. *Org. Lett.* **2003,** *5* (18), 3329-32.

115. Avram, L.; Cohen, Y., Discrimination of guests encapsulation in large hexameric molecular capsules in solution: pyrogallol[4]arene versus resorcin[4]arene capsules. *J. Am. Chem. Soc.* **2003,** *125* (52), 16180-1.

116. Slovak, S.; Cohen, Y., The effect of alcohol structures on the interaction mode with the hexameric capsule of resorcin[4]arene. *Chem. Eur. J.* **2012,** *18* (27), 8515-20.

117. Evan-Salem, T.; Baruch, I.; Avram, L.; Cohen, Y.; Palmer, L. C.; Rebek, J., Jr., Resorcinarenes are hexameric capsules in solution. *Proc. Natl. Acad. Sci. U.S.A.* **2006,** *103* (33), 12296-300.

118. Horiuchi, S.; Tanaka, H.; Sakuda, E.; Arikawa, Y.; Umakoshi, K., Encapsulation and Enhanced Luminescence Properties of Ir(III) Complexes within a Hexameric Self-Assembled Capsule. *Chem. Eur. J.* **2016,** *22* (49), 17533-17537.

119. Mileo, E.; Yi, S.; Bhattacharya, P.; Kaifer, A. E., Probing the inner space of resorcinarene molecular capsules with nitroxide guests. *Angew. Chem. Int. Ed.* **2009,** *48* (29), 5337-40.

120. Zhang, Q.; Catti, L.; Kaila, V. R. I.; Tiefenbacher, K., To catalyze or not to catalyze: elucidation of the subtle differences between the hexameric capsules of pyrogallolarene and resorcinarene. *Chem. Sci.* **2017,** *8* (2), 1653-1657.

121. Yariv-Shoushan, S.; Cohen, Y., Encapsulated or Not Encapsulated? Ammonium Salts Can Be Encapsulated in Hexameric Capsules of Pyrogallol[4]arene. *Org. Lett.* **2016,** *18* (5), 936-9.

122. Chapin, J. C.; Kvasnica, M.; Purse, B. W., Molecular encapsulation in pyrogallolarene hexamers under nonequilibrium conditions. *J. Am. Chem. Soc.* **2012,** *134* (36), 15000-9.

123. Journey, S. N.; Teppang, K. L.; Garcia, C. A.; Brim, S. A.; Onofrei, D.; Addison, J. B.; Holland, G. P.; Purse, B. W., Mechanically induced pyrogallol[4]arene hexamer assembly in the solid state extends the scope of molecular encapsulation. *Chem. Sci.* **2017,** *8* (11), 7737-7745.

124. Beaudoin, D.; Rominger, F.; Mastalerz, M., Chirality-Assisted Synthesis of a Very Large Octameric Hydrogen-Bonded Capsule. *Angew. Chem. Int. Ed.* **2016,** *55* (50), 15599-15603.

125. Jans, A. C. H.; Caumes, X.; Reek, J. N. H., Gold Catalysis in (Supra)Molecular Cages to Control Reactivity and Selectivity. *ChemCatChem* **2019,** *11* (1), 287-297.

126. Cavarzan, A.; Scarso, A.; Sgarbossa, P.; Strukul, G.; Reek, J. N., Supramolecular control on chemo- and regioselectivity via encapsulation of (NHC)-Au catalyst within a hexameric self-assembled host. *J. Am. Chem. Soc.* **2011,** *133* (9), 2848-51.

127. Cavarzan, A.; Reek, J. N. H.; Trentin, F.; Scarso, A.; Strukul, G., Substrate selectivity in the alkyne hydration mediated by NHC-Au(I) controlled by encapsulation of the catalyst within a hydrogen bonded hexameric host. *Catal. Sci. Technol.* **2013,** *3* (11), 2898-2901.

128. Jans, A. C.; Gomez-Suarez, A.; Nolan, S. P.; Reek, J. N., A Switchable Gold Catalyst by Encapsulation in a Self-Assembled Cage. *Chem. Eur. J.* **2016,** *22* (42), 14836-14839.

129. Bianchini, G.; Scarso, A.; La Sorella, G.; Strukul, G., Switching the activity of a photoredox catalyst through reversible encapsulation and release. *Chem. Commun.* **2012,** *48* (99), 12082-4.

130. Bianchini, G.; La Sorella, G.; Canever, N.; Scarso, A.; Strukul, G., Efficient isonitrile hydration through encapsulation within a hexameric self-assembled capsule and selective inhibition by a photo-controllable competitive guest. *Chem. Commun.* **2013,** *49* (46), 5322-4.

131. Zhang, Q.; Tiefenbacher, K., Hexameric resorcinarene capsule is a Bronsted acid: investigation and application to synthesis and catalysis. *J. Am. Chem. Soc.* **2013,** *135* (43), 16213-9.

132. Köster, J. M.; Tiefenbacher, K., Elucidating the Importance of Hydrochloric Acid as a Cocatalyst for Resorcinarene-Capsule-Catalyzed Reactions. *ChemCatChem* **2018,** *10* (14), 2941-2944.

133. Giust, S.; La Sorella, G.; Sperni, L.; Fabris, F.; Strukul, G.; Scarso, A., Supramolecular Catalysis in the Synthesis of Substituted 1 H-Tetrazoles from Isonitriles by a Self-Assembled Hexameric Capsule. *Asian J. Org. Chem.* **2015,** *4* (3), 217-220.

134. La Sorella, G.; Sperni, L.; Strukul, G.; Scarso, A., Supramolecular Encapsulation of Neutral Diazoacetate Esters and Catalyzed 1,3-Dipolar Cycloaddition Reaction by a Self-Assembled Hexameric Capsule. *ChemCatChem* **2015,** *7* (2), 291-296.

135. Catti, L.; Tiefenbacher, K., Intramolecular hydroalkoxylation catalyzed inside a self-assembled cavity of an enzyme-like host structure. *Chem. Commun.* **2015,** *51* (5), 892-4.

136. Catti, L.; Pothig, A.; Tiefenbacher, K., Host-Catalyzed Cyclodehydration-Rearrangement Cascade Reaction of Unsaturated Tertiary Alcohols. *Adv. Synth. Catal.* **2017,** *359* (8), 1331-1338.

137. La Sorella, G.; Sperni, L.; Ballester, P.; Strukul, G.; Scarso, A., Hydration of aromatic alkynes catalyzed by a self-assembled hexameric organic capsule. *Catal. Sci. Technol.* **2016,** *6* (15), 6031-6036.

138. Caneva, T.; Sperni, L.; Strukul, G.; Scarso, A., Efficient epoxide isomerization within a self-assembled hexameric organic capsule. *RSC Adv.* **2016,** *6* (87), 83505-83509.

139. Zhang, Q.; Catti, L.; Pleiss, J.; Tiefenbacher, K., Terpene Cyclizations inside a Supramolecular Catalyst: Leaving-Group-Controlled Product Selectivity and Mechanistic Studies. *J. Am. Chem. Soc.* **2017,** *139* (33), 11482-11492.

140. Zhang, Q.; Tiefenbacher, K., Sesquiterpene Cyclizations inside the Hexameric Resorcinarene Capsule: Total Synthesis of delta-Selinene and Mechanistic Studies. *Angew. Chem. Int. Ed.* **2019,** *58* (36), 12688-12695.

141. Zhang, Q.; Rinkel, J.; Goldfuss, B.; Dickschat, J. S.; Tiefenbacher, K., Sesquiterpene Cyclisations Catalysed inside the Resorcinarene Capsule and Application in the Short Synthesis of Isolongifolene and Isolongifolenone. *Nat. Catal.* **2018,** *1* (8), 609-615.

142. Syntrivanis, L. D.; Nemethova, I.; Schmid, D.; Levi, S.; Prescimone, A.; Bissegger, F.; Major, D. T.; Tiefenbacher, K., Four-Step Access to the Sesquiterpene Natural Product Presilphiperfolan-1beta-ol and Unnatural Derivatives via Supramolecular Catalysis. *J. Am. Chem. Soc.* **2020,** *142* (12), 5894-5900.

143. Brauer, T. M.; Zhang, Q.; Tiefenbacher, K., Iminium Catalysis inside a Self-Assembled Supramolecular Capsule: Modulation of Enantiomeric Excess. *Angew. Chem. Int. Ed.* **2016,** *55* (27), 7698-701.

144. Brauer, T. M.; Zhang, Q.; Tiefenbacher, K., Iminium Catalysis inside a Self-Assembled Supramolecular Capsule: Scope and Mechanistic Studies. *J. Am. Chem. Soc.* **2017,** *139* (48), 17500-17507.

145. Catti, L.; Tiefenbacher, K., Bronsted Acid-Catalyzed Carbonyl-Olefin Metathesis inside a Self-Assembled Supramolecular Host. *Angew. Chem. Int. Ed.* **2018,** *57* (44), 14589-14592.

146. Gambaro, S.; De Rosa, M.; Soriente, A.; Talotta, C.; Floresta, G.; Rescifina, A.; Gaeta, C.; Neri, P., A hexameric resorcinarene capsule as a hydrogen bonding catalyst in the conjugate addition of pyrroles and indoles to nitroalkenes. *Org. Chem. Front.* **2019,** *6* (14), 2339-2347.

147. La Manna, P.; De Rosa, M.; Talotta, C.; Rescifina, A.; Floresta, G.; Soriente, A.; Gaeta, C.; Neri, P., Synergic Interplay Between Halogen Bonding and Hydrogen Bonding in the Activation of a Neutral Substrate in a Nanoconfined Space. *Angew. Chem. Int. Ed.* **2020,** *59* (2), 811-818.

148. La Manna, P.; Talotta, C.; De Rosa, M.; Soriente, A.; Gaeta, C.; Neri, P., An Atom-Economical Method for the Formation of Amidopyrroles Exploiting the Self-Assembled Resorcinarene Capsule. *Org. Lett.* **2020,** *22* (7), 2590-2594.

149. Rackauskaite, D.; Bergquist, K. E.; Shi, Q.; Sundin, A.; Butkus, E.; Warnmark, K.; Orentas, E., A Remarkably Complex Supramolecular Hydrogen-Bonded Decameric Capsule Formed from an Enantiopure C(2)-Symmetric Monomer by Solvent-Responsive Aggregation. *J. Am. Chem. Soc.* **2015,** *137* (33), 10536-46.

150. Markiewicz, G.; Jenczak, A.; Kolodziejski, M.; Holstein, J. J.; Sanders, J. K. M.; Stefankiewicz, A. R., Selective C70 encapsulation by a robust octameric nanospheroid held together by 48 cooperative hydrogen bonds. *Nat. Commun.* **2017,** *8*, 15109.

151. Gerkensmeier, T.; Mattay, J.; Nather, C., A new type of calixarene: Octahydroxypyridine[4]arenes. *Chem. Eur. J.* **2001,** *7* (2), 465-474.

152. Letzel, M. C.; Decker, B.; Rozhenko, A. B.; Schoeller, W. W.; Mattay, J., Encapsulated guest molecules in the dimer of octahydroxypyridine[4]arene. *J. Am. Chem. Soc.* **2004,** *126* (31), 9669-74.

153. Evan-Salem, T.; Cohen, Y., Octahydroxypyridine[4]arene self-assembles spontaneously to form hexameric capsules and dimeric aggregates. *Chem. Eur. J.* **2007,** *13* (27), 7659-63.

154. Kiesila, A.; Beyeh, N. K.; Moilanen, J. O.; Puttreddy, R.; Gotz, S.; Rissanen, K.; Barran, P.; Lutzen, A.; Kalenius, E., Thermodynamically driven self-assembly of pyridinearene to hexameric capsules. *Org. Biomol. Chem.* **2019,** *17* (29), 6980-6984.

155. Jordan, J. H.; Gibb, B. C., Molecular containers assembled through the hydrophobic effect. *Chem. Soc. Rev.* **2015,** *44* (2), 547-85.

156. Gibb, C. L.; Gibb, B. C., Well-defined, organic nanoenvironments in water: the hydrophobic effect drives a capsular assembly. *J. Am. Chem. Soc.* **2004,** *126* (37), 11408-9.

157. Gibb, C. L.; Gibb, B. C., Templated assembly of water-soluble nano-capsules: inter-phase sequestration, storage, and separation of hydrocarbon gases. *J. Am. Chem. Soc.* **2006,** *128* (51), 16498-9.

158. Kaanumalle, L. S.; Gibb, C. L.; Gibb, B. C.; Ramamurthy, V., Controlling photochemistry with distinct hydrophobic nanoenvironments. *J. Am. Chem. Soc.* **2004,** *126* (44), 14366-7.

159. Kondo, K.; Suzuki, A.; Akita, M.; Yoshizawa, M., Micelle-like molecular capsules with anthracene shells as photoactive hosts. *Angew. Chem. Int. Ed.* **2013,** *52* (8), 2308-12.

160. Kondo, K.; Suzuki, A.; Akita, M.; Yoshizawa, M., Micellar Polyaromatic Capsules: Enhanced Emissive Properties through Shell-Functionalization. *Eur. J. Org. Chem.* **2014,** *2014* (33), 7389-7394.

161. Suzuki, A.; Kondo, K.; Akita, M.; Yoshizawa, M., Atroposelective self-assembly of a molecular capsule from amphiphilic anthracene trimers. *Angew. Chem. Int. Ed.* **2013,** *52* (31), 8120-3.

162. Kondo, K.; Akita, M.; Nakagawa, T.; Matsuo, Y.; Yoshizawa, M., A V-shaped polyaromatic amphiphile: solubilization of various nanocarbons in water and enhanced photostability. *Chem. Eur. J.* **2015,** *21* (36), 12741-6.

163. Kondo, K.; Akita, M.; Yoshizawa, M., Solubility Switching of Metallophthalocyanines and Their Larger Derivatives upon Encapsulation. *Chem. Eur. J.* **2016,** *22* (6), 1937-1940.

164. Omagari, T.; Suzuki, A.; Akita, M.; Yoshizawa, M., Efficient Catalytic Epoxidation in Water by Axial N-Ligand-Free Mn-Porphyrins within a Micellar Capsule. *J. Am. Chem. Soc.* **2016,** *138* (2), 499-502.

165. Kishimoto, M.; Kondo, K.; Akita, M.; Yoshizawa, M., A pH-responsive molecular capsule with an acridine shell: catch and release of large hydrophobic compounds. *Chem. Commun.* **2017,** *53* (8), 1425-1428.

166. Catti, L.; Kishida, N.; Kai, T.; Akita, M.; Yoshizawa, M., Polyaromatic nanocapsules as photoresponsive hosts in water. *Nat. Commun.* **2019,** *10* (1), 1948.

167. Gilday, L. C.; Robinson, S. W.; Barendt, T. A.; Langton, M. J.; Mullaney, B. R.; Beer, P. D., Halogen Bonding in Supramolecular Chemistry. *Chem. Rev.* **2015,** *115* (15), 7118-95.

168. Aakeroy, C. B.; Rajbanshi, A.; Metrangolo, P.; Resnati, G.; Parisi, M. F.; Desper, J.; Pilati, T., The quest for a molecular capsule assembled via halogen bonds. *Crystengcomm* **2012,** *14* (20), 6366-6368.

169. Dumele, O.; Trapp, N.; Diederich, F., Halogen bonding molecular capsules. *Angew. Chem. Int. Ed.* **2015,** *54* (42), 12339-44.

170. Dumele, O.; Schreib, B.; Warzok, U.; Trapp, N.; Schalley, C. A.; Diederich, F., Halogen-Bonded Supramolecular Capsules in the Solid State, in Solution, and in the Gas Phase. *Angew. Chem. Int. Ed.* **2017,** *56* (4), 1152-1157.

171. Beyeh, N. K.; Pan, F.; Rissanen, K., A Halogen-Bonded Dimeric Resorcinarene Capsule. *Angew. Chem. Int. Ed.* **2015,** *54* (25), 7303-7.

172. Turunen, L.; Peuronen, A.; Forsblom, S.; Kalenius, E.; Lahtinen, M.; Rissanen, K., Tetrameric and Dimeric [NI(+) N] Halogen-Bonded Supramolecular Cages. *Chem. Eur. J.* **2017,** *23* (48), 11714-11718.

173. Benz, S.; Lopez-Andarias, J.; Mareda, J.; Sakai, N.; Matile, S., Catalysis with Chalcogen Bonds. *Angew. Chem. Int. Ed.* **2017,** *56* (3), 812-815.

174. Ho, P. C.; Szydlowski, P.; Sinclair, J.; Elder, P. J.; Kubel, J.; Gendy, C.; Lee, L. M.; Jenkins, H.; Britten, J. F.; Morim, D. R.; Vargas-Baca, I., Supramolecular macrocycles reversibly assembled by Te(...)O chalcogen bonding. *Nat. Commun.* **2016,** *7*, 11299.

175. Mastalerz, M., Porous Shape-Persistent Organic Cage Compounds of Different Size, Geometry, and Function. *Acc. Chem. Res.* **2018,** *51* (10), 2411-2422.

176. Zhang, G.; Mastalerz, M., Organic cage compounds--from shape-persistency to function. *Chem. Soc. Rev.* **2014,** *43* (6), 1934-47.

177. Little, M. A.; Cooper, A. I., The Chemistry of Porous Organic Molecular Materials. *Adv. Funct. Mater.* **2020,** *30* (41), 1909842.

178. Quan, M. L. C.; Cram, D. J., Constrictive binding of large guests by a hemicarcerand containing four portals. *J. Am. Chem. Soc.* **2002,** *113* (7), 2754-2755.

179. Liu, X.; Liu, Y.; Li, G.; Warmuth, R., One-pot, 18-component synthesis of an octahedral nanocontainer molecule. *Angew. Chem. Int. Ed.* **2006,** *45* (6), 901-4.

180. Liu, Y.; Liu, X.; Warmuth, R., Multicomponent dynamic covalent assembly of a rhombicuboctahedral nanocapsule. *Chem. Eur. J.* **2007,** *13* (32), 8953-9.

181. Sun, J.; Warmuth, R., Rational design of a nanometre-sized covalent octahedron. *Chem. Commun.* **2011,** *47* (33), 9351-3.

182. Liu, X.; Warmuth, R., Solvent effects in thermodynamically controlled multicomponent nanocage syntheses. *J. Am. Chem. Soc.* **2006,** *128* (43), 14120-7.

183. Wierzbicki, M.; Glowacka, A. A.; Szymanski, M. P.; Szumna, A., A chiral member of the family of organic hexameric cages. *Chem. Commun.* **2017,** *53* (37), 5200-5203.

184. Brutschy, M.; Schneider, M. W.; Mastalerz, M.; Waldvogel, S. R., Porous organic cage compounds as highly potent affinity materials for sensing by quartz crystal microbalances. *Adv. Mater.* **2012,** *24* (45), 6049-52.

185. Song, Q.; Jiang, S.; Hasell, T.; Liu, M.; Sun, S.; Cheetham, A. K.; Sivaniah, E.; Cooper, A. I., Porous Organic Cage Thin Films and Molecular-Sieving Membranes. *Adv. Mater.* **2016,** *28* (13), 2629-37.

186. Zhang, J. H.; Xie, S. M.; Chen, L.; Wang, B. J.; He, P. G.; Yuan, L. M., Homochiral Porous Organic Cage with High Selectivity for the Separation of Racemates in Gas Chromatography. *Anal. Chem.* **2015,** *87* (15), 7817-24.

187. Kewley, A.; Stephenson, A.; Chen, L. J.; Briggs, M. E.; Hasell, T.; Cooper, A. I., Porous Organic Cages for Gas Chromatography Separations. *Chem. Mater.* **2015,** *27* (9), 3207-3210.

7. Bibliographic Data of Complete Publications

The following chapter provides the bibliographic data of the publications included in this thesis. Summaries can be found in Section 5.1.

Requirements for Terpene Cyclizations inside the Supramolecular Resorcinarene Capsule: Bound Water and its Protonation Determine the Catalytic Activity

Severin Merget[a], Lorenzo Catti[b], GiovanniMaria Piccini[c], Konrad Tiefenbacher*[a, d]

[a] Department of Chemistry, University of Basel, Mattenstrasse 24a, CH-4058 Basel, Switzerland

[b] Address at the time of publication: Laboratory for Chemistry and Life Sciences, Tokyo Institute of Technology, 4259 Nagatsuta, Midori-ku, Yokohama 226-8503, Japan
Current Address:

[c] Department of Chemistry and Applied Biosciences, ETH Zurich, c/o USI Campus, Via Giuseppe Buffi 13, CH-6900 Lugano, Switzerland; Facoltàdi Informatica, Istituto di Scienze Computazionali, Universitàdella SvizzeraItaliana (USI), Via Giuseppe Buffi 13, CH-6900 Lugano, Switzerland

[d] Department of Biosystems Science and Engineering, ETH Zürich, Mattenstrasse 26, CH-4058 Basel, Switzerland

*Corresponding Author: konrad.tiefenbacher@unibas.ch; tkonrad@ethz.ch

Originally published in: *J. Am. Chem. Soc.* **2020**, *142*, 4400−4410

DOI: 10.1021/jacs.9b13239

URL: https://pubs.acs.org/doi/abs/10.1021/jacs.9b13239

Concentration-dependent Self-assembly of an Unusually Large Hexameric Hydrogen-bonded Molecular Cage

Severin Merget[a], Lorenzo Catti[b], Shani Zev[c], Dan T. Major[c], Nils Trapp[d] and Konrad Tiefenbacher*[a, e]

[a] Department of Chemistry, University of Basel, Mattenstrasse 24a, CH-4058 Basel, Switzerland

[b] WPI Nano Life Science Institute (WPI-NanoLSI), Kanazawa University, Kakuma-machi, Kanazawa 920-1192, Japan

[c] Department of Chemistry and Institute for Nanotechnology & Advanced Materials, Bar-Ilan University, Ramat-Gan 52900, Israel

[d] Department of Chemistry, Laboratorium für Organische Chemie, ETH Zurich, Vladimir-Prelog-Weg 3, CH-, 8093, Zurich, Switzerland

[e] Department of Biosystems Science and Engineering, ETH Zürich, Mattenstrasse 26, CH-4058 Basel, Switzerland

*Corresponding Author: konrad.tiefenbacher@unibas.ch; tkonrad@ethz.ch

Originally published in: *Chem. Eur. J.* **2021**, *27*, 4447−4453

DOI: 10.1002/chem.202005046

URL: https://chemistry-europe.onlinelibrary.wiley.com/doi/10.1002/chem.202005046

8. Reprints and Reprint Permissions

8.1 American Chemical Society

The manuscript published in *Journal of the American Chemical Society* and scheme 13 were reproduced with permission of American Chemical Society.

Requirements for Terpene Cyclizations inside the Supramolecular Resorcinarene Capsule: Bound Water and its Protonation Determine the Catalytic Activity

Merget, S., Catti, L., Piccini, G.M., Tiefenbacher, K. *J. Am. Chem. Soc.* **2020**, *142*, 4400−4410

DOI: 10.1021/jacs.9b13239

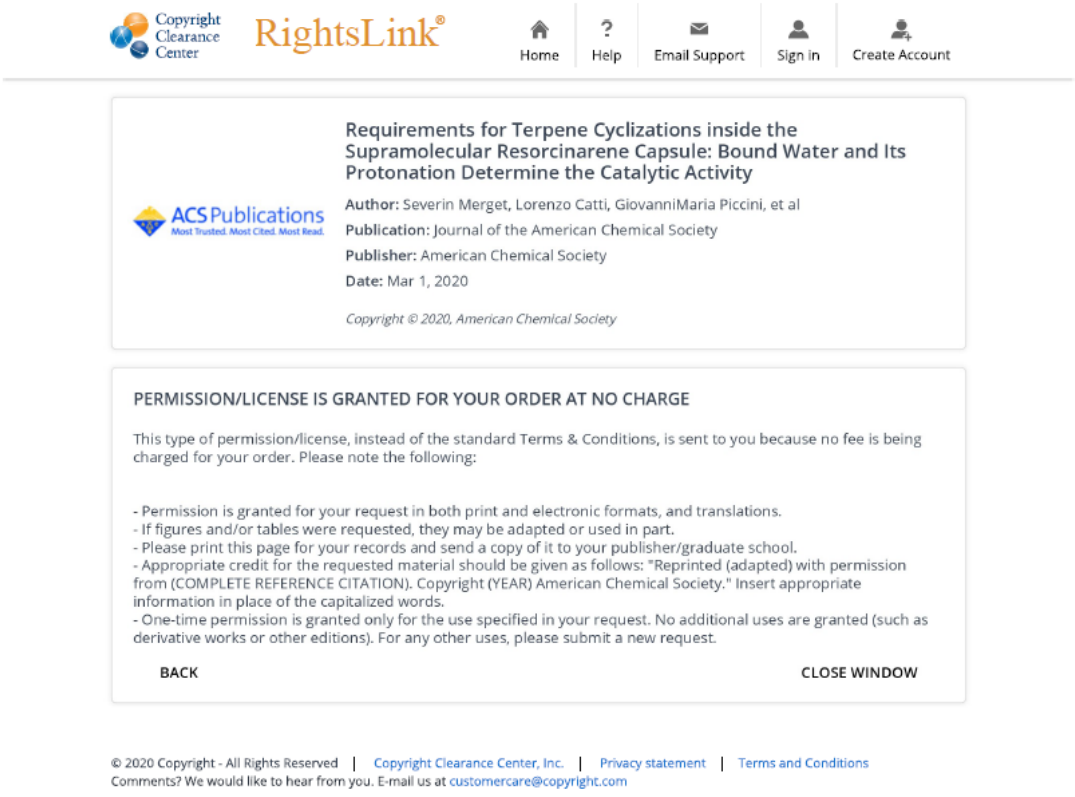

Scheme 18 was partly reproduced from reference[139] with permission of American Chemical Society.

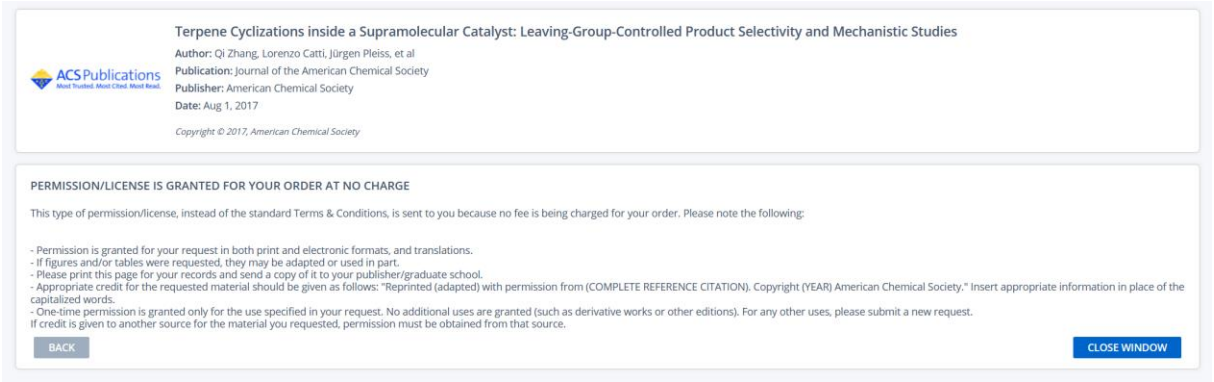

Terpene Cyclizations inside a Supramolecular Catalyst: Leaving-Group-Controlled Product Selectivity and Mechanistic Studies

Author: Qi Zhang, Lorenzo Catti, Jürgen Pleiss, et al
Publication: Journal of the American Chemical Society
Publisher: American Chemical Society
Date: Aug 1, 2017

Copyright © 2017, American Chemical Society

PERMISSION/LICENSE IS GRANTED FOR YOUR ORDER AT NO CHARGE

This type of permission/license, instead of the standard Terms & Conditions, is sent to you because no fee is being charged for your order. Please note the following:

- Permission is granted for your request in both print and electronic formats, and translations.
- If figures and/or tables were requested, they may be adapted or used in part.
- Please print this page for your records and send a copy of it to your publisher/graduate school.
- Appropriate credit for the requested material should be given as follows: "Reprinted (adapted) with permission from (COMPLETE REFERENCE CITATION). Copyright (YEAR) American Chemical Society." Insert appropriate information in place of the capitalized words.
- One-time permission is granted only for the use specified in your request. No additional uses are granted (such as derivative works or other editions). For any other uses, please submit a new request.

If credit is given to another source for the material you requested, permission must be obtained from that source.

BACK CLOSE WINDOW

Scheme 20 was partly reproduced from reference[144] with permission of American Chemical Society.

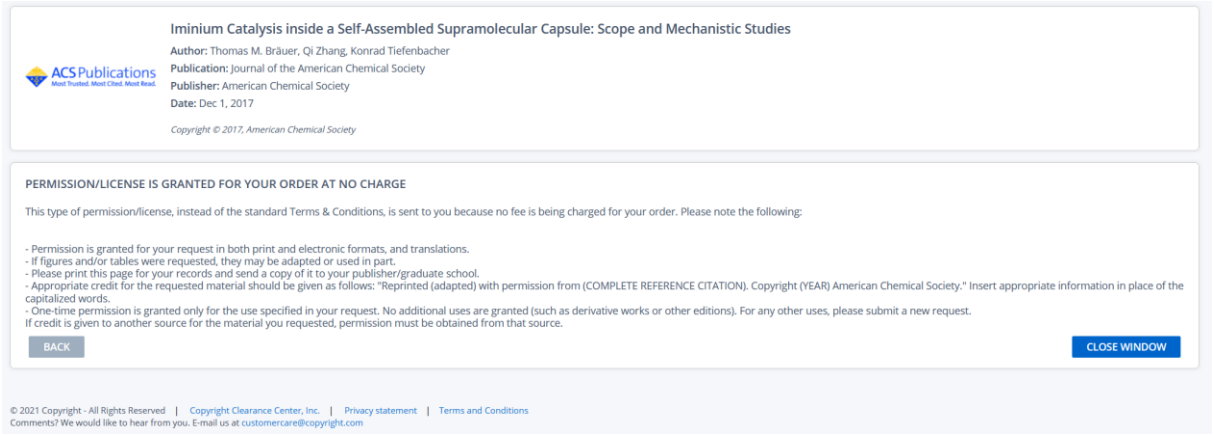

Iminium Catalysis inside a Self-Assembled Supramolecular Capsule: Scope and Mechanistic Studies

Author: Thomas M. Bräuer, Qi Zhang, Konrad Tiefenbacher
Publication: Journal of the American Chemical Society
Publisher: American Chemical Society
Date: Dec 1, 2017

Copyright © 2017, American Chemical Society

PERMISSION/LICENSE IS GRANTED FOR YOUR ORDER AT NO CHARGE

This type of permission/license, instead of the standard Terms & Conditions, is sent to you because no fee is being charged for your order. Please note the following:

- Permission is granted for your request in both print and electronic formats, and translations.
- If figures and/or tables were requested, they may be adapted or used in part.
- Please print this page for your records and send a copy of it to your publisher/graduate school.
- Appropriate credit for the requested material should be given as follows: "Reprinted (adapted) with permission from (COMPLETE REFERENCE CITATION). Copyright (YEAR) American Chemical Society." Insert appropriate information in place of the capitalized words.
- One-time permission is granted only for the use specified in your request. No additional uses are granted (such as derivative works or other editions). For any other uses, please submit a new request.

If credit is given to another source for the material you requested, permission must be obtained from that source.

BACK CLOSE WINDOW

JACS
JOURNAL OF THE AMERICAN CHEMICAL SOCIETY
pubs.acs.org/JACS
Article

Requirements for Terpene Cyclizations inside the Supramolecular Resorcinarene Capsule: Bound Water and Its Protonation Determine the Catalytic Activity

Severin Merget, Lorenzo Catti, GiovanniMaria Piccini, and Konrad Tiefenbacher*

Cite This: J. Am. Chem. Soc. 2020, 142, 4400−4410
Read Online
ACCESS | Metrics & More | Article Recommendations | Supporting Information

ABSTRACT: The elucidation of the requirements for efficient catalysis within supramolecular host systems is an important prerequisite for developing novel supramolecular catalysts. The resorcinarene hexamer has recently been shown to be the first supramolecular catalyst to promote the tail-to-head terpene cyclization in a biomimetic fashion. We herein present the synthesis of a number of resorcinarene-based macrocycles composed of different ratios of resorcinol and pyrogallol units capable of self-assembly and compare the corresponding assemblies regarding their catalytic activity in the cyclization of monoterpenes. The assemblies were investigated in detail with respect to a number of properties including the encapsulation of substrate and ion pairs, the structural incorporation of water, and the response to externally added acid (HCl). The results obtained strongly indicate that water incorporated into the hydrogen-bond network of the self-assembled structure plays an integral role for catalysis, effectively acting as a *proton shuttle* to activate the encapsulated substrate. These findings are also supported by molecular dynamics simulations, providing further insight into the protonation pathway and the relative energies of the intermediates involved.

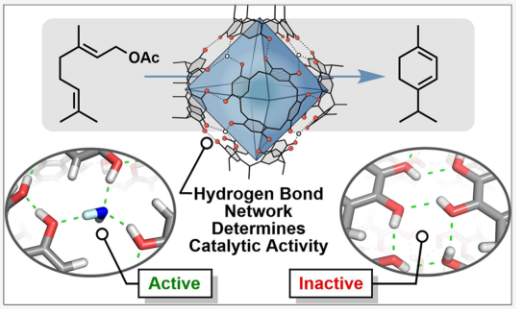

INTRODUCTION

The catalytic power and selectivity displayed by natural enzymes still serves as inspiration and role model for many organic chemists working in the broad field of catalysis.[1] Chemists successfully mimicked some aspects of enzyme catalysis utilizing self-assembled supramolecular host structures.[2,3]

Numerous reactions within different host structures have been reported; however, their catalytic efficiency and selectivity usually do not rival their natural counterparts. To close this gap, and to design new, more efficient catalysts, it is essential to understand the fundamental requirements for catalytic activity in these artificial systems.

One of the most frequently applied supramolecular catalyst is the hexameric capsule **I** (Figure 1a). It self-assembles from six units of resorcinarene **1** and eight molecules of water in apolar media such as chloroform.[4] A number of reactions involving mainly cationic transition states have been reported using structure **I** as a catalyst.[2k,n,q−s] A prime example is the successful catalysis of the tail-to-head terpene (THT) cyclization inside **I** developed by our group,[5] which utilizes the supramolecular cavity to enable a reaction that is very difficult to perform in bulk solution.[6] Terpenes form one of the largest classes of natural products with remarkable structural diversity. Many members exhibit interesting biological activity, making them suitable lead compounds for drug development.[7] Since most compounds in this class require considerable synthetic effort and are often not available in significant quantity, an efficient method to access these compounds from rather simple precursors would provide a powerful tool to the organic synthetic community. Utilizing capsule **I** as an aromatic cavity with some similarities to natural cyclase enzymes, we were able to showcase some first examples: A four-step total synthesis of isolongifolene,[5c] the first total synthesis of δ-selinene,[5d] as well as a four-step synthesis of the complex tricyclic presilphiperfolan-1β-ol,[8] which is difficult to access via other means. Interestingly, the closely related hexamer **II**,[9] which is formed from six units of pyrogallolarene **2** (Figure 1b), has been found to be catalytically inactive in THT cyclizations.[10] The reason for its inactivity, however, remained unknown. We previously speculated that either its low intrinsic acidity[10] or its inability to bind ion pairs is the cause for this observation. To clarify this issue, we decided to closely investigate assemblies **I** and **II**, as well as the related macrocycles **3**−**5** (Figure 1d), featuring different ratios of resorcinol and pyrogallol units. Additionally, the electron-deficient tetrafluori-

Received: December 9, 2019
Published: February 7, 2020

https://dx.doi.org/10.1021/jacs.9b13239
J. Am. Chem. Soc. 2020, 142, 4400−4410

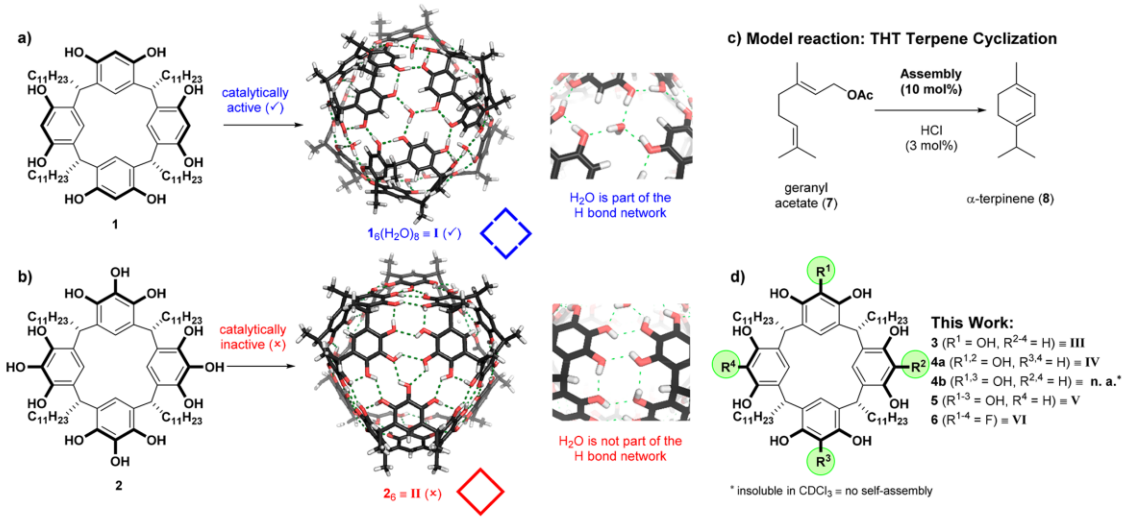

Figure 1. (a) Self-assembly of **I** from six units of **1** and eight water molecules, four of which are not fully saturated within the hydrogen-bond network and can function as hydrogen-bond donor at the inside of the cavity. (b) Self-assembly of **II** from six units of **2** forming a fully saturated hydrogen-bond network without water. (c) THT cyclization of geranyl acetate (**7**) forming α-terpinene (**8**). (d) Macrocycles **3**–**6** corresponding to assemblies **III**–**VI**.

nated resorcinarene derivative **6** was selected. As the main test reaction, we chose the THT cyclization of geranyl acetate (**7**) to α-terpinene (**8**, Figure 1c, Scheme S1), a reaction which was shown to undergo a "non-stop" cyclization inside **I**.[5a]

Concerning the prerequisites for catalytic activity, we considered the following steps in the catalytic cycle as potentially decisive (Scheme 1): (a) For a successful conversion inside the

Scheme 1. Potentially Decisive Steps of the Catalytic Cycle[a]

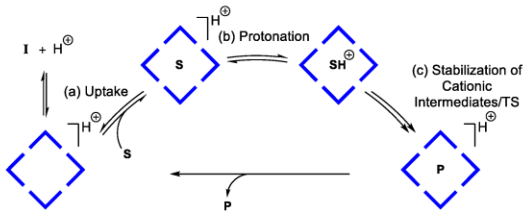

[a]S = Substrate, TS = Transition States, P = Products.

molecular capsule, the substrate has to be encapsulated. Therefore, substrate uptake in the different assemblies was explored first. (b) The substrate has to be activated by protonation.[5b] Protonation in an apolar solvent like chloroform leads to the formation of ion pairs. Consequently, we next investigated the ability of the assemblies to encapsulate ion pairs. (c) Cationic intermediates and transition states have very likely to be stabilized via cation-π interactions. Accordingly, we included an electron-deficient derivative (i.e., **6**) featuring four additional fluorine substituents in the study, as it should display reduced cation-π stabilization.

Here, we report efficient synthetic routes to macrocycles **3**–**6** (Figure 1d), their ability to self-assemble to the hexameric capsules **III**–**VI**, and provide evidence that water being incorporated into the hydrogen-bond network of the corresponding assemblies plays a crucial role for the efficient catalytic cyclization of monoterpenes.

RESULTS AND DISCUSSION

Synthesis of Macrocycles 3–6 and Investigation of Their Self-assembling Properties. First, it was necessary to develop a reliable route to access the macrocycles **3**–**6**, in pure form on a preparative scale (Scheme 2). While there has been a report about directly cyclizing different ratios of resorcinol and pyrogallol with the corresponding aldehyde to obtain macrocycles **3**–**5** by Atwood et al., these reactions yielded very complex mixtures that were not separable in our hands.[9d] To circumvent these separation issues, a more controlled route utilizing tetrabromo-derivative **9** was developed (Scheme 2). Compound **9** is accessible via literature procedures in two steps from resorcinarene **1** on decagram scale.[11] It was partially debrominated by treatment with specific amounts of *n*-butyllithium and, subsequently, methanol. The remaining aryl bromides were then converted in situ into phenolic moieties using *n*-butyllithium and trimethylborate followed by the addition of $NaOH/H_2O_2$.[12] This yielded biased mixtures of the octamethylated compounds **10**–**12**, which were separable by column chromatography. The tetrafluorinated compound **13** was accessed in a similar way from **9** using halogen-lithium exchange followed by the addition of the electrophilic fluorine reagent *N*-fluorobenzenesulfonimide (NFSI).[13] The removal of the methyl protecting groups was achieved by stirring in the presence of boron tribromide at room temperature for several days,[14] yielding compounds **3**–**6** in moderate to good yields and in analytically pure form (see Supporting Information Chapter 12). The products were recrystallized and subsequently washed with a H_2O/MeOH mixture to remove any acid traces (see Supporting Information for details). Aside from compound **4b**, featuring two distal pyrogallol units, all macrocycles were soluble in chloroform and self-assembled to hexameric capsules related to **I** and **II**. DOSY-NMR experiments[15] provided diffusion

https://dx.doi.org/10.1021/jacs.9b13239
J. Am. Chem. Soc. 2020, 142, 4400−4410

Scheme 2. Synthesis of the Macrocycles 3−6[a]

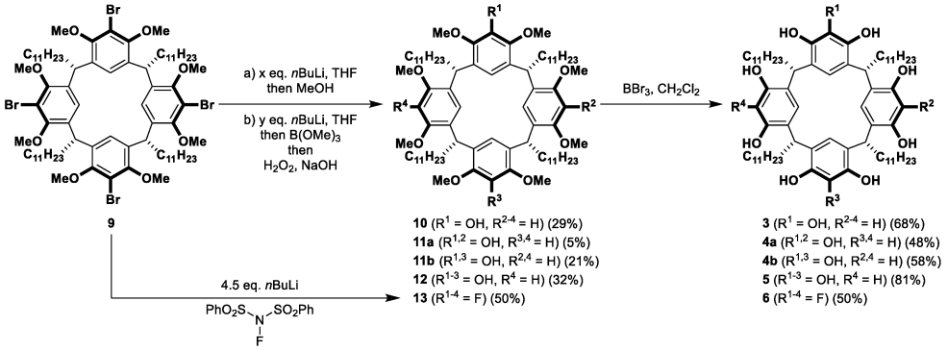

[a]Synthesis of the macrocycles **3**−**6** starting from the literature known compound **9**.[11]

values for the new assemblies very close to those of assemblies **I** and **II** (see Table S2). Self-assembly was further corroborated by the fact that assemblies **III**−**VI** show uptake of ammonium salts (i.e., NBu_4Br (**14**), Figure S18) indicated by the strong upfield shift of the guest protons due to the aromatic shielding effect. We, therefore, concluded that the obtained macrocycles form assemblies resembling the structures of **I** and **II**. However, note that, in the case of the assemblies **III**−**V**, the structures are not as symmetric and clearly defined as in **I** and **II**. Because of the lower degree of symmetry of the macrocycles, different isomers of hexameric capsules are formed. The broad signals in the ^{1}H NMR spectra recorded in $CDCl_3$ suggest that there is more than one assembly present and that these are interconverting. Solid-state structures could not be obtained, since crystal formation is hindered by the dynamic nature of the assemblies and the long flexible alkyl chains. Besides, crystal structures do not always correlate with structures present in solution as illustrated by macrocycle **5**.[9d] While we cannot exclude the presence of the previously reported, X-ray-based donut-shaped structure,[9d] none of the experiments we performed hinted at such an assembly in solution. In the case of assembly **VI**, the NMR spectrum closely resembles that of the resorcinarene-based capsule **I**, indicating a similar structure (see Supporting Information for the energy-optimized structure).

Evaluation of the Catalytic Activity in the Cyclization of Monoterpenes. With assemblies **I**−**VI** in hand, the cyclization of geranyl acetate (**7**, Figure 1c) as the model reaction was investigated employing the optimized conditions reported previously by our group for assembly **I**.[5b] HCl is added as a cocatalyst, which, unable to catalyze the reaction by itself, works in a synergistic fashion with the assembly. As reported by us,[10] no reaction was observed with assembly **II** (Figure 2e), while assembly **I** (Figure 2a) catalyzed the formation of α-terpinene (**8**) from acetate **7** in 30−35% yield. The reaction proceeds in good selectivity with other common cyclization products (Figure 2g) such as eucalyptol (**15**), terpinolene (**16**), limonene (**17**), γ-terpinene (**18**), and isoterpinolene (**19**) being only formed in minor quantities (<10% yield). Assembly **III** (Figure 2b), formed from monomer **3**, featuring one additional hydroxyl group compared to resorcinarene **1**, also displayed catalytic activity and likewise yielded α-terpinene (**8**) as the main product, albeit in a lower yield. When employing assembly **IV** (Figure 2c), the conversion of substrate remained significant, but the overall yield of cyclization products dropped significantly. We attribute this fact to a side reaction in which phenolic groups of **4a** react with the highly reactive cationic intermediates of the cyclization reaction. This was also observed for **I** in an earlier report and confirmed by isolation.[5a] In the current study, these alkylation products were detected by electrospray ionization−mass spectrometry (ESI-MS) analysis of the reaction mixtures (see Figures S9−S14) in the cases of the assemblies **I**, **III**, and **IV**. DOSY-NMR measurements during the reaction indicate that the assemblies stay largely intact (Supporting Information Chapter 7.4). Interestingly, assembly **V** (Figure 2d) with three pyrogallol units showed no catalytic activity in this cyclization reaction. The reaction in the presence of assembly **VI** (Figure 2f) featuring subunits with fluorine substituents proceeded very slowly. Similar results were obtained when the reaction was conducted with the intrinsically more reactive nerol (**20**) as the substrate (see Figure S3 for the reaction profiles). Assemblies **I**, **III**, and **IV** showed comparable behavior with only small differences in product selectivity. Initially, mainly α-terpineol (**25**) is formed, which is then further converted to eucalyptol (**15**), the major product after 72 h (30−38% yield). In the case of the fluorinated assembly **VI**, the formation of α-terpineol (**25**) in combination with traces of eucalyptol (**15**) (4% after 72 h) indicates a reaction profile similar to the one of assembly **I**, with the conversion being, however, again significantly slower. Assembly **II** shows no activity, while the closely related assembly **V** leads to considerable conversion (60% conversion after 72 h, Table 1, entry 1). At first glance, this seemed surprising, since assembly **V** showed no conversion with geranyl acetate (**7**). To understand this observation, control experiments with assembly **V** were conducted (Table 1). No conversion was observed in the absence of **V** with HCl present (entry 2). Blocking assembly **V** with tetrabutyl ammonium bromide (**14**) did not halt the reaction completely (13%, entry 3), indicating that the reaction is not only taking place within the cavity in that case. This was further corroborated by substituting assembly **V** with 4-hexyl resorcinol (**21**), which also led to some conversion of nerol (**20**) (10%, entry 5) after 3 d. Moreover, the product distribution of entry 1 indicated that the reaction likely takes place outside/on the outer surface of the capsule. The main products are limonene (**17**) and α-terpineol (**25**), which are also formed in regular solution experiments under acidic conditions[16] and in the presence of 4-hexyl resorcinol (**21**).

Additionally, the absence of eucalyptol (**15**), which is usually formed to a significant degree when the reaction takes place within the assembly (i.e., in assembly **I**), indicates a conversion

https://dx.doi.org/10.1021/jacs.9b13239
J. Am. Chem. Soc. 2020, 142, 4400−4410

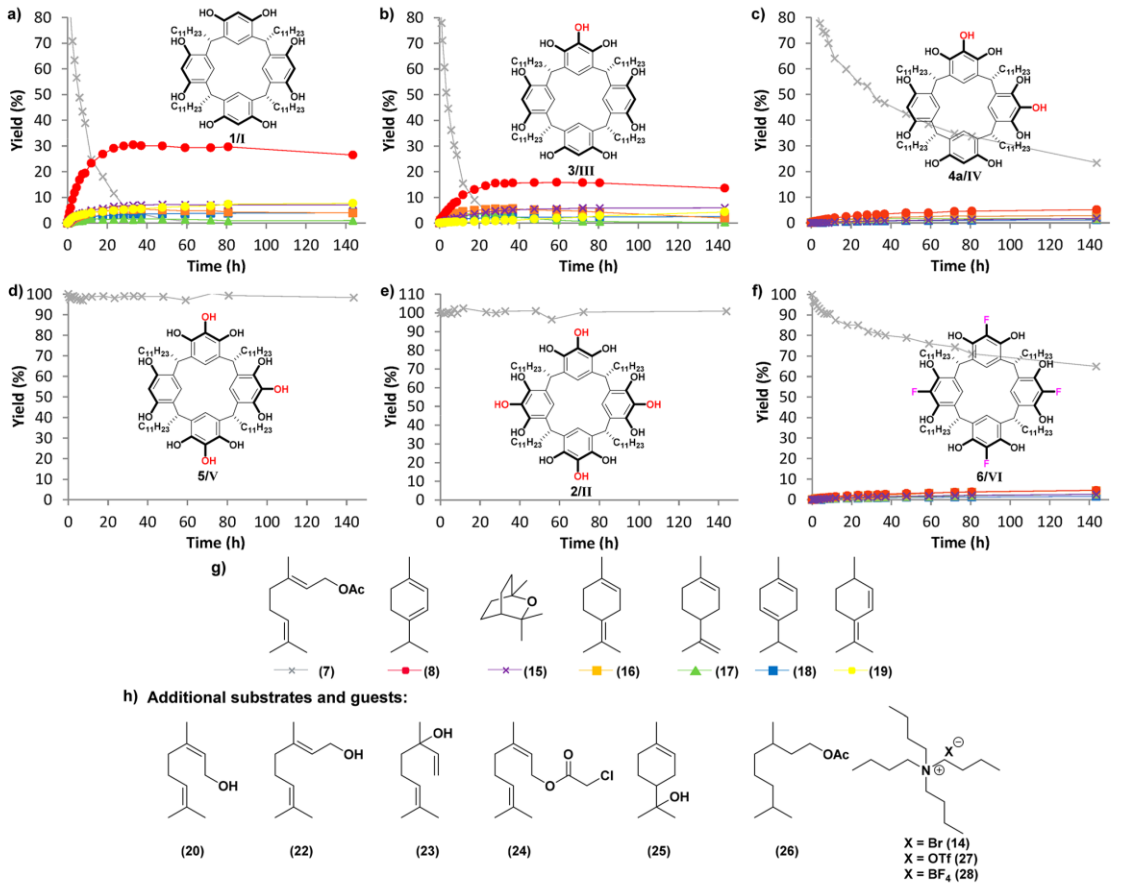

Figure 2. (a–f): Gas chromatography-based reaction profiles of assemblies **I**, **III**, **IV**, **V**, **II**, and **VI** with geranyl acetate (**7**) as substrate (reaction conditions: 33.3 mmol/L of **7**, 10 mol % assembly, 3 mol % HCl, in $CDCl_3$ at 30 °C). (g) Substrate **7** and reaction products. (h) Additional substrates and guests.

outside the assembly. Taken together, these results indicate that, in this case, the reaction is taking place mainly outside/on the outer surface of assembly **V** presumably via hydrogen bonding (Table 1, entry 5), due to the higher reactivity of nerol (**20**). What causes the difference in capsules **II** and **V**? It is likely that the perfect hydrogen-bond network[9b] of **II** prevents activation of nerol via hydrogen bonds. Also note that assembly **V** proved to be an inefficient catalyst in the cyclization of other substrates (Figure 2h) such as geraniol (**22**), linalool (**23**), and neryl chloroacetate (**24**), all of which showed less than 15% conversion after 72 h. In the cases where traces of product were detected, these correspond again to limonene (**17**) and α-terpineol (**25**), indicating that the conversion is likely taking place in solution rather than inside **V** (Figures S5–S7). In summary, the cyclization studies revealed that assemblies **I**, **III**, **IV**, and **VI** are active supramolecular catalysts for the THT cyclization, while **II** and **V** are inactive.

Uptake Studies. Substrate uptake is a prerequisite for catalysis inside the capsule. To elucidate a potential correlation between catalytic inactivity and inability of substrate uptake, a set of NMR experiments was performed. For this purpose, the saturated substrate analogue **26** (Figure 2h), which is not converted in the presence of assemblies **I**–**VI** and HCl, was employed. Host and guest solutions in chloroform were mixed in the ratios used for cyclization (1:10) in the presence of HCl at 0

Table 1. Control Experiments for the Nerol (20) Cyclization with Assembly V under Standard Reaction Conditions (33.3 mmol/L of 20, 3 mol % HCl, in $CDCl_3$ at 30 °C)

Entry	Catalyst (mol%)	Additive (mol%)	Conversion (%) [a] (72 h)
1	**V** (10)	-	60
2	-	-	-
3	**V** (10)	*n*-Bu_4NBr (**14**) (15)	13
4	-	*n*-Bu_4NBr (**14**) (15)	-
5	-	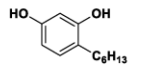 (**21**) (240)	10

[a]Determined by gas chromatography.

https://dx.doi.org/10.1021/jacs.9b13239
J. Am. Chem. Soc. 2020, 142, 4400–4410

°C and immediately submitted to NMR spectroscopy. The samples were then stored at 30 °C and monitored by ^{1}H NMR. Guest uptake over time was determined via ^{1}H NMR analysis (Table 2), by comparison of the respective assembly signals

Table 2. Encapsulation of Substrate Analogue 26[a]

entry	assembly	encapsulation[b] after 6 h (%)	encapsulation[b] after 48 h (%)
1	**I**	1.3	3.1
2	**III**	1.0	1.4
3	**IV**	0.3	0.7
4	**V**	0.5	1.5
5	**II**	0.6	1.0
6	**VI**	0.3	2.3

[a]Encapsulation of substrate analogue **26** by assemblies **I**–**VI** under reaction conditions (33.3 mmol/L of **26**, 10 mol % assembly, 3 mol % HCl, in $CDCl_3$ at 30 °C). [b]Determined by ^{1}H NMR integration.

(internal standard) and the signal of "free" **26**. The values given are calculated assuming that directly after addition no encapsulation is observed. Table 2 shows that the amount of nonencapsulated substrate **26** is decreasing with time in all cases, indicating a gradual encapsulation of **26** by all assemblies to varying degrees (for full details see Tables S4–S9). This is further supported by the appearance of small signals below 0.5 ppm in the respective ^{1}H NMR spectra, which continued to increase when the samples were monitored over a longer period of time (see Figures S15 and S16). Since all assemblies investigated, including the catalytically inactive assemblies **II** and **V**, showed some uptake of guest **26**, a direct correlation between catalytic activity and encapsulation of substrate could not be established.

Encapsulation of Ion Pairs. After encapsulation, protonation of the substrate with HCl in the apolar solvent chloroform will form an ion pair. Therefore, we investigated the ability of the different assemblies to encapsulate ion pairs. While **I** readily encapsulates ammonium salts (e.g., tetrabutylammonium bromide (TBAB) **14**) as ion pairs, the encapsulation of anions in assembly **II** has been shown to be energetically unfavorable.[10] The binding of anions can be easily investigated with ^{19}F NMR when utilizing fluorine-containing anions (e.g., triflate). Figure 3 shows the ^{19}F NMR spectra of the assemblies **I**–**VI** in the presence of 1.0 equiv of tetrabutylammonium triflate (**27**). In all cases, the presence of the assembly causes a

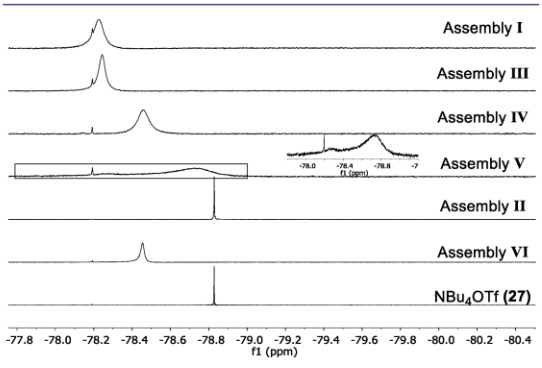

Figure 3. ^{19}F NMR spectra of assemblies **I**–**VI** (3.33 mmol/L) in the presence of 1.0 equiv of NBu_4OTf (**27**) in $CDCl_3$.

shift and broadening of the signal corresponding to the triflate anion, with the sole exception being assembly **II**, where no effect on the triflate signal was observed. When tetrabutylammonium tetrafluoroborate (**28**) was employed, similar results were obtained (Figures S19 and S20). This is in agreement with the ability of all assemblies beside **II** to encapsulate ammonium salts such as TBAB (see also Supporting Information Chapter 8.3). Importantly, the catalytically inactive assembly **V** is able to bind ion pairs in contrast to the inactive assembly **II**. In conclusion, the ability to encapsulate ion pairs does not correlate with the catalytic activity of assemblies **I**–**VI**.

Protonation Studies. During the cyclization studies, we recognized that some ^{1}H NMR signals of several assemblies changed upon the addition of HCl as cocatalyst. Therefore, this phenomenon was investigated in more detail. For this purpose, chloroform solutions of the assemblies **I**–**VI** were titrated with HCl (3.33 mmol/L of assemblies **I**–**VI**, 0.0–1.0 equiv HCl added to the same sample). The results (Figure 4) show that, in four cases (**I**, **III**, **IV**, and **VI**, Figure 4a–c,f), the signals corresponding to the phenol groups as well as the water signal broaden with increasing amounts of HCl. We attributed these changes to the protonation of the assemblies by the external acid. In contrast, the signals corresponding to the phenol groups of the assemblies **II** and **V** (Figure 4d,e) remain unaffected by the added acid, and also the water signal only broadens to a very small extent when compared to the other assemblies (Figure 4a–c,f). This indicates that assemblies **II** and **V** are not protonated by the external acid, at least on the ^{1}H NMR (500 MHz) time scale.[17] A protonation of the phenolic groups of **II** and **V** in the presence of unbound water seems unlikely considering the pK_a values of H_3O^+ (pK_a = 0)[18] and protonated phenols (pK_a ≈ −6).[19] The integrity of the assemblies **I**–**VI** in the presence of 1.0 equiv of HCl was confirmed by DOSY-NMR experiments (see Supporting Information Chapter 10 for details). Importantly, the observed protonation of the host correlates well with the observed catalytic activity of the respective assemblies in the cyclization of monoterpenes.

Water as Integral Part of the Assembly. As mentioned before, the main structural difference between assemblies **I** and **II** is the incorporation of water into the hydrogen-bond network. This can be directly observed in the ^{1}H NMR spectra in $CDCl_3$, where the water signal in the presence of **I** is significantly downfield shifted, while it remains largely unaffected with **II** (Figure 4a,e, 0.0 equiv of HCl). The shift is associated with the incorporation of water into the capsular hydrogen-bond network.[20] Water being incorporated into the assembly and free water in solution are in fast exchange on the ^{1}H NMR time scale; therefore, only one averaged water signal is observed. The magnitude of the downfield shift depends on the total amount of water present in the solution, with a low water content leading to a stronger shift. Cohen et al. reported a method based on DOSY-NMR experiments to determine the water content in **I** and **II**.[20]

If water is not part of the assembly, like in **II**, its diffusion value is independent of the total water amount in the sample (e.g., assembly **II**, Figure 5e). However, if water is an integral part of the capsule, its diffusion value converges to the value of the assembly when the total amount of water decreases (assembly **I**, Figure 5a). Varying the water content of chloroform solutions of the novel catalytically active assemblies **III**, **IV**, and **VI** (Figure 5b,c,f) indicated that, in these cases, water is part of the hydrogen-bond network, similar to structure **I** (Figure 5a). In contrast, the data obtained for the inactive assembly **V** (Figure 5d) imply that water does not take part in the formation of

https://dx.doi.org/10.1021/jacs.9b13239
J. Am. Chem. Soc. 2020, 142, 4400–4410

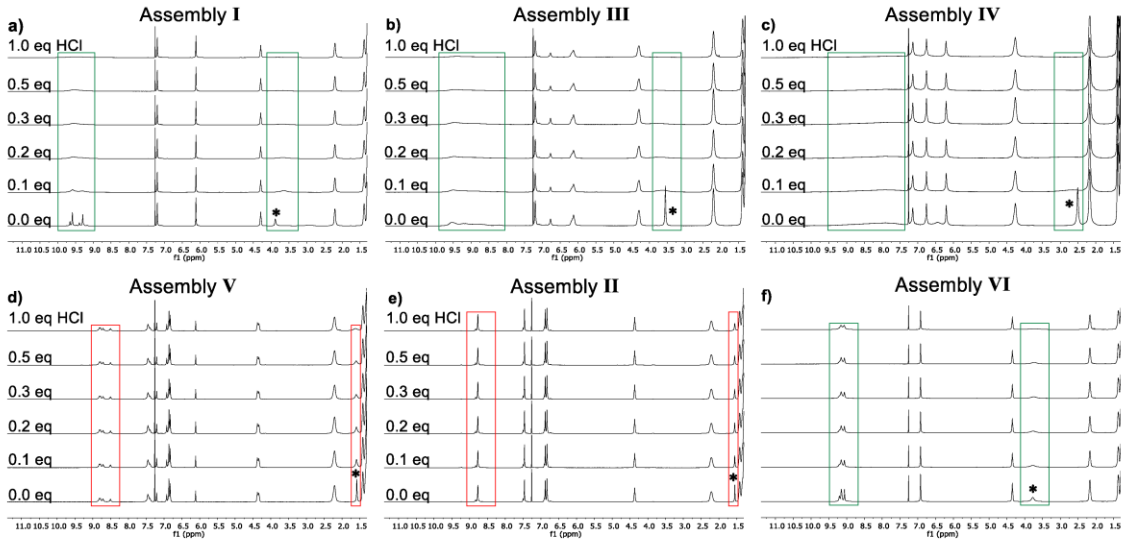

Figure 4. (a–f) NMR titration of the respective assembly (3.33 mmol/L) with HCl (0.0–1.0 equiv). Representative signals corresponding to phenol moieties and water are highlighted (green for catalytically active, red for catalytically inactive). The water signals are marked with an asterisk (*).

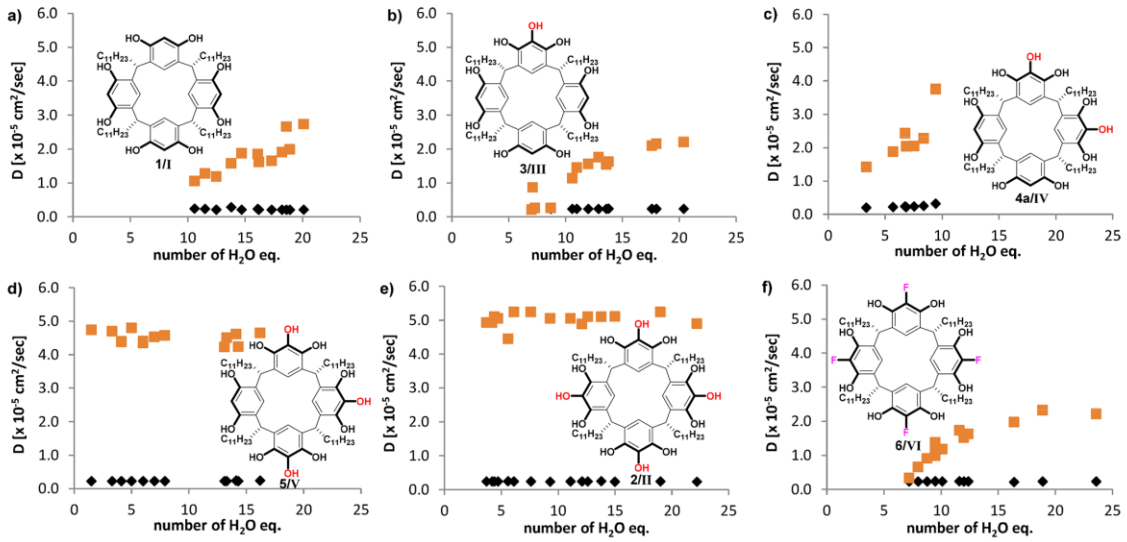

Figure 5. (a–f) Influence of the water content on the diffusion coefficients *D* of the assemblies (◆) and water (red ■). Experiments were performed in $CDCl_3$ solutions of the assemblies (3.33–1.67 mmol/L).

assembly **V**; the same observation as was made for structure **II** (see Supporting Information for a molecular model of assembly **V**). Note that, in the case of assembly **IV**, due to an overlap between the water signal and signals of the assembly, only a few measurements resulted in reliable data points concerning the diffusion value of water. However, considering that the water signal is shifted significantly and that the diffusion values obtained are significantly lower than the values observed for the assemblies containing no water, we concluded that water is part of the hydrogen-bond network of assembly **IV**.

In conclusion, the incorporation of water into the hydrogen-bond network of the assembly correlates well with the catalytic activity observed. Interestingly, the assemblies containing water in the hydrogen-bond network also displayed enhanced protonation in the presence of HCl (see previous section). These observations indicate a central role of the bound water molecules for the catalytic activity.

Molecular Dynamics Simulations. The results presented in the previous two sections indicate that water being part of the hydrogen-bond network is essential in the protonation of the assembly by an external acid, thereby enabling catalysis within the host structures **I**, **III**, **IV**, and **VI**. To learn more details about the protonation event inside the capsule, we turned to molecular dynamics (MD) simulations. Specifically, capsule **I** containing

https://dx.doi.org/10.1021/jacs.9b13239
J. Am. Chem. Soc. 2020, 142, 4400–4410

encapsulated geranyl acetate (7) and external HCl was submitted to quantum mechanics/molecular mechanics (QM/MM) (density functional theory (DFT), PBE,[21] +D level[22]) MD simulations at 300 K using the CP2K code.[23] The QM region consisted of six resorcinol units belonging to three adjacent resorcinarene molecules, one water molecule, one HCl molecule, and geranyl acetate (7), whereas the rest of assembly **I** and the chloroform solvent molecules were treated at the MM level (see Supporting Information for computational details).

As the proton transfer from HCl to the carbonyl oxygen of substrate **7** involves separate, relevant metastable states separated by high free energy barriers along the reaction path, standard MD is not suitable. Therefore, the sampling of the process was enhanced using Metadynamics[24] (MetaD) implemented in the PLUMED2 code.[25] To characterize the complex free energy landscape describing the proton migration from HCl throughout the complex hydrogen-bond network, we used the method recently developed by Grifoni et al.[26]

The simulation can be summarized as follows: (i) Energetically, the most favored pathway involves a direct protonation of the water at the capsule surface by HCl (Figure 6a, state **A** → **B**). The alternative pathway involving protonation of a phenol group, followed by rapid proton migration to a water molecule, is less likely (Figure S23). (ii) The formed chloride of the H_3O^+/Cl^- ion pair is stabilized by coordination to the surrounding phenol groups of the resorcinarene molecules. It replaces the hydronium ion in the hydrogen-bond network of capsule **I** and shifts the hydronium ion below the inner surface of the capsule (state **B**). (iii) Finally, the hydronium ion and the carbonyl of the geranyl acetate substrate form a very compact complex, sharing the proton (state **C**). Similar structures have been observed in other computational studies focusing on the acid-catalyzed ester hydrolysis.[27]

To further analyze the results, we calculated the free energy surface following the reweighting procedure previously described.[28] To extract useful and chemically meaningful information on the protonation process, two collective variables (CV_1 and CV_2) describing the progressive protonation reaction of the carbonyl oxygen were selected. To be general in describing the fundamental chemical features, we used coordination numbers. These functions count how many atoms of a specific species are found within a cutoff sphere from the central atom. In the present case, CV_1 accounts for the proximity of the carbonyl oxygen and the water oxygen atoms. At the starting point of the simulation (Figure 6b, state **A**), CV_1 is close to zero; after the formation of the final hydronium-carbonyl complex (state **C**), it will be ∼1, as the water molecule gets close to the carbonyl oxygen. The second variable (CV_2) accounts for the number of hydrogen atoms in close proximity to the water-oxygen. At the starting point of the simulation (state **A**), CV_2 is 2, corresponding to the number of covalent bonds in the neutral water molecule. As the proton transfer proceeds, CV_2 increases.

The minimum free energy path[29] (MFEP) along the free energy surface is depicted in Figure 6a. This curve represents the minimum energy required during the process. It is worth noticing that state **B** in which the H_3O^+/Cl^- ion pair is formed is the most stable state. The chloride anion is well-stabilized by the surrounding phenol groups at the surface of the capsule (see Figure S24). The estimated energy barrier for the dissociation process is only ∼1.5 kJ·mol^{-1}, much lower than the thermal barrier ($k_BT \approx 2.5$ kJ·mol^{-1}). The picture is different when we consider the formation of the carbonyl/hydronium complex of

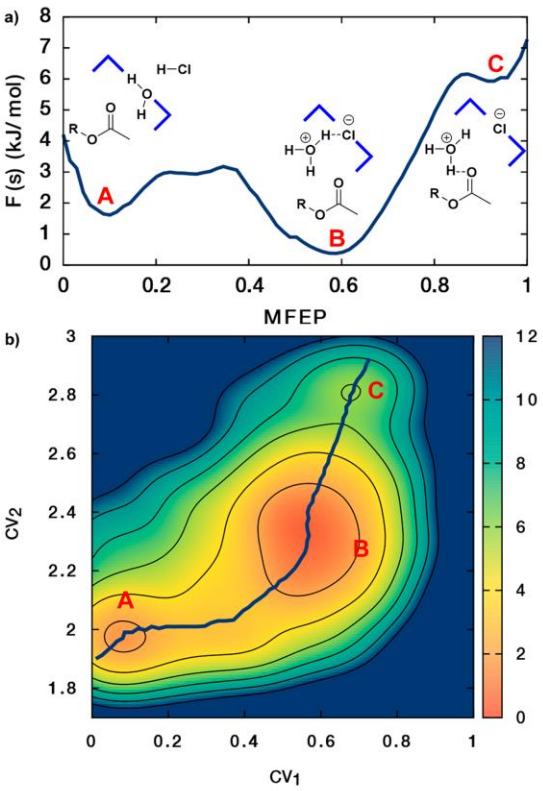

Figure 6. (a) Free energy along the MFEP showing the three states' (A, B, and C) relative stabilities and free energy barriers separating them. (b) Free energy surface for the geranyl acetate (7) protonation by means of HCl as cocatalyst for assembly **I** along the coordination of the carbonyl oxygen with the water oxygen atom (CV_1) and the coordination of the water oxygen atoms with the acidic hydrogen atoms (CV_2). Letters A, B, and C label the minima corresponding to the metastable states referring to the initial neutral state, the intermediate formation of the H_3O^+/Cl^- ion pair, and the final protonation of the carbonyl oxygen by H_3O^+. The blue line passing through the three states represents the MFEP connecting them. The color bar represents the energy reported (in kJ·mol^{-1}).

state **C**. Its formation is slowed by a larger barrier of ∼6 kJ·mol^{-1}, and state **C** is less stable than state **B**. Again, this result is in line with previous computational findings.[27]

The calculations, therefore, provide further evidence that water is indeed essential for the proton transfer process from the cocatalyst HCl onto the encapsulated substrate.

■ CONCLUSION

The experimental results obtained in this study are summarized in Table 3. Taken together, these results strongly indicate that the decisive requirement for catalytic activity in the context of terpene cyclization is the incorporation of water molecules into the hydrogen-bond network of the assembly. The crucial water molecule functions as a proton shuttle, delivering the proton onto the encapsulated substrate. If water is not incorporated into the assembly, this protonation mode is prevented, rendering these hosts catalytically inactive. This holds true even in the case where the host is able to encapsulate the substrate and stabilize

https://dx.doi.org/10.1021/jacs.9b13239
J. Am. Chem. Soc. 2020, 142, 4400−4410

Table 3. Comparison of Properties of Macrocycles 1−6 and the Corresponding Assemblies I−VI Indicating a Correlation between Water Being Part of the Hydrogen-Bond Network and Catalytic Activity in the THT Cyclization

Macrocycle /Assembly	Catalysis	Substrate Binding	Anion Binding	Water	Proto-nation
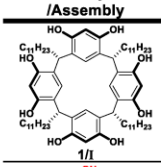 1/I	✓	✓	✓	✓	✓
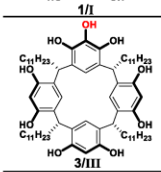 3/III	✓	✓	✓	✓	✓
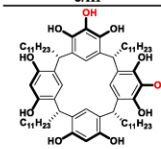 4a/IV	✓	✓	✓	✓	✓
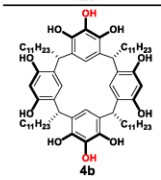 4b	n. d.[a]	n. d.[a]	n. d.[a]	n. d.[a]	n. d.[a]
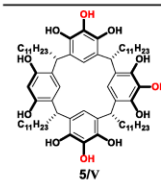 5/V	✗	✓	✓	✗	✗
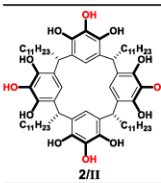 2/II	✗	✓	✗	✗	✗
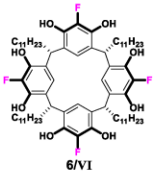 6/VI	✓	✓	✓	✓	✓

[a]Not determined due to the insolubility of **4b** in $CDCl_3$.

ion pairs (assembly **V**, Table 3, entry 5). This finding has furthermore been validated by calculations, which confirm that the proposed intermediary states constitute the minimum free energy path.

Interestingly, the proposed protonation pathway may also provide insights into the puzzling observation that the chloride counteranion of the HCl cocatalyst does not interfere with the cationic cyclization cascade. Control experiments with HCl, as well as other Bronsted or Lewis acids,[5a,6,30] usually lead to counteranion quenching of cationic intermediates. Since the chloride anion is bound at the capsule surface (Figure 6a), it is prevented from quenching cationic intermediates inside the cavity of the capsule.

SUMMARY

In summary, we presented the synthesis and characterization of four new macrocycles **3**−**5** composed of different ratios of resorcinol and pyrogallol units as well as a new tetrafluorinated resorcinarene derivative **6**. With the exception of compound **4b**, all derivatives self-assemble to dynamic, hexameric hydrogen-bonded assemblies in chloroform solution. The new assemblies **III**−**VI**, together with assemblies **I** and **II**, were studied in detail and compared with respect to their catalytic activity in the monoterpene cyclization, their ability to encapsulate terpene substrates and ion pairs, their response to acid additive, and the amount of water incorporated into the hydrogen-bond network. The experimental results strongly indicate a correlation between the catalytic activity and water being part of the assembly. QM/MM molecular dynamics simulations provided insights into the specific role of the water molecule in the protonation process of the encapsulated substrate. The incorporated water molecules likely act as a proton shuttle by transferring the proton from the acid cocatalyst HCl to the encapsulated substrate, which initiates the cyclization. Since the chloride counteranion is replacing one water molecule in the hydrogen-bond network, it is immobilized and does not interfere with the cationic cyclization cascade reaction.

These findings finally reveal the activation mechanism inside capsule **I** and decipher the prerequisites for catalytic activity. It, therefore, represents an important step toward the rational design of new supramolecular catalyst systems. We expect this finding to make a significant impact on future developments in the field of supramolecular catalysis, since the proposed model is likely transferable to other types of host systems.

ASSOCIATED CONTENT

Supporting Information

The Supporting Information is available free of charge at https://pubs.acs.org/doi/10.1021/jacs.9b13239.

Illustrated hydrogen-bond network (CDX)

Experimental details and NMR spectra of new compounds (PDF)

AUTHOR INFORMATION

Corresponding Author

Konrad Tiefenbacher − *Department of Chemistry, University of Basel, CH-4058 Basel, Switzerland; Department of Biosystems Science and Engineering, ETH Zürich, CH-4058 Basel, Switzerland;* orcid.org/0000-0002-3351-6121; Email: konrad.tiefenbacher@unibas.ch, tkonrad@ethz.ch

Authors

Severin Merget − *Department of Chemistry, University of Basel, CH-4058 Basel, Switzerland*

Lorenzo Catti − *WPI Nano Life Science Institute (WPI-NanoLSI), Kanazawa University, Kakuma-machi, Kanazawa 920-1192, Japan;* orcid.org/0000-0003-0727-0620

https://dx.doi.org/10.1021/jacs.9b13239
J. Am. Chem. Soc. 2020, 142, 4400−4410

GiovanniMaria Piccini − *Department of Chemistry and Applied Biosciences, ETH Zurich, CH-6900 Lugano, Switzerland; Facoltàdi Informatica, Istituto di Scienze Computazionali, Università della Svizzera Italiana, CH-6900 Lugano, Switzerland;* orcid.org/0000-0002-3511-4281

Complete contact information is available at: https://pubs.acs.org/10.1021/jacs.9b13239

Notes

The authors declare no competing financial interest.

■ ACKNOWLEDGMENTS

This work was supported by funding from the European Research Council Horizon 2020 Programme (ERC Starting Grant No. 714620-TERPENECAT) and the Swiss National Science Foundation as part of the NCCR Molecular Systems Engineering. We thank PD Dr. D. Häussinger for assistance with the DOSY-NMR measurements. L.C. thanks JSPS and the Alexander von Humboldt Foundation for a postdoctoral fellowship. GM.P. thanks Prof. M. Parrinello for fruitful discussions and E. Grifoni for support and analysis of metadynamics simulations. All calculations were run on the ETHZ Euler-IV cluster.

■ REFERENCES

(1) (a) Kirby, A. J. Enzyme Mechanisms, Models, and Mimics. *Angew. Chem., Int. Ed. Engl.* **1996**, *35* (7), 706−724. (b) Motherwell, W. B.; Bingham, M. J.; Six, Y. Recent progress in the design and synthesis of artificial enzymes. *Tetrahedron* **2001**, *57* (22), 4663−4686. (c) Garcia-Viloca, M.; Gao, J.; Karplus, M.; Truhlar, D. G. How Enzymes Work: Analysis by Modern Rate Theory and Computer Simulations. *Science* **2004**, *303* (5655), 186−195. (d) Zhang, X.; Houk, K. N. Why Enzymes Are Proficient Catalysts: Beyond the Pauling Paradigm. *Acc. Chem. Res.* **2005**, *38* (5), 379−385. (e) Gao, J.; Ma, S.; Major, D. T.; Nam, K.; Pu, J.; Truhlar, D. G. Mechanisms and Free Energies of Enzymatic Reactions. *Chem. Rev.* **2006**, *106* (8), 3188−3209. (f) Warshel, A.; Sharma, P. K.; Kato, M.; Xiang, Y.; Liu, H.; Olsson, M. H. M. Electrostatic Basis for Enzyme Catalysis. *Chem. Rev.* **2006**, *106* (8), 3210−3235. (g) Ringe, D.; Petsko, G. A. How Enzymes Work. *Science* **2008**, *320* (5882), 1428−1429. (h) Kamerlin, S. C. L.; Warshel, A. At the dawn of the 21st century: Is dynamics the missing link for understanding enzyme catalysis? *Proteins: Struct., Funct., Genet.* **2010**, *78* (6), 1339−1375.

(2) For reviews see: (a) Pluth, M. D.; Bergman, R. G.; Raymond, K. N. Proton-Mediated Chemistry and Catalysis in a Self-Assembled Supramolecular Host. *Acc. Chem. Res.* **2009**, *42* (10), 1650−1659. (b) Yoshizawa, M.; Klosterman, J. K.; Fujita, M. Functional Molecular Flasks: New Properties and Reactions within Discrete, Self-Assembled Hosts. *Angew. Chem., Int. Ed.* **2009**, *48* (19), 3418−3438. (c) Meeuwissen, J.; Reek, J. N. Supramolecular catalysis beyond enzyme mimics. *Nat. Chem.* **2010**, *2* (8), 615−21. (d) Wiester, M. J.; Ulmann, P. A.; Mirkin, C. A. Enzyme Mimics Based Upon Supramolecular Coordination Chemistry. *Angew. Chem., Int. Ed.* **2011**, *50* (1), 114−137. (e) Marchetti, L.; Levine, M. Biomimetic Catalysis. *ACS Catal.* **2011**, *1* (9), 1090−1118. (f) Ajami, D.; Rebek, J. More Chemistry in Small Spaces. *Acc. Chem. Res.* **2013**, *46* (4), 990−999. (g) Raynal, M.; Ballester, P.; Vidal-Ferran, A.; van Leeuwen, P. W. N. M. Supramolecular catalysis. Part 2: artificial enzyme mimics. *Chem. Soc. Rev.* **2014**, *43* (5), 1734−1787. (h) Leenders, S. H.; Gramage-Doria, R.; de Bruin, B.; Reek, J. N. Transition metal catalysis in confined spaces. *Chem. Soc. Rev.* **2015**, *44* (2), 433−48. (i) Brown, C. J.; Toste, F. D.; Bergman, R. G.; Raymond, K. N. Supramolecular catalysis in metal-ligand cluster hosts. *Chem. Rev.* **2015**, *115* (9), 3012−35. (j) Zarra, S.; Wood, D. M.; Roberts, D. A.; Nitschke, J. R. Molecular containers in complex chemical systems. *Chem. Soc. Rev.* **2015**, *44* (2), 419−432. (k) Catti, L.; Zhang, Q.; Tiefenbacher, K. Self-Assembled Supramolecular Structures as Catalysts for Reactions Involving Cationic Transition States. *Synthesis* **2016**, *48* (03), 313−328. (l) Levin, M. D.; Kaphan, D. M.; Hong, C. M.; Bergman, R. G.; Raymond, K. N.; Toste, F. D. Scope and Mechanism of Cooperativity at the Intersection of Organometallic and Supramolecular Catalysis. *J. Am. Chem. Soc.* **2016**, *138* (30), 9682−93. (m) Catti, L.; Zhang, Q.; Tiefenbacher, K. Advantages of Catalysis in Self-Assembled Molecular Capsules. *Chem. - Eur. J.* **2016**, *22* (27), 9060−9066. (n) Zhang, Q.; Catti, L.; Tiefenbacher, K. Catalysis inside the Hexameric Resorcinarene Capsule. *Acc. Chem. Res.* **2018**, *51* (9), 2107−2114. (o) Mouarrawis, V.; Plessius, R.; van der Vlugt, J. I.; Reek, J. N. H. Confinement Effects in Catalysis Using Well-Defined Materials and Cages. *Front. Chem.* **2018**, *6*, 623. (p) Hong, C. M.; Bergman, R. G.; Raymond, K. N.; Toste, F. D. Self-Assembled Tetrahedral Hosts as Supramolecular Catalysts. *Acc. Chem. Res.* **2018**, *51* (10), 2447−2455. (q) Zhu, Y.; Rebek, J., Jr; Yu, Y. Cyclizations catalyzed inside a hexameric resorcinarene capsule. *Chem. Commun.* **2019**, *55* (25), 3573−3577. (r) Gaeta, C.; Talotta, C.; De Rosa, M.; La Manna, P.; Soriente, A.; Neri, P. The Hexameric Resorcinarene Capsule at Work: Supramolecular Catalysis in Confined Spaces. *Chem. - Eur. J.* **2019**, *25* (19), 4899−4913. (s) Zhang, Q.; Catti, L.; Syntrivanis, L. D.; Tiefenbacher, K. En route to terpene natural products utilizing supramolecular cyclase mimetics. *Nat. Prod. Rep.* **2019**, *36*, 1619−1627. (t) Cohen, Y.; Slovak, S.; Avram, L. Hydrogen Bond Hexameric Capsules: Structures, Host-Guest Interactions, Guest Affinities, and Catalysis. In *Calixarenes and Beyond;* Neri, P., Sessler, J. L., Wang, M.-X., Eds.; Springer International Publishing: Cham, Switzerland, 2016; pp 811−842.

(3) For recent examples see: (a) Wei, J.; Zhao, L.; He, C.; Zheng, S.; Reek, J. N. H.; Duan, C. Metal-Organic Capsules with NADH Mimics as Switchable Selectivity Regulators for Photocatalytic Transfer Hydrogenation. *J. Am. Chem. Soc.* **2019**, *141* (32), 12707−12716. (b) Jans, A. C. H.; Caumes, X.; Reek, J. N. H. Gold Catalysis in (Supra)Molecular Cages to Control Reactivity and Selectivity. *ChemCatChem* **2019**, *11* (1), 287−297. (c) Jongkind, L. J.; Elemans, J.; Reek, J. N. H. Cofactor Controlled Encapsulation of a Rhodium Hydroformylation Catalyst. *Angew. Chem., Int. Ed.* **2019**, *58* (9), 2696−2699. (d) Bender, T. A.; Bergman, R. G.; Raymond, K. N.; Toste, F. D. A Supramolecular Strategy for Selective Catalytic Hydrogenation Independent of Remote Chain Length. *J. Am. Chem. Soc.* **2019**, *141* (30), 11806−11810. (e) Bender, T. A.; Morimoto, M.; Bergman, R. G.; Raymond, K. N.; Toste, F. D. Supramolecular Host-Selective Activation of Iodoarenes by Encapsulated Organometallics. *J. Am. Chem. Soc.* **2019**, *141* (4), 1701−1706. (f) Takezawa, H.; Kanda, T.; Nanjo, H.; Fujita, M. Site-Selective Functionalization of Linear Diterpenoids through U-Shaped Folding in a Confined Artificial Cavity. *J. Am. Chem. Soc.* **2019**, *141* (13), 5112−5115. (g) La Manna, P.; De Rosa, M.; Talotta, C.; Rescifina, A.; Floresta, G.; Soriente, A.; Gaeta, C.; Neri, P. Synergic Interplay Between Halogen Bonding and Hydrogen Bonding in the Activation of a Neutral Substrate in a Nanoconfined Space. *Angew. Chem., Int. Ed.* **2020**, *59*, 811. (h) Gambaro, S.; De Rosa, M.; Soriente, A.; Talotta, C.; Floresta, G.; Rescifina, A.; Gaeta, C.; Neri, P. A hexameric resorcinarene capsule as a hydrogen bonding catalyst in the conjugate addition of pyrroles and indoles to nitroalkenes. *Org. Chem. Front.* **2019**, *6* (14), 2339−2347. (i) Gambaro, S.; La Manna, P.; De Rosa, M.; Soriente, A.; Talotta, C.; Gaeta, C.; Neri, P. The Hexameric Resorcinarene Capsule as a Brønsted Acid Catalyst for the Synthesis of Bis(heteroaryl)methanes in a Nanoconfined Space. *Front. Chem.* **2019**, *7*, 687 DOI: 10.3389/fchem.2019.00687. (j) Angamuthu, V.; Petroselli, M.; Rahman, F.-U.; Yu, Y.; Rebek, J. Binding orientation and reactivity of alkyl α,ω-dibromides in water-soluble cavitands. *Org. Biomol. Chem.* **2019**, *17* (21), 5279−5282. (k) Köster, J. M.; Häussinger, D.; Tiefenbacher, K. Activation of Primary and Secondary Benzylic and Tertiary Alkyl (sp3)C-F Bonds Inside a Self-Assembled Molecular Container. *Front. Chem.* **2019**, *6* (639). DOI: 10.3389/fchem.2018.00639

(4) (a) MacGillivray, L. R.; Atwood, J. L. A chiral spherical molecular assembly held together by 60 hydrogen bonds. *Nature* **1997**, *389* (6650), 469−472. (b) Avram, L.; Cohen, Y. Spontaneous Formation of Hexameric Resorcinarene Capsule in Chloroform Solution as Detected

by Diffusion NMR. *J. Am. Chem. Soc.* **2002**, *124* (51), 15148−15149. (c) Avram, L.; Cohen, Y.; Rebek, J., Jr Recent advances in hydrogen-bonded hexameric encapsulation complexes. *Chem. Commun.* **2011**, *47* (19), 5368−5375.

(5) (a) Zhang, Q.; Tiefenbacher, K. Terpene cyclization catalysed inside a self-assembled cavity. *Nat. Chem.* **2015**, *7* (3), 197−202. (b) Zhang, Q.; Catti, L.; Pleiss, J.; Tiefenbacher, K. Terpene Cyclizations inside a Supramolecular Catalyst: Leaving-Group-Controlled Product Selectivity and Mechanistic Studies. *J. Am. Chem. Soc.* **2017**, *139* (33), 11482−11492. (c) Zhang, Q.; Rinkel, J.; Goldfuss, B.; Dickschat, J. S.; Tiefenbacher, K. Sesquiterpene Cyclisations Catalysed inside the Resorcinarene Capsule and Application in the Short Synthesis of Isolongifolene and Isolongifolenone. *Nat. Catal.* **2018**, *1* (8), 609−615. (d) Zhang, Q.; Tiefenbacher, K. Sesquiterpene Cyclizations inside the Hexameric Resorcinarene Capsule: Total Synthesis of delta-Selinene and Mechanistic Studies. *Angew. Chem., Int. Ed.* **2019**, *58* (36), 12688−12695.

(6) Pronin, S. V.; Shenvi, R. A. Synthesis of highly strained terpenes by non-stop tail-to-head polycyclization. *Nat. Chem.* **2012**, *4* (11), 915−920.

(7) (a) Croteau, R. Biosynthesis and catabolism of monoterpenoids. *Chem. Rev.* **1987**, *87* (5), 929−954. (b) Cane, D. E. Enzymic formation of sesquiterpenes. *Chem. Rev.* **1990**, *90* (7), 1089−1103. (c) Christianson, D. W. Structural Biology and Chemistry of the Terpenoid Cyclases. *Chem. Rev.* **2006**, *106* (8), 3412−3442. (d) Degenhardt, J.; Köllner, T. G.; Gershenzon, J. Monoterpene and sesquiterpene synthases and the origin of terpene skeletal diversity in plants. *Phytochemistry* **2009**, *70* (15), 1621−1637. (e) Dickschat, J. S. Isoprenoids in three-dimensional space: the stereochemistry of terpene biosynthesis. *Nat. Prod. Rep.* **2011**, *28* (12), 1917−1936. (f) Miller, D. J.; Allemann, R. K. Sesquiterpene synthases: passive catalysts or active players? *Nat. Prod. Rep.* **2012**, *29* (1), 60−71. (g) Dickschat, J. S. Bacterial terpene cyclases. *Nat. Prod. Rep.* **2016**, *33* (1), 87−110. (h) Christianson, D. W. Structural and Chemical Biology of Terpenoid Cyclases. *Chem. Rev.* **2017**, *117* (17), 11570−11648.

(8) Syntrivanis, L.-D.; Levi, S.; Prescimone, A.; Major, D. T.; Tiefenbacher, K. Four-Step Access to the Sesquiterpene Natural Product Presilphiperfolan-1β-ol and Unnatural Derivatives via Supramolecular Catalysis. *ChemRxiv* **2019**, DOI: 10.26434/chemrxiv.9891341.v1.

(9) (a) Gerkensmeier, T.; Iwanek, W.; Agena, C.; Fröhlich, R.; Kotila, S.; Näther, C.; Mattay, J. Self-Assembly of 2,8,14,20-Tetraisobutyl-5,11,17,23-tetrahydroxyresorc[4]arene. *Eur. J. Org. Chem.* **1999**, *1999* (9), 2257−2262. (b) Atwood, J. L.; Barbour, L. J.; Jerga, A. Hydrogen-bonded molecular capsules are stable in polar media. *Chem. Commun.* **2001**, No. 22, 2376−2377. (c) Shivanyuk, A.; Rebek, J., Jr. Hydrogen-bonded capsules in polar, protic solvents. *Chem. Commun.* **2001**, No. 22, 2374−2375. (d) Atwood, J. L.; Barbour, L. J.; Jerga, A. Organization of the interior of molecular capsules by hydrogen bonding. *Proc. Natl. Acad. Sci. U. S. A.* **2002**, *99* (8), 4837−4841. (e) Avram, L.; Cohen, Y. Discrimination of Guests Encapsulation in Large Hexameric Molecular Capsules in Solution: Pyrogallol[4]arene versus Resorcin[4]arene Capsules. *J. Am. Chem. Soc.* **2003**, *125* (52), 16180−16181. (f) Avram, L.; Cohen, Y. Hexameric Capsules of Lipophilic Pyrogallolarene and Resorcinarene in Solutions as Probed by Diffusion NMR: One Hydroxyl Makes the Difference. *Org. Lett.* **2003**, *5* (18), 3329−3332. (g) Shivanyuk, A.; Friese, J. C.; Döring, S.; Rebek, J. Solvent-Stabilized Molecular Capsules. *J. Org. Chem.* **2003**, *68* (17), 6489−6496. (h) Avram, L.; Cohen, Y. Self-Recognition, Structure, Stability, and Guest Affinity of Pyrogallol[4]arene and Resorcin[4]-arene Capsules in Solution. *J. Am. Chem. Soc.* **2004**, *126* (37), 11556−11563. (i) Guralnik, V.; Avram, L.; Cohen, Y. Unique Organization of Solvent Molecules Within the Hexameric Capsules of Pyrogallol[4]-arene in Solution. *Org. Lett.* **2014**, *16* (21), 5592−5595. (j) Avram, L.; Goldbourt, A.; Cohen, Y. Hexameric Capsules Studied by Magic Angle Spinning Solid-State NMR Spectroscopy: Identifying Solvent Molecules in Pyrogallol[4]arene Capsules. *Angew. Chem., Int. Ed.* **2016**, *55* (3), 904−7.

(10) Zhang, Q.; Catti, L.; Kaila, V. R. I.; Tiefenbacher, K. To catalyze or not to catalyze: elucidation of the subtle differences between the hexameric capsules of pyrogallolarene and resorcinarene. *Chem. Sci.* **2017**, *8* (2), 1653−1657.

(11) (a) Elidrisi, I.; Negin, S.; Bhatt, P. V.; Govender, T.; Kruger, H. G.; Gokel, G. W.; Maguire, G. E. M. Pore formation in phospholipid bilayers by amphiphilic cavitands. *Org. Biomol. Chem.* **2011**, *9* (12), 4498−4506. (b) Pietraszkiewicz, M.; Prus, P.; Pietraszkiewicz, O. Synthesis of novel, boron-containing cavitands derived from calix[4]-resorcinarenes and their molecular recognition of biologically important polyols in Langmuir films. *Tetrahedron* **2004**, *60* (47), 10747−10752. (c) Tan, S.-D.; Chen, W.-H.; Satake, A.; Wang, B.; Xu, Z.-L.; Kobuke, Y. Tetracyanoresorcin[4]arene as a pH dependent artificial acetylcholine receptor. *Org. Biomol. Chem.* **2004**, *2* (19), 2719−2721.

(12) (a) Irwin, J. L.; Sherburn, M. S. Practical Synthesis of Selectively Functionalized Cavitands. *J. Org. Chem.* **2000**, *65* (2), 602−605. (b) Irwin, J. L.; Sherburn, M. S. Optimized Synthesis of Cavitand Phenol Bowls. *J. Org. Chem.* **2000**, *65* (18), 5846−5848.

(13) Yamada, S.; Gavryushin, A.; Knochel, P. Convenient Electrophilic Fluorination of Functionalized Aryl and Heteroaryl Magnesium Reagents. *Angew. Chem., Int. Ed.* **2010**, *49* (12), 2215−2218.

(14) Punna, S.; Meunier, S.; Finn, M. G. A Hierarchy of Aryloxide Deprotection by Boron Tribromide. *Org. Lett.* **2004**, *6* (16), 2777−2779.

(15) Avram, L.; Cohen, Y. Diffusion NMR of molecular cages and capsules. *Chem. Soc. Rev.* **2015**, *44* (2), 586−602.

(16) Cori, O.; Chayet, L.; Perez, L. M.; Bunton, C. A.; Hachey, D. Rearrangement of linalool, geraniol, nerol and their derivatives. *J. Org. Chem.* **1986**, *51* (8), 1310−1316.

(17) Bryant, R. G. The NMR time scale. *J. Chem. Educ.* **1983**, *60* (11), 933.

(18) Silverstein, T. P.; Heller, S. T. pKa Values in the Undergraduate Curriculum: What Is the Real pKa of Water? *J. Chem. Educ.* **2017**, *94* (6), 690−695.

(19) Lambrechts, H. J. A.; Cerfontain, H. Solutes in sulfuric acid. Part IX. Effect of para-substitution on the ionization of the oxonium ions of phenol and anisole. *Recueil des Travaux Chimiques des Pays-Bas* **1983**, *102* (6), 299−301.

(20) Avram, L.; Cohen, Y. The Role of Water Molecules in a Resorcinarene Capsule As Probed by NMR Diffusion Measurements. *Org. Lett.* **2002**, *4* (24), 4365−4368.

(21) Perdew, J. P.; Burke, K.; Ernzerhof, M. Generalized Gradient Approximation Made Simple. *Phys. Rev. Lett.* **1996**, *77* (18), 3865−3868.

(22) Grimme, S.; Antony, J.; Ehrlich, S.; Krieg, H. A consistent and accurate ab initio parametrization of density functional dispersion correction (DFT-D) for the 94 elements H-Pu. *J. Chem. Phys.* **2010**, *132* (15), 154104.

(23) Laino, T.; Mohamed, F.; Laio, A.; Parrinello, M. An Efficient Linear-Scaling Electrostatic Coupling for Treating Periodic Boundary Conditions in QM/MM Simulations. *J. Chem. Theory Comput.* **2006**, *2* (5), 1370−1378.

(24) (a) Laio, A.; Parrinello, M. Escaping free-energy minima. *Proc. Natl. Acad. Sci. U. S. A.* **2002**, *99* (20), 12562−12566. (b) Barducci, A.; Bussi, G.; Parrinello, M. Well-Tempered Metadynamics: A Smoothly Converging and Tunable Free-Energy Method. *Phys. Rev. Lett.* **2008**, *100* (2), 020603.

(25) Bonomi, M.; Bussi, G.; Camilloni, C.; Tribello, G. A.; Banáš, P.; Barducci, A.; Bernetti, M.; Bolhuis, P. G.; Bottaro, S.; Branduardi, D.; Capelli, R.; Carloni, P.; Ceriotti, M.; Cesari, A.; Chen, H.; Chen, W.; Colizzi, F.; De, S.; De La Pierre, M.; Donadio, D.; Drobot, V.; Ensing, B.; Ferguson, A. L.; Filizola, M.; Fraser, J. S.; Fu, H.; Gasparotto, P.; Gervasio, F. L.; Giberti, F.; Gil-Ley, A.; Giorgino, T.; Heller, G. T.; Hocky, G. M.; Iannuzzi, M.; Invernizzi, M.; Jelfs, K. E.; Jussupow, A.; Kirilin, E.; Laio, A.; Limongelli, V.; Lindorff-Larsen, K.; Löhr, T.; Marinelli, F.; Martin-Samos, L.; Masetti, M.; Meyer, R.; Michaelides, A.; Molteni, C.; Morishita, T.; Nava, M.; Paissoni, C.; Papaleo, E.; Parrinello, M.; Pfaendtner, J.; Piaggi, P.; Piccini, G.; Pietropaolo, A.;

https://dx.doi.org/10.1021/jacs.9b13239
J. Am. Chem. Soc. 2020, 142, 4400−4410

Pietrucci, F.; Pipolo, S.; Provasi, D.; Quigley, D.; Raiteri, P.; Raniolo, S.; Rydzewski, J.; Salvalaglio, M.; Sosso, G. C.; Spiwok, V.; Šponer, J.; Swenson, D. W. H.; Tiwary, P.; Valsson, O.; Vendruscolo, M.; Voth, G. A.; White, A.; The, P. c. Promoting transparency and reproducibility in enhanced molecular simulations. *Nat. Methods* **2019**, *16* (8), 670−673.

(26) Grifoni, E.; Piccini, G.; Parrinello, M. Microscopic description of acid−base equilibrium. *Proc. Natl. Acad. Sci. U. S. A.* **2019**, *116* (10), 4054−4057.

(27) (a) Gómez-Bombarelli, R.; Calle, E.; Casado, J. Mechanisms of Lactone Hydrolysis in Acidic Conditions. *J. Org. Chem.* **2013**, *78* (14), 6880−6889. (b) Shi, H.; Wang, Y.; Hua, R. Acid-catalyzed carboxylic acid esterification and ester hydrolysis mechanism: acylium ion as a sharing active intermediate via a spontaneous trimolecular reaction based on density functional theory calculation and supported by electrospray ionization-mass spectrometry. *Phys. Chem. Chem. Phys.* **2015**, *17* (45), 30279−30291.

(28) Valsson, O.; Tiwary, P.; Parrinello, M. Enhancing Important Fluctuations: Rare Events and Metadynamics from a Conceptual Viewpoint. *Annu. Rev. Phys. Chem.* **2016**, *67* (1), 159−184.

(29) (a) Jonsson, H.; Mills, G.; Jacobsen, K. W. Nudged elastic band method for finding minimum energy paths of transitions. In *Classical and Quantum Dynamics in Condensed Phase Simulations;* World Scientific, 1998; pp 385−404. (b) Maragliano, L.; Fischer, A.; Vanden-Eijnden, E.; Ciccotti, G. String method in collective variables: Minimum free energy paths and isocommittor surfaces. *J. Chem. Phys.* **2006**, *125* (2), 024106.

(30) (a) Andersen, N. H.; Syrdal, D. D. Chemical simulation of the biogenesis of cedrene. *Tetrahedron Lett.* **1972**, *13* (24), 2455−2458. (b) Ohta, Y.; Hirose, Y. Electrophile Induced Cyclization of Farnesol. *Chem. Lett.* **1972**, *1* (3), 263−266. (c) McCormick, J. P.; Barton, D. L. Studies in 85% H3PO4—II: On the role of the α-terpinyl cation in cyclic monoterpene genesis. *Tetrahedron* **1978**, *34* (3), 325−330.

https://dx.doi.org/10.1021/jacs.9b13239
J. Am. Chem. Soc. 2020, 142, 4400−4410

8.2 John Wiley and Sons

The manuscript published in *Chemisty – A European Journal* and schemes 32 and 33 were reproduced with permission of John Wiley and Sons.

Concentration-dependent Self-assembly of an Unusually Large Hexameric Hydrogen-bonded Molecular Cage

Merget, S., Catti, L., Zev, S, Major, D. T., Trapp, N., Tiefenbacher, K. *Chem. Eur. J.* **2021**, *27*, 4447−4453

DOI: 10.1002/chem.202005046

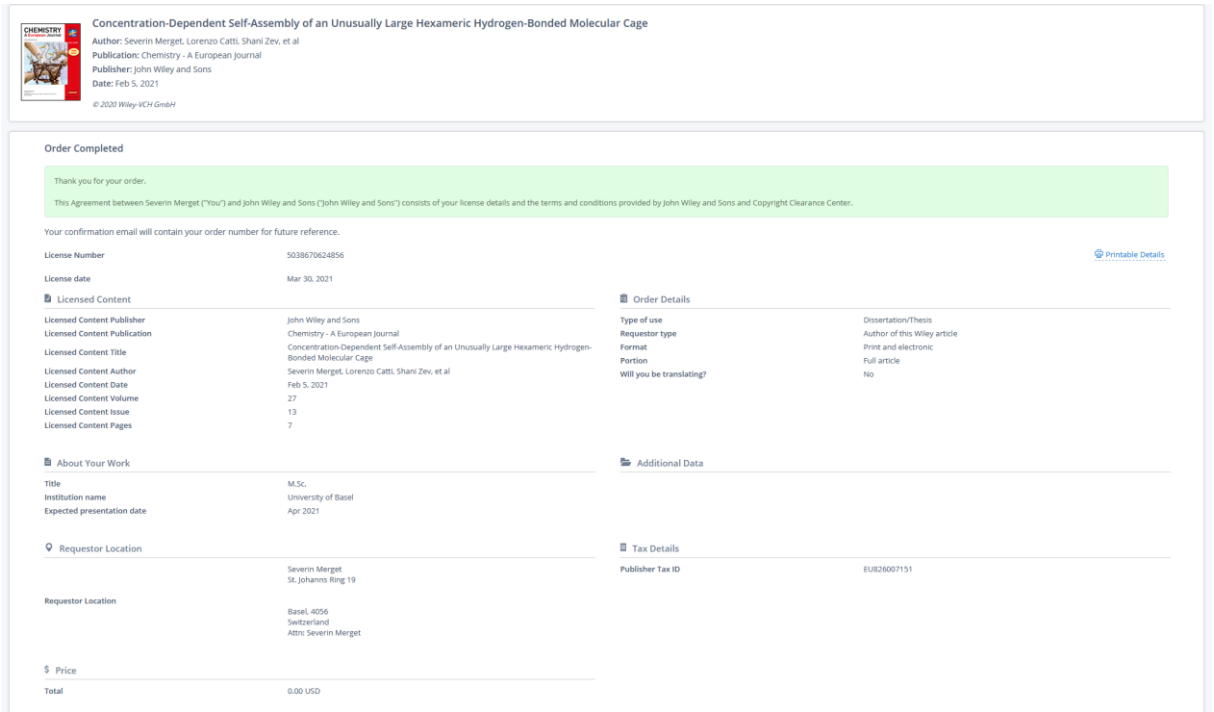

Concentration-Dependent Self-Assembly of an Unusually Large Hexameric Hydrogen-Bonded Molecular Cage
Author: Severin Merget, Lorenzo Catti, Shani Zev, et al
Publication: Chemistry - A European Journal
Publisher: John Wiley and Sons
Date: Feb 5, 2021
© 2020 Wiley-VCH GmbH

Order Completed

Thank you for your order.

This Agreement between Severin Merget ("You") and John Wiley and Sons ("John Wiley and Sons") consists of your license details and the terms and conditions provided by John Wiley and Sons and Copyright Clearance Center.

Your confirmation email will contain your order number for future reference.

Printable Details

License Number	5038670624856
License date	Mar 30, 2021

Licensed Content

Licensed Content Publisher	John Wiley and Sons
Licensed Content Publication	Chemistry - A European Journal
Licensed Content Title	Concentration-Dependent Self-Assembly of an Unusually Large Hexameric Hydrogen-Bonded Molecular Cage
Licensed Content Author	Severin Merget, Lorenzo Catti, Shani Zev, et al
Licensed Content Date	Feb 5, 2021
Licensed Content Volume	27
Licensed Content Issue	13
Licensed Content Pages	7

Order Details

Type of use	Dissertation/Thesis
Requestor type	Author of this Wiley article
Format	Print and electronic
Portion	Full article
Will you be translating?	No

About Your Work

Title	M.Sc.
Institution name	University of Basel
Expected presentation date	Apr 2021

Additional Data

Requestor Location

Severin Merget
St. Johanns Ring 19

Requestor Location

Basel, 4056
Switzerland
Attn: Severin Merget

Tax Details

Publisher Tax ID	EU826007151

$ Price

Total	0.00 USD

Chemistry–A European Journal
Full Paper
doi.org/10.1002/chem.202005046
Check for updates
Chemistry Europe
European Chemical Societies Publishing

Cage Compounds | *Hot Paper*

Concentration-Dependent Self-Assembly of an Unusually Large Hexameric Hydrogen-Bonded Molecular Cage

Severin Merget,[a] Lorenzo Catti,[b] Shani Zev,[c] Dan T. Major,[c] Nils Trapp,[d] and Konrad Tiefenbacher*[a, e]

Abstract: The sizes of available self-assembled hydrogen-bond-based supramolecular capsules and cages are rather limited. The largest systems have volumes of approximately 1400–2300 Å^3. Herein, we report a large, hexameric cage based on intermolecular amide–amide dimerization. The unusual structure with openings, reminiscent of covalently linked cages, is held together by 24 hydrogen bonds. With a diameter of 2.3 nm and a cavity volume of ~2800 Å^3, the assembly is larger than any previously known capsule/cage structure relying exclusively on hydrogen bonds. The self-assembly process in chlorinated, organic solvents was found to be strongly concentration dependent, with the monomeric form prevailing at low concentrations. Additionally, the formation of host–guest complexes with fullerenes (C_{60} and C_{70}) was observed.

Introduction

The self-assembly of molecular capsules and cages using non-covalent interactions such as hydrogen bonds,[1,2] halogen bonds[3] or hydrophobic interactions[4] has been studied intensively over the last decades. Interestingly, in the case of hydrogen-bond-based systems, the size of the assemblies formed has remained rather modest. The octameric capsule (Figure 1 a) reported by the Mastalerz group in 2016 is the largest structure, with a diameter of approximately 1.8 nm (V~2300 Å^3).[2b]

In contrast, the self-assembly of cages through covalent bonds[5] and especially metal–ligand interactions[6] has furnished much larger structures with volumes of up to 157000 Å^3 and more than a hundred components.[7] What causes this size discrepancy? Metal–ligand self-assembly is highly predictable concerning the number of ligands binding to the metal center and the angle between these ligands. In contrast, hydrogen bonding is less predictable. While a linear binding mode is ideal, large deviations are tolerated. Moreover, different binding motives can be observed (e.g., bifurcation of the hydrogen bond) that can further complicate a rational design. Most importantly, however, the linearity of the hydrogen bond requires the design and synthesis of curved building blocks, while in the case of metal–ligand self-assembly the curvature can be imparted by the metal binding site. These factors reduce the predictability of the self-assembly process through hydrogen bonds, and in many cases the formation of extended networks is observed.[2b,8] These problems can be overcome to a large extent by designing dimeric systems.[1,9] Unfortunately, the synthetic effort usually scales with the size of the building blocks, rendering this approach challenging when trying to obtain larger assemblies. Among the noteworthy exceptions are the hexameric resorcinarene[10] and pyrogallolarene[11] capsules (d~1.8 nm; V~ 1400 Å^3), the Stefankiewicz[2c] capsule (d~1.9 nm; V~1700 Å^3) and the largest example by the Mastalerz group[2b] (d~1.8 nm; V~2300 Å^3) already mentioned before (Figure 1 a).

Another striking feature of most multimeric assemblies based on hydrogen bonding is the formation of a "closed-shell" capsule, effectively isolating the interior from the surrounding solvent. This is in stark contrast to metal–ligand-based[5] and covalently linked cages[6] many of which have large openings. Such open structures are of interest not only since the pores potentially offer an additional binding site, but also because they allow small molecules to diffuse in and out of the cavity without the need for partial disassembly required for closed-shell capsules. Furthermore, the pores potentially

[a] S. Merget, Prof. Dr. K. Tiefenbacher
Department of Chemistry, University of Basel
Mattenstrasse 24a, 4058 Basel (Switzerland)
E-mail: konrad.tiefenbacher@unibas.ch
[b] Dr. L. Catti
WPI Nano Life Science Institute (WPI-NanoLSI)
Kanazawa University
Kakuma-machi, Kanazawa 9201192 (Japan)
[c] S. Zev, Prof. Dr. D. T. Major
Department of Chemistry and Institute for Nanotechnology & Advanced Materials, Bar-Ilan University
Ramat-Gan 52900 (Israel)
[d] Dr. N. Trapp
Laboratorium für Organische Chemie, ETH Zürich
Vladimir-Prelog-Weg 3, 8093, Zürich (Switzerland)
[e] Prof. Dr. K. Tiefenbacher
Department of Biosystems Science and Engineering
ETH Zürich
Mattenstrasse 26, 4058 Basel (Switzerland)
E-mail: tkonrad@ethz.ch
Supporting information and the ORCID identification numbers for the authors of this article can be found under: https://doi.org/10.1002/chem.202005046.

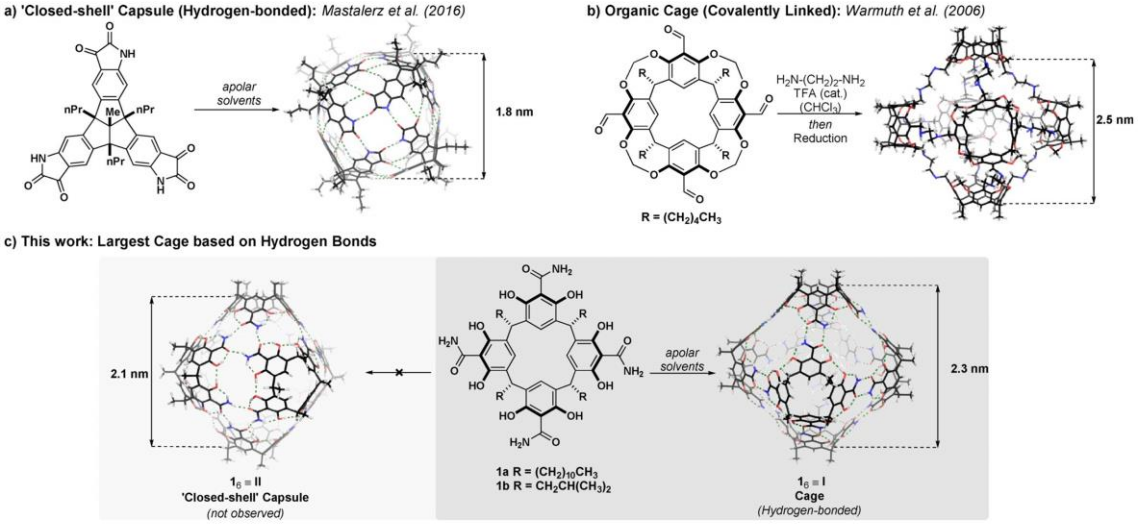

Figure 1. Molecular models of a) the octameric structure reported by Mastalerz, b) the covalently linked cage reported by Warmuth and c) structure **I** reported herein, assembled from six units of **1a** (R residues are omitted for clarity).

offer the possibility for further modification of the assembly. Warmuth and co-workers have pioneered the assembly of covalent organic cages based on methylene bridged resorcinarene derivatives.[12] (Figure 1b). The cages are formed using dynamic covalent imine chemistry and feature openings of considerable size ($d \sim 8$ Å). The approach[13] has been extended towards chiral hydrazone cages by Szumna and co-workers using resorcinarene derivatives with unfunctionalized phenol groups.[14]

In order to construct a very large assembly based on hydrogen bonds, we decided to synthesize the tetraamide-functionalized resorcinarene **1a** (Figure 1c). Interestingly, this building block would be suited to self-assembly into two structurally very different hexameric structures, according to our initial molecular modeling. A direct amide–amide dimerization would form an unusually large cage structure **I**, while an amide trimerization binding motive would form a smaller closed-shell capsule **II** (Figure 1c).

Herein, we present our results concerning the self-assembly of the organic cage **I** with an internal cavity volume of ~2800 Å^3—to the best of our knowledge the largest cage structure that relies solely on hydrogen bonding.

Results and Discussion

First, a reliable synthetic route to macrocycle **1a** had to be developed (Figure 2a). Starting from resorcinarene, the tetrabrominated compound **2a** was accessible on the decagram scale following bromination and methylation according to a literature procedure.[15] Initial attempts to access tetraamide **3a** from **2a** by cyanide coupling followed by hydrolysis proved futile, due to the unreactive nature of the nitrile compound. Ultimately, the introduction of the four amide moieties was achieved in 47% yield by treatment of **2a** with an excess of *n*-butyllithium, followed by addition of trimethylsilyl isocyanate (TMSNCO) as the electrophile. Finally, the methyl protecting groups were removed with trimethylsilyl iodide (TMSI) to yield macrocycle **1a** in 74% yield. Derivative **1b** featuring shorter *iso*-butyl chains was synthesized along the same route and used for X-ray structure analysis (see the Supporting Information for details).

Crystals were obtained by slow evaporation of a saturated solution of **1b** in diethylether/nitrobenzene (10:1) at room temperature. Two types of structures were identified, using this protocol. Occasionally, **1b** crystallized forming a wave-like structure (Figure 2b) that could be solved using small mole-

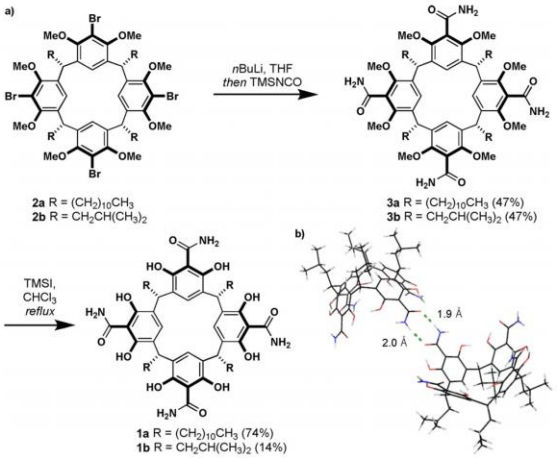

Figure 2. a) Synthesis of **1a** and **1b** from **2a** and **2b**, respectively. b) Representation of the wave-like crystal structure of **1b** obtained from diethyl ether/nitrobenzene. Solvent molecules are omitted for clarity.

cule methods and was also found when employing other solvents (i.e., toluene) for crystallization. In this structure the intermolecular amide–amide hydrogen bonding is evident with measured NH—O=C distances of 1.9–2.0 Å.[16] In most cases however, the crystals obtained showed a much larger cubic unit cell ($a = 3.7$ nm) with a maximum resolution of 1.2 Å, suggesting a large self-assembled structure. Unfortunately, disordered solvent molecules within the cavity prevented solving of this larger structure with small molecule methods.

Although macrocycle **1a** contains several polar groups on its upper rim it was found to be well soluble ($\geq 50\ \mu mol\ mL^{-1}$, $\geq 64\ mg\ mL^{-1}$) in apolar, chlorinated solvents (i.e. $CDCl_3$, CD_2Cl_2, [D_2]tetrachloroethane ([D_2]TCE)) as well as aromatic solvents (C_6D_6, [D_8]toluene). The relevant low-field regions of the ^{1}H NMR spectra in different solvents, including [D_6]acetone that prevents hydrogen-bond-based self-assembly, are displayed in Figure 3. The spectra in apolar solvents show largely similar features: 1) the two amide NH protons (C and D) resonate at a similar chemical shift in the range of 8.50–9.50 ppm, indicating that they both participate in the hydrogen bond network; 2) the protons corresponding to the phenol groups (A and B) differ quite significantly with proton A (16.0–17.0 ppm) being highly deshielded due to the hydrogen bond with the neighboring carbonyl group, while proton B (9.70–10.8 ppm) forms a hydrogen bond with the phenol-group at the adjacent aromatic ring and experiences a weaker downfield shift (see the Supporting Information for 2D NMR data). All major peaks correspond to a single diffusing entity ($D = 2.39 \pm 0.005 \times 10^{-10}\ m^2\ s^{-1}$ in $CDCl_3$ (5 mM)) as indicated by DOSY NMR in different solvents (see the Supporting Information). The hydrodynamic radius (r_h) in apolar solvents was estimated to be 1.81–1.96 nm, which indicates an assembly of higher order[2b,17] similar in size to previously reported hexameric structures.[18] The spectrum of **1a** (20 mM) in $CDCl_3$ as wells as [D_2]TCE, features additional small peaks and shoulders next to the OH signals (A and B) and at 5.84 ppm (red dots in Figure 3), beside the main peaks (green dots). We found the ratio between the main peaks and these smaller signals to be highly dependent on the concentration of the NMR sample (Figure 4b). Furthermore, DOSY NMR spectra revealed a significantly higher diffusion coefficient of the signals marked with

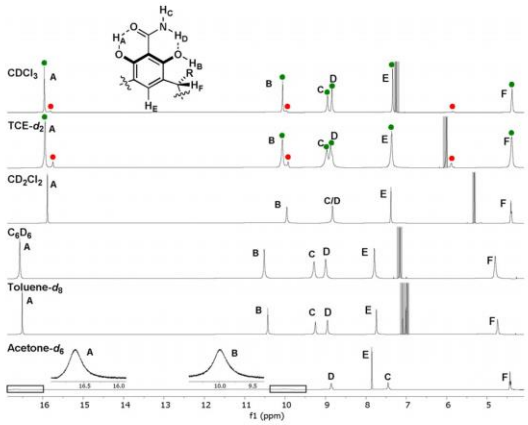

Figure 3. Partial ^{1}H NMR spectra of **1a** (20 mmol L^{-1}) in different solvents. ●: Signals corresponding to the main species **I**; ●: signals corresponding to the monomeric species **1a**. Solvent peaks are marked in gray.

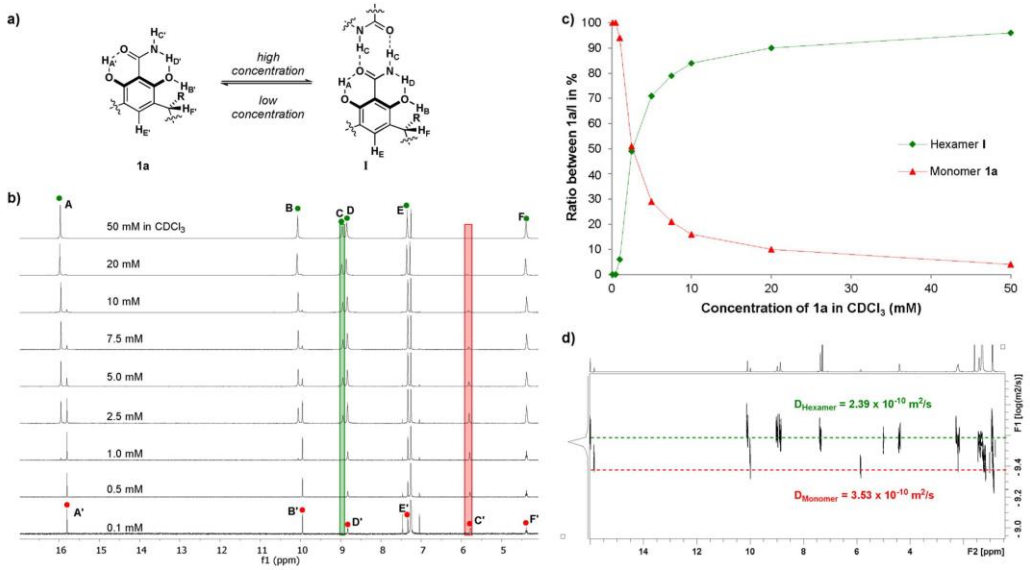

Figure 4. a) Concentration-dependent assembly process between monomer **1a** (●) and hexamer **I** (●) in nonpolar solvents. b) Partial ^{1}H NMR spectra of **1a/I** in $CDCl_3$ at different concentrations (0.1–50 mM based on **1a**). c) Ratio between monomer **1a** and hexamer **I** as a function of the monomer concentration. d) DOSY NMR spectrum of **1a/I** (5.0 mM) showing the different diffusion coefficients for **1a** and **I**.

the red dots ($D = 3.53 \pm 0.021 \times 10^{-10}$ m^2 s^{-1} (5 mM in $CDCl_3$)) indicating a much smaller species (Figure 4d). Upon varying the concentration, it became evident that at low concentration the small species is preferred while at high concentration the hexameric structure **I** is formed predominantly (Figure 4c). The strong upfield shift from 8.98 to 5.78 ppm of NH proton C′ (highlighted in red in Figure 4b) indicates the loss of a strong hydrogen bond in the smaller species as compared to the larger one.[19] The loss of a strong hydrogen bond at atom C′ indicates that the smaller species is the monomeric species **1a**. In the hexameric structure, one of the NH-protons (C) forms an intermolecular hydrogen bond with the carbonyl moiety of a second macrocycle leading to a significant deshielding. This hydrogen bond is lost in the monomeric species and the NH proton (C′) experiences an upfield shift.[20]

In contrast, the chemical environment of the protons involved in intramolecular hydrogen bonds (A′, B′, D′$H_{A'}$, $H_{B'}$, $H_{D'}$) remains rather similar and only a small shift is observed at different concentrations.

Similar trends are observed in the [D_6]acetone solution of **1a** (Figure 3), as the self-assembly process is suppressed by the solvent. The spectrum is in fact comparable to the one of **1a** in $CDCl_3$ at lower concentration (Figure 4b), although the difference for the two NH protons (C′ and D′) is not as pronounced in [D_6]acetone; presumably because proton C′ still experiences some deshielding due to hydrogen bonding with the solvent. Varying the concentration of **1a** in [D_2]TCE and CD_2Cl_2 (see the Supporting Information) as well as in aromatic solvents (C_6D_6, [D_8]toluene) led to similar results concerning a second smaller species prevailing at low concentration.

Interestingly, a study concerning the self-assembly of the pyridinearene macrocycle **4** (Figure 5a) by Cohen and co-workers[18c] revealed analogous behavior. Also in this case two species were distinguished by DOSY NMR in $CDCl_3$: a large hexameric capsule ($D = 2.36 \times 10^{-10}$ m^2 s^{-1}) and a smaller species ($D = 3.50 \times 10^{-10}$ m^2 s^{-1} in $CDCl_3$) assigned as a dimer. The addition of trifluoroacetic acid (TFA) led to disassembly and allowed the observation of the monomer in solution ($D = 4.31 \times 10^{-10}$ m^2 s^{-1}).

In our case the diffusion coefficients of both species **1a** and **I** were found to be concentration dependent (Figure 5b). At low concentrations, where the assembled species **I** is effectively absent, the diffusion coefficient of the small species increases to reach values of up to 4.83×10^{-10} m^2 s^{-1} (1.0 mM in $CDCl_3$) with decreasing concentration, which is in good agreement with values previously reported for pyridinearene **4** in its monomeric form. To obtain an independent reference for the monomeric form the globally methyl protected resorcinarene derivative **5** was used, which cannot self-assemble. Macrocycle **5** was accordingly found to have a diffusion coefficient of 4.86×10^{-10} m^2 s^{-1} (5.0 mM in $CDCl_3$), which is in good agreement with the value obtained for **1a** at low concentration. In con-

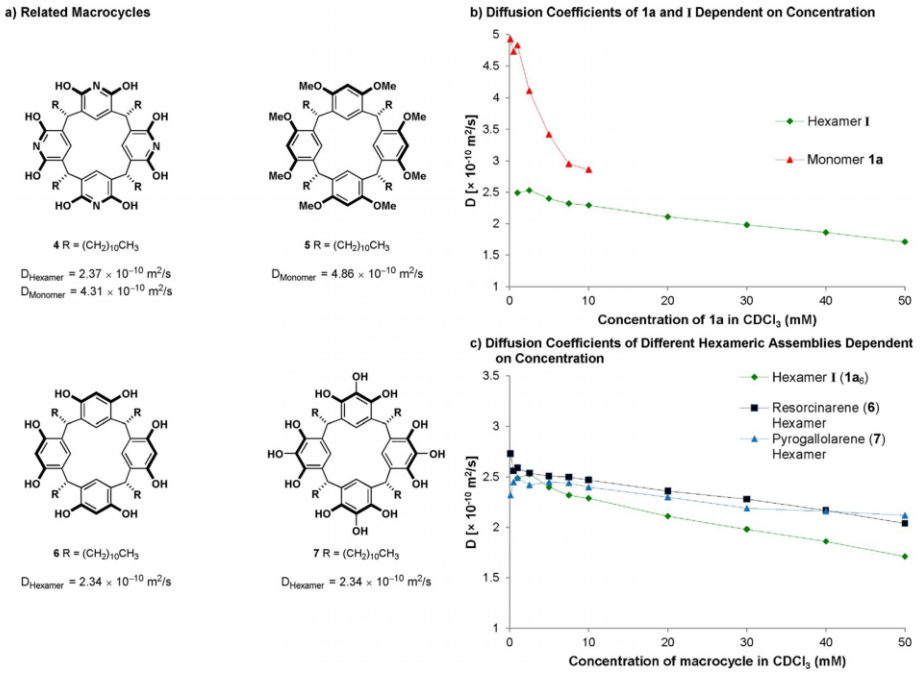

Figure 5. a) Related macrocycles: pyridinearene **4**, octamethylated resorcinarene derivative **5**, resorcinarene **6** and pyrogallarene **7**, and their respective diffusion coefficients in $CDCl_3$. b) Concentration dependence of the diffusion coefficients of the monomeric species **1a** and the hexameric species **I** (1 mM −50 mM in $CDCl_3$). c) Comparison of the diffusion coefficients of the related hexameric assemblies based on macrocycles **1a**, **6** and **7** at different concentrations(1 mM −50 mM in $CDCl_3$).

trast, at high concentrations the assembled species **I** prevails and the diffusion coefficient decreases to reach 1.71×10^{-10} m^2s^{-1} at 50 mM in $CDCl_3$ indicating the formation of a large, discrete assembly. As the decreasing diffusion coefficient might be simply caused by an increase in viscosity at higher macrocycle concentrations, we compared the behavior to the well-known resorcinarene[10] and pyrogallolarene[11] hexamers assembling from macrocycles **6** and **7**, respectively (Figure 5c). In all cases the diffusion coefficient decreases at higher concentration, however, the effect is much more pronounced for macrocycle **1a** which indicates that indeed the hexamer **I** is significantly larger than the resorcinarene and pyrogallarene based hexamers. Assuming that for all assemblies the contribution of the alkyl feet is similar, the hydrodynamic radius determined from the respective diffusion coefficient (measured at 50 mM) correlates very well with the molecular models (Table S4). For the resorcinarene hexamer ($r_h=1.99$ nm; estimated $r=2.01$ nm) and the pyrogallolarene hexamer ($r_h=1.91$ nm; estimated $r=1.97$ nm), an excellent correlation was observed. Also the proposed structure of cage-like hexamer **I** ($r_h=2.36$ nm) displays a very good fit to the molecular model (estimated r = 2.39 nm). As the alternative closed-shell structure **II** does not match the observed hydrodynamic radius, we excluded this option. In conclusion, the DOSY NMR investigations provided evidence that strongly support the formation of the cage-like hexamer **I**.

EXSY-spectra of a 5.0 mM sample of **1a** in $CDCl_3$, corresponding to a monomer:hexamer ratio of 29:71, were obtained using different mixing times.[21] The results revealed an exchange barrier of 16–17 kcal mol^{-1} between the two species.[17b]

Assembly **I** was also studied at different temperatures (20 mM in $CDCl_3$) by using variable temperature (VT) NMR spectroscopy. While lowering the temperature to −45 °C resulted in considerable broadening and decreasing quality of the spectra, at higher temperatures (up to 55 °C) coalescence of the peaks associated with monomer **1a** and hexamer **I** was observed. This indicates that the peaks are indeed two different species of the same compound, which are in equilibrium.

The results presented above are in agreement with the hypothesis that in chlorinated solvents a dynamic, concentration dependent self-assembly process between monomer and hexamer is observed (Figure 4a). The self-assembly of **I** exhibits a critical aggregation concentration of about 3 mM in $CDCl_3$ (Figure 4c). Once this concentration is reached hexamer **I** is formed in a cooperative fashion while other multimeric species remain undetectable at least by NMR spectroscopy. Based on this conclusion the association constant K_a between monomer **1a** and hexamer **I** can be formulated as [Eq. (1)]:

$$K_a=\frac{[\text{hexamer}]}{[\text{monomer}]^6} \quad (1)$$

and was found to be $6.12\pm1.35\times10^{13}$ $mol^{-5}L^5$ in $CDCl_3$.

Finally, assembly **I** was investigated concerning its host–guest chemistry. Supramolecular structures have been used in the past to selectively bind fullerenes for separation purposes and to modulate the electronic properties of fullerenes.[2c,22] To our delight the spherical C_{60} and C_{70} fullerenes proved to be suitable guest molecules for cage **I** (Table 1, entries 1 and 2) most likely due to favorable dispersive interactions and potentially π–π-interactions with the cage walls. The encapsulation of C_{60} within the cavity of cage **I** was indicated by a downfield shift of the C_{60}-carbon signal in the ^{13}C NMR spectra in $CDCl_3$. Due to the low solubility of C_{60} in $CDCl_3$ or potentially as a result of fast guest exchange on the time scale of ^{13}C NMR we were unable to observe a second signal corresponding to non-encapsulated C_{60}, even in the presence of excess guest. Using C_{70} in [D_8]toluene in the presence of **I** similar results were obtained. The low solubility and the absence of slow exchange prevented the determination of binding constants by ^{13}C NMR. Due to the low concentrations required for UV/Vis spectroscopy that prevent the self-assembly of **I**, this technique was also not applicable. To still gain some insight into the encapsulation process by NMR spectroscopy, the soluble ethyl and *tert*-butyl malonyl derivatives of C_{60} and C_{70} were synthesized. The encapsulation of these derivatives was indicated by the appearance of a second set of upfield shifted signals (slow exchange) in the ^1H NMR in presence of **I**. As only one set of well-defined guest signals was observed, a 1:1 binding mode was assumed. Additional evidence for encapsulation was provided by DOSY NMR experiments showing similar diffusion coefficients for host **I** and the encapsulated guest molecules (see the Supporting Information). Association constants were accordingly determined from the integrals of free and encapsulated guest. The binding constants were found to range from 750 to 2220 M^{-1} (entries 3–6) with C_{60} derivatives binding slightly stronger than the corresponding C_{70} derivatives. Contrastingly, in presence of the hexameric resorcinarene and pyrogallolarene capsules no indication for the encapsulation of $C_{60}((CH(CO_2Et)_2)$ was observed. These results are interpreted as additional evidence for the formation of a large, discrete cage **I**, which is able to accommodate large, spherical molecules.

Table 1. Encapsulation of guest molecules within assembly **I**.

	Guest[a]	K_a [M^{-1}]		Guest[a]	K_a [M^{-1}]
1	C_{60}	n.d.[b]	4	$C_{60}(CH(CO_2tBu))$	790[c]
2	C_{70}	n.d.[b]	5	$C_{70}(CH(CO_2Et))$	910[c]
3	$C_{60}(CH(CO_2Et))$	2220[c]	6	$C_{70}(CH(CO_2tBu))$	750[c]

[a] **1a**/guest ratio = 6:1 or 12:1, **1a** 20 mM in $CDCl_3$, 16 h @ 50 °C. [b] n.d. = not determined due to low solubility. [c] Determined by ^1H NMR integration.

Although the results of the DOSY NMR measurements and the binding motif observed in the solid state (Figure 2b) indicate the formation of the larger cage-like structure **I**, we decided also to investigate the energy differences between the two possible hexameric assemblies **I** and **II** with computational methods. According to our gas-phase calculations, the cage structure **I** is lower in energy by 4.5–17.2 kcal mol^{-1} than the alternative closed-shell structure **II**, depending on the DFT method and the basis set used (Table S8). Also in chloroform, an energy preference for structure **I** in the range of 1.8–

14.0 kcal mol^{-1} was observed (Table S9). This energetic difference may be a result of stronger interunit hydrogen bonds formed in the cage structure **I**. Both the cage **I** and closed-shell structure **II** have 24 interunit hydrogen bonds, but these are shorter in the former by 0.04–0.05 Å, depending on the DFT method used (Table S10). These results are fully in line with the experimental findings of this study.

Conclusions

In summary, we have presented the rational design and synthesis of a new supramolecular assembly based on hydrogen bonding. Cage **I** spontaneously self-assembles in chloroform and other chlorinated solvents owing to intermolecular amide–amide hydrogen bonding as evidenced by detailed NMR studies and indicated by solid-state structures. With an internal cavity volume of approximately 2800 Å^3, cage **I** represents, to the best of our knowledge, the largest capsule/cage structure to date based solely on hydrogen bonding. Comparative DFT studies revealed a significant energy difference between two possible hexameric structures, clearly favoring the self-assembly of **I**. Investigation of the properties of assembly **I** in apolar solvents revealed a strong concentration dependence of the self-assembly process and an affinity for fullerenes, which are encapsulated with moderate binding constants. Remarkably, cage **I** is held together by only 24 intermolecular hydrogen bonds all based on simple amide–amide dimerization, whereas most other assemblies of this class feature a much more complex hydrogen-bonding network. Furthermore, the cage has large openings commonly associated with covalently linked cages but unusual for hydrogen-bonded assemblies. We believe that porous structures such as the one presented could potentially be advantageous as they offer an additional handle for further modifications and/or alternative binding sites to obtain heteroassemblies. In general, the simplification of the binding pattern achieved here is expected to aid rational development of future systems and we are confident that the results presented here will help to design new, more sophisticated assemblies in order to overcome the current limitations of size and the encapsulation of large molecules within hydrogen-bonded structures.

Acknowledgements

This work was supported by funding from the European Research Council Horizon 2020 Programme (ERC Starting Grant 714620—TERPENECAT) and the Swiss National Science Foundation as part of the NCCR Molecular Systems Engineering. We thank P.D. Dr. Daniel Häussinger and Fabian Bissegger for assistance with the DOSY NMR and VT NMR measurements as well as Dr. Michael Pfeffer for HRMS analysis. L.C. thanks the Japan Society for the Promotion of Science and the Alexander von Humboldt Foundation for a postdoctoral fellowship. This work was also supported by a grant from the Israeli Science Foundation (grant 1683/18; D.T.M.).

Conflict of Interests

The authors declare no conflict of interests.

Keywords: amides · fullerenes · host–guest complexes · self-assembly · supramolecular chemistry

[1] For reviews see: a) L. Avram, Y. Cohen, J. Rebek, Jr, *Chem. Commun.* **2011**, *47*, 5368 – 5375; b) D. Ajami, J. Rebek, Jr, *Acc. Chem. Res.* **2013**, *46*, 990 – 999; c) L. Adriaenssens, P. Ballester, *Chem. Soc. Rev.* **2013**, *42*, 3261 – 3277; d) L. J. Liu, J. Rebek in *Hydrogen Bonded Supramolecular Structures* (Eds.: Z.-T. Li, L.-Z. Wu), Springer, Heidelberg, **2015**, pp. 227 – 248.

[2] For recent examples see: a) D. Rackauskaite, K. E. Bergquist, Q. Shi, A. Sundin, E. Butkus, K. Warnmark, E. Orentas, *J. Am. Chem. Soc.* **2015**, *137*, 10536 – 10546; b) D. Beaudoin, F. Rominger, M. Mastalerz, *Angew. Chem. Int. Ed.* **2016**, *55*, 15599 – 15603; *Angew. Chem.* **2016**, *128*, 15828 – 15832; c) G. Markiewicz, A. Jenczak, M. Kolodziejski, J. J. Holstein, J. K. M. Sanders, A. R. Stefankiewicz, *Nat. Commun.* **2017**, *8*, 15109; d) A. Kiesila, N. K. Beyeh, J. O. Moilanen, R. Puttreddy, S. Gotz, K. Rissanen, P. Barran, A. Lutzen, E. Kalenius, *Org. Biomol. Chem.* **2019**, *17*, 6980 – 6984; e) K. Eichstaedt, K. Szpotkowski, M. Grajda, M. Gilski, S. Wosicki, M. Jaskolski, A. Szumna, *Chem. Eur. J.* **2019**, *25*, 3091 – 3097; f) H. Jedrzejewska, A. Szumna, *Chem. Sci.* **2019**, *10*, 4412 – 4421; g) Y. S. Park, Y. Kim, K. Paek, *Org. Lett.* **2019**, *21*, 8300 – 8303.

[3] a) N. K. Beyeh, F. Pan, K. Rissanen, *Angew. Chem. Int. Ed.* **2015**, *54*, 7303 – 7307; *Angew. Chem.* **2015**, *127*, 7411 – 7415; b) O. Dumele, N. Trapp, F. Diederich, *Angew. Chem. Int. Ed.* **2015**, *54*, 12339 – 12344; *Angew. Chem.* **2015**, *127*, 12516 – 12521; c) L. Turunen, U. Warzok, R. Puttreddy, N. K. Beyeh, C. A. Schalley, K. Rissanen, *Angew. Chem. Int. Ed.* **2016**, *55*, 14033 – 14036; *Angew. Chem.* **2016**, *128*, 14239 – 14242; d) O. Dumele, B. Schreib, U. Warzok, N. Trapp, C. A. Schalley, F. Diederich, *Angew. Chem. Int. Ed.* **2017**, *56*, 1152 – 1157; *Angew. Chem.* **2017**, *129*, 1172 – 1177; e) L. Turunen, A. Peuronen, S. Forsblom, E. Kalenius, M. Lahtinen, K. Rissanen, *Chem. Eur. J.* **2017**, *23*, 11714 – 11718.

[4] a) C. L. Gibb, B. C. Gibb, *J. Am. Chem. Soc.* **2004**, *126*, 11408 – 11409; b) A. Suzuki, K. Kondo, M. Akita, M. Yoshizawa, *Angew. Chem. Int. Ed.* **2013**, *52*, 8120 – 8123; *Angew. Chem.* **2013**, *125*, 8278 – 8281; c) J. H. Jordan, B. C. Gibb, *Chem. Soc. Rev.* **2015**, *44*, 547 – 585; d) A. Suzuki, M. Akita, M. Yoshizawa, *Chem. Commun.* **2016**, *52*, 10024 – 10027.

[5] a) G. Zhang, M. Mastalerz, *Chem. Soc. Rev.* **2014**, *43*, 1934 – 1947; b) M. Mastalerz, *Acc. Chem. Res.* **2018**, *51*, 2411 – 2422; c) M. A. Little, A. I. Cooper, *Adv. Funct. Mater.* **2020**, *30*, 1909842; d) T. Hasell, A. I. Cooper, *Nat. Rev. Mater.* **2016**, *1*, 16053.

[6] a) M. J. Wiester, P. A. Ulmann, C. A. Mirkin, *Angew. Chem. Int. Ed.* **2011**, *50*, 114 – 137; *Angew. Chem.* **2011**, *123*, 118 – 142; b) T. R. Cook, Y. R. Zheng, P. J. Stang, *Chem. Rev.* **2013**, *113*, 734 – 777; c) S. H. Leenders, R. Gramage-Doria, B. de Bruin, J. N. Reek, *Chem. Soc. Rev.* **2015**, *44*, 433 – 448; d) D. Zhang, T. K. Ronson, J. R. Nitschke, *Acc. Chem. Res.* **2018**, *51*, 2423 – 2436; e) C. M. Hong, R. G. Bergman, K. N. Raymond, F. D. Toste, *Acc. Chem. Res.* **2018**, *51*, 2447 – 2455; f) M. Yoshizawa, L. Catti, *Acc. Chem. Res.* **2019**, *52*, 2392 – 2404.

[7] a) D. Fujita, Y. Ueda, S. Sato, H. Yokoyama, N. Mizuno, T. Kumasaka, M. Fujita, *Chem* **2016**, *1*, 91 – 101; b) D. Fujita, Y. Ueda, S. Sato, N. Mizuno, T. Kumasaka, M. Fujita, *Nature* **2016**, *540*, 563 – 566.

[8] a) K. Müller-Dethlefs, P. Hobza, *Chem. Rev.* **2000**, *100*, 143 – 168; b) P. A. Wood, F. H. Allen, E. Pidcock, *CrystEngComm* **2009**, *11*, 1563 – 1571.

[9] C. Gaeta, C. Talotta, M. De Rosa, P. La Manna, A. Soriente, P. Neri, *Chem. Eur. J.* **2019**, *25*, 4899 – 4913.

[10] L. R. MacGillivray, J. L. Atwood, *Nature* **1997**, *389*, 469 – 472.

[11] T. Gerkensmeier, W. Iwanek, C. Agena, R. Frohlich, S. Kotila, C. Nather, J. Mattay, *Eur. J. Org. Chem.* **1999**, 2257 – 2262.

[12] a) X. Liu, Y. Liu, G. Li, R. Warmuth, *Angew. Chem. Int. Ed.* **2006**, *45*, 901 – 904; *Angew. Chem.* **2006**, *118*, 915 – 918; b) X. Liu, R. Warmuth, *J. Am. Chem. Soc.* **2006**, *128*, 14120 – 14127; c) J. Sun, R. Warmuth, *Chem. Commun.* **2011**, *47*, 9351 – 9353.

[13] K. Kobayashi, M. Yamanaka, *Chem. Soc. Rev.* **2015**, *44*, 449 – 466.

[14] M. Wierzbicki, A. A. Glowacka, M. P. Szymanski, A. Szumna, *Chem. Commun.* **2017**, *53*, 5200 – 5203.
[15] C. Schäfer, J. Mattay, *Photochem. Photobiol. Sci.* **2004**, *3*, 331 – 333.
[16] R. Taylor, O. Kennard, W. Versichel, *Acta Crystallogr. B Struct. Sci.* **1984**, *40*, 280 – 288.
[17] a) H. C. Chen, S. H. Chen, *J. Phys. Chem.* **1984**, *88*, 5118 – 5121; b) A. Macchioni, G. Ciancaleoni, C. Zuccaccia, D. Zuccaccia, *Chem. Soc. Rev.* **2008**, *37*, 479 – 489.
[18] a) L. Avram, Y. Cohen, *Org. Lett.* **2002**, *4*, 4365 – 4368; b) L. Avram, Y. Cohen, *Org. Lett.* **2003**, *5*, 3329 – 3332; c) T. Evan-Salem, Y. Cohen, *Chem. Eur. J.* **2007**, *13*, 7659 – 7663.
[19] M. H. Abraham, R. J. Abraham, W. E. Acree, Jr, A. E. Aliev, A. J. Leo, W. L. Whaley, *J. Org. Chem.* **2014**, *79*, 11075 – 11083.
[20] a) J. R. Neale, N. B. Richter, K. E. Merten, K. G. Taylor, S. Singh, L. C. Waite, N. K. Emery, N. B. Smith, J. Cai, W. M. Pierce, Jr, *Bioorg. Med. Chem. Lett.* **2009**, *19*, 680 – 683; b) D. Joarder, S. Gayen, R. Sarkar, R. Bhattacharya, S. Roy, D. K. Maiti, *J. Org. Chem.* **2019**, *84*, 8468 – 8480.
[21] S. Y. Chang, H. Y. Jang, K. S. Jeong, *Chem. Eur. J.* **2003**, *9*, 1535 – 1541.
[22] a) S. J. Park, O. H. Kwon, K. S. Lee, K. Yamaguchi, D. J. Jang, J. I. Hong, *Chem. Eur. J.* **2008**, *14*, 5353 – 5359; b) N. Kishi, M. Akita, M. Kamiya, S. Hayashi, H. F. Hsu, M. Yoshizawa, *J. Am. Chem. Soc.* **2013**, *135*, 12976 – 12979; c) J. Camacho Gonzalez, S. Mondal, F. Ocayo, R. Guajardo-Maturana, A. Muñoz-Castro, *Int. J. Quantum Chem.* **2019**, *120*, e26080; d) X. Chang, S. Lin, G. Wang, C. Shang, Z. Wang, K. Liu, Y. Fang, P. J. Stang, *J. Am. Chem. Soc.* **2020**, *142*, 15950 – 15960.

Manuscript received: November 20, 2020
Accepted manuscript online: December 21, 2020
Version of record online: February 5, 2021

Severin Merget

Born 7/20/1991
in Munich

Education

05/2017 – 04/2021 **PhD Program (Chemistry)**
University of Basel, Switzerland

10/2010 – 04/2017 **Chemistry Studies (Master of Science)**
Technical University, Munich
Final grade: 1,4

2008 – 2010 **High School Diploma**
Max-Planck-Gymnasium, Munich
Final grade: 1,6

2007 – 2008 **Year Abroad**
Rockridge Secondary School, Vancouver, Canada

Research Projects

Since 05/2017 **PhD Project**
Novel Hydrogen-bonded Supramolecular Assemblies from Resorcinarene-derived Macrocycles & Elucidation of the Prerequisites for Terpene Cyclizations inside the Resorcinarene Capsule

Supervisor: Prof. Dr. Konrad Tiefenbacher

06/2016 – 01/2017 **Master Thesis**
Synthesis of Resorcin[4]arene Derivatives and the Study of their Supramolecular Properties
Supervisor: Prof. Dr. Konrad Tiefenbacher
Grade: 1,0

10/2015 – 12/2015 **Research Internship**
Investigations concerning the Optical Response of Supported Silver Clusters Towards Thiol Ligands
Supervisors: Dr. Tobias Lünskens, Prof. Dr. Ulrich Heitz
Grade: 1,0

05/2015 – 08/2015 **Research Internship**
Studies Towards the Total Synthesis of Merilacton A Derivatives
Supervisors: Dr. Johannes Richers, Prof. Dr. Konrad Tiefenbacher
Grade: 1,0

04/2014 – 09/2014 **Research Internship**
Studies Towards the Synthesis of the Skeleton of Plicamine-Type Alkaloids
Supervisors: Dr. Karl-Heinz Rimböck, Prof. Dr. Thorsten Bach
Grade: 1,0

05/2013 – 08/2013 **Bachelor Thesis**
SHG-Spectroscopy of Supported Ag Clusters and Charaterization of Supported Ligand-stabilized Ag Particles
Supervisors: Dr. Tobias Lünskens, Prof. Dr. Ulrich Heitz
Grade: 1,3